ORGANOMETALLIC CHEMISTRY SUPPORTED BY THE PNP PINCER FRAMEWORK FOR BOTH EARLY AND LATE TRANSITION METALS

A Thesis

by

CHRISTINA MARIE BRAMMELL

Submitted to the Office of Graduate Studies of
Texas A&M University
in partial fulfillment of the requirements for the degree of

MASTER OF SCIENCE

Approved by:

Chair of Committee,	Oleg V. Ozerov
Committee Members,	Francois P. Gabbaï
	Donald J. Darensbourg
	Carl D. Laird
Head of Department,	David H. Russell

December 2012

Major Subject: Chemistry

ABSTRACT

Tridentate “pincer” ligands provide a unique balance of stability and reactivity in organometallic chemistry. The development of diarylamido-based PNP pincer ligands has led to many applications in catalysis, including the potential to facilitate unique chemical transformations at transition metal centers. The main objective of this thesis was to explore transition metal chemistry supported by the PNP pincer framework for both early and late transition metals. In Chapter I, the history behind the design and synthesis of pincer complexes is described. The advantages and disadvantages of various pincer ligands are reviewed to show the reasoning behind the synthesis of the PNP pincer framework.

Chapter II discusses the synthesis of novel Hf and Ta complexes involving the PNP ligand. Reactions of (PNP)$HfCl_3$ with large alkyl Grignards led to double alkylation and triple alkylation was achieved with methyl Grignard. (PNP)$HfMe_3$ and (PNP)$Hf(CH_2SiMe_3)_2Cl$ displayed remarkably irregular coordination environments about hafnium, in contrast to the approximately octahedral structure of (PNP)$HfCl_3$. (PNP)$HfMe_3$ was found to be thermally stable at 75 °C, whereas thermolysis of (PNP)$Hf(CH_2SiMe_3)_2Cl$ under similar conditions led to a mixture of products. The major decomposition product is believed to be a Hf alkylidene complex on the basis of in situ NMR spectroscopic observations (e.g., δ 248.2 ppm in the $^{13}C\{^1H\}$ NMR spectrum).[27] The reaction of (PNP)TaF_4 with an excess of ethyl Grignard led primarily to the double alkylation product, (PNP)$Ta(CH_2CH_3)_2F_2$. Repeating this reaction in the presence of

excess ethyl Grignard and dioxane resulted in the formation of an ethylene complex, (PNP)Ta(=$CHCH_3$)(C_2H_4).

In Chapter III, a C-C reductive elimination study is described comparing two pincer ligand scaffolds: ^{Me}(PNP) ligand and TH(PNP) ligand. The tied ligand has previously been found to be more sterically demanding than the untied ligand, which has allowed for faster N-C cleavage, faster oxidative addition and a more selective alkyne dimerization catalyst. This study reveals that the tied ligand complex, TH(PNP)Rh($C_6H_4CF_3$)(Ph), undergoes slower reductive elimination of *p*-Ph-$C_6H_4CF_3$ (< 4% after 7 h at 38 °C; $t_{1/2}$ = 7.7 h at 64 °C; $t_{1/2}$ = 2.13 h at 75 °C) than ^{Me}(PNP)Rh($C_6H_4CF_3$)(Ph) ($t_{1/2}$ = 15.6 min at 38 °C).

DEDICATION

To my husband.

ACKNOWLEDGEMENTS

I would like to thank my advisor, Dr. Oleg V. Ozerov, for his education, support, patience and encouragement during my Master's study.

I would like to thank my committee members, Dr. D. J. Darensbourg, Dr. F. P. Gabbaï, and Dr. C. D. Laird, for their time, guidance and support throughout the course of this research.

I am also very thankful to Professor Bruce Foxman, Dr. Chun-Hsing Chen, Dr. Andrey A. Yakovenko and Dr. David Herbert for their work on X-ray crystallography.

I would like to thank all members of the Ozerov group, the present and the past, for their friendship and helpful discussions: Dr. Deborha Bacciu, Dr. Dan Smith, Dr. David Herbert, Dr. Jia Zhou, Dr. Claudia Fafard, Dr. Yanjun Zhu, Dr. Weixing Gu, Dr. Morgan MacInnis, Mayank Puri, Laura Gerber, Dan Graham, Emily Pelton, Billy McCulloch, Rafael Huacuja, Rodrigo Ramirez, Jillian Davidson, Sam Timpa, Chun-I Lee, Loren Press, Aaron Hollas, Jessica DeMott, Adam Miller, Chandra Mouli Palit, Chis Penn, Chan Park, Samantha Yruegas and Chelsea Mandell.

I would like to thank my siblings: Britney, Heather and Harrison, as well as my best friends: Lindsey and Jessica, for their encouragement and belief that I can accomplish anything I set my mind to. Finally and most importantly, I would like to thank my wonderful, understanding and loving husband for his patience and support.

TABLE OF CONTENTS

Page

ABSTRACT ii

DEDICATION iv

ACKNOWLEDGEMENTS v

TABLE OF CONTENTS vi

LIST OF FIGURES viii

LIST OF SCHEMES xi

LIST OF TABLES xiii

CHAPTER I INTRODUCTION: PINCER LIGANDS 1

Pincer Ligands 1
History of Pincer Ligands 3
Early and Late Metal PNP Chemistry 6

CHAPTER II EARLY METAL CHEMISTRY: HAFNIUM AND TANTALUM 8

Metal Carbon Bonds 8
Alpha-Abstraction, Alpha-Agostic Interactions and Characterization 10
Use of the PNP Pincer Ligand in Early Transition Metal Chemistry 14
Results and Discussion 18
Synthesis and Solution Characterization of (PNP)HfX_3 Complexes 18
Thermolysis of (PNP)$HfMe_3$ (**37**) and (PNP)$Hf(CH_2SiMe_3)_2Cl$ (**38**) 21
Single Crystal X-ray Diffraction Studies 23
Synthesis and Characterization of Additional (PNP)HfX_3 Complexes 29
Halide Exchange Reactions with (PNP)TaF_4 36
Synthesis of (PNP)Ta(alkyl) Complexes 40
Attempted C-C Bond Cleavage Reactions 46
Experimental 49
General Considerations 49

CHAPTER III A REDUCTIVE ELIMINATION STUDY: UNTIED VS TIED PNP LIGANDS 66

Reductive Elimination/ Oxidative Addition 66
Synthesis of the Untied PNP Ligand 70
Synthesis of the Tied PNP Ligand 72
Results of the C-C Reductive Elimination Study 75
Experimental 84
General Considerations 84

CHAPTER IV CONCLUSION: PNP PINCER LIGAND CHEMISTRY 93

Conclusion 93

REFERENCES 95

LIST OF FIGURES

Page

Figure 1 General scheme for a pincer ligand coordinated to a metal center 1

Figure 2 Metal complexes of anionic and neutral pincer ligands 2

Figure 3 PNP ligand design 5

Figure 4 Soft-Hard-Soft binding motif 7

Figure 5 Example of alkylidene (left) and carbene (right) 8

Figure 6 First synthesized and characterized metal alkylidene 9

Figure 7 Molecular orbitals of an metal alkylidene 9

Figure 8 Alpha-agostic interaction within metal alkylidenes 12

Figure 9 POV-Ray[61] rendition of an ORTEP[62] drawing (50% probability ellipsoids) of (PNP)$HfCl_3$ (**36**) with hydrogen atoms and benzene solvent molecule omitted for clarity 23

Figure 10 POV-Ray[61] rendition of an ORTEP[62] drawing (50% probability ellipsoids) of (PNP)$HfMe_3$ (**37**) with hydrogen atoms omitted for clarity 24

Figure 11 POV-Ray[61] rendition of an ORTEP[62] drawing (50% probability ellipsoids) of (PNP)$Hf(CH_2SiMe_3)_2Cl$ (**38**) with hydrogen atoms omitted for clarity 24

Figure 12 Views[61-62] down the N-Hf axis in (PNP)$HfCl_3$ (**36**, left), (PNP)$HfMe_3$ (**37**, center) and and (PNP)$Hf(CH_2SiMe_3)_2Cl$ (**38,** right). Only the atoms directly bound to the Hf centers shown. 25

Figure 13 POV-Ray[61] rendition of an ORTEP[62] drawing (50% probability ellipsoids) of (PNP)$Hf(CH_2SiMe_3)_2OTf$ (**43**) with hydrogen atoms omitted for clarity 33

Figure 14 View[61-62] of atoms directly bound to the Hf center displayed for (PNP)$Hf(CH_2SiMe_3)_2OTf$ (**43**) 34

Figure 15 POV-Ray[61] rendition of an ORTEP[62] drawing (50% probability ellipsoids) of (PNP)TaF_4 (**45**)[25] with hydrogen atoms omitted for clarity 37

Figure 16 POV-Ray[61] rendition of an ORTEP[62] drawing (50% probability ellipsoids) of (PNP)Ta($CHCH_3$)(C_2H_4) (**52**) with hydrogen atoms omitted for clarity 43

Figure 17 View[61-62] of atoms directly bound to the Ta center displayed for (PNP)Ta($CHCH_3$)(C_2H_4) (**52**) 44

Figure 18 Untied ^{Me}(PNP) and tied TH(PNP) ligands 68

Figure 19 Untied ^{Me}(PNP)PdCl(left) and tied TH(PNP)PdCl (right) complexes 68

Figure 20 ^{1}H NMR spectrum of TH(PNP)Rh($C_6H_4CF_3$)Cl (**69**) in C_6D_6 with residual ether and pentane 74

Figure 21 Reductive elimination study at 38 °C. Peaks from left to right: *p*-Ph$C_6H_4CF_3$, ^{Me}(PNP)Rh(C_6H_5)($C_6H_4CF_3$) (**70**), ^{Me}(PNP)Rh($C_6H_4CF_3$)Cl (**59**) 76

Figure 22 Plot illustrating the first-order reductive elimination of *p*-Ph$C_6H_4CF_3$ from **70** at different concentrations of PhCl 77

Figure 23 C-C reductive elimination at 75 °C. Peaks from left to right: TH(PNP)Rh(C_6H_5)($C_6H_4CF_3$) (**72**), TH(PNP)Rh($C_6H_4CF_3$)Cl (**69**), and *p*-Ph$C_6H_4CF_3$ 78

Figure 24 Plot illustrating the first-order reductive elimination of *p*-Ph$C_6H_4CF_3$ from **72** (red) 64 °C, $t_{1/2}$ = 7.7 h (blue) 75 °C, $t_{1/2}$ = 2.13 h 79

Figure 25 Possible coplanarity of **72** at the transition state 80

Figure 26 POV-Ray[61] rendition of an ORTEP[62] drawing (50% probability ellipsoids) of (PNP)Rh(Ph)Br (**76**) with hydrogen atoms omitted for clarity 81

Figure 27 POV-Ray[61] rendition of an ORTEP[62] drawing (50% probability ellipsoids) of TH(PNP)Rh(C_6H_4Me)Cl (**75**) with hydrogen atoms omitted for clarity 81

Figure 28 Views[61-62] down the N-Rh axis in (PNP)Rh(Ph)Br (**76**, left) and TH(PNP)Rh(C_6H_4Me)Cl (**75**, right). Only the atoms directly bound to the Rh centers are shown..... 82

Figure 29 Plot illustrating the first-order reductive elimination of *p*-$PhC_6H_4CF_3$ from **70** at different concentrations of PhCl with rate constants..... 90

LIST OF SCHEMES

		Page
Scheme 1	Interesting reactivity with PCP Ligand	3
Scheme 2	New synthesis of a (PNP)H ligand (**12**)	4
Scheme 3	Formation of alkylidene through α-abstraction mechanism	10
Scheme 4	Role of sterics in the formation of an alkylidene	11
Scheme 5	Role of PMe_3 in the formation of an alkylidene[42]	12
Scheme 6	First examples of Zr and Hf alkylidenes[49-50]	14
Scheme 7	Zirconium alkylidenes with the (PNP)H ligand[3,23,27,51]	15
Scheme 8	Ti alkylidene/yne and its remarkable reactivity[54]	16
Scheme 9	^{Si}PNP polyalkyls with M = Zr, Hf[55]	16
Scheme 10	Rearrangement from titanium alkylidene to imide[41]	17
Scheme 11	Preparation of (PNP)HfX_3 complexes	19
Scheme 12	Thermolysis of **37** and **38**	21
Scheme 13	Various routes toward the synthesis of an alkylidene with (PNP)$Hf(CH_2SiMe_3)_2Cl$ (**38**)	30
Scheme 14	Preparation of (PNP)$Hf(CH_2SiMe_3)_2Me$ (**40**)	30
Scheme 15	Preparation of (PNP)$Hf(CH_2SiMe_3)_2(C_6H_5)$ (**42**)	31
Scheme 16	Preparation of (PNP)$Hf(CH_2SiMe_3)_2OTf$ (**43**)	32
Scheme 17	Preparation of (PNP)$HfMe_2(NHC_6H_4F)$ (**44**)	35
Scheme 18	Synthesis of (PNP)TaF_4 (**45**)[25]	37
Scheme 19	Synthesis of [(PNP)Ta] halide complexes	38

Scheme 20 Reaction of (PNP)TaF_4 (**45**) with ethyl magnesium chloride to make(PNP)$TaF_2(CH_2CH_3)_2$ (**51**)..... 41

Scheme 21 Reaction of (PNP)TaF_4 (**45**) with ethyl magnesium chloride and dioxane to make (PNP)Ta($CHCH_3$)(C_2H_4) (**52**) 42

Scheme 22 Plausible mechanistic route for formation of (PNP)Ta($CHCH_3$)(C_2H_4) (**52**)..... 46

Scheme 23 Rare example of C=C bond cleavage[68-69] 47

Scheme 24 Series of attempted C=C bond cleavage reactions 48

Scheme 25 Reductive elimination and oxidative addition 66

Scheme 26 An example of ligand dissociation prior to reductive elimination 67

Scheme 27 Reductive elimination from a Pd(II)/Pd(0) three-coordinate system 68

Scheme 28 Synthesis of untied ^{Me}(PNP)Rh($C_6H_4CF_3$)Cl (**59**)..... 71

Scheme 29 Simplified synthesis of TH(PNP)Me (**66**)..... 72

Scheme 30 Synthesis of tied TH(PNP)Rh($C_6H_4CF_3$)Cl (**69**)..... 73

Scheme 31 Reductive elimination study comparing the untied and tied PNP ligands with a rhodium center..... 75

LIST OF TABLES

Page

Table 1 J_{CH} coupling data for selected alkylidene complexes[43-45] 13

Table 2 Summary of select bond distances and angles in (PNP)$HfCl_3$ (**36**), (PNP)$HfMe_3$ (**37**), and (PNP)$Hf(CH_2SiMe_3)_2Cl$ (**38**) 26

Table 3 Summary of select bond distances and angles in (PNP)$Hf(CH_2SiMe_3)_2OTf$ (**43**) 35

Table 4 Halide exchanges with (PNP)TaF_4 (**45**) and corresponding ^{31}P and ^{19}F chemical shifts 40

Table 5 Summary of select bond distances and angles in (PNP)$Ta(CHCH_3)(C_2H_4)$ (**52**) 45

Table 6 Comparison of the crystal structures for the tied and untied ligands 83

CHAPTER I

INTRODUCTION: PINCER LIGANDS

Pincer Ligands

Pincer ligands are a common name for tridentate ligands consisting of three non-metal atoms that coordinate to a metal center, creating two heterocyclic rings (Figure 1). The general form for naming pincer ligands is EXE, which refers to two flanking donor atoms ”E” and one central donor atom “X”.

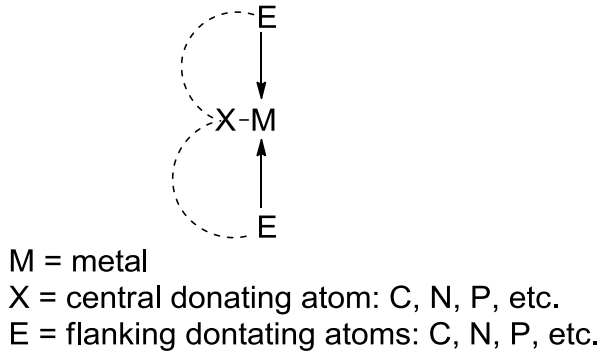

Figure 1. General scheme for a pincer ligand coordinated to a metal center.

Some examples are shown in Figure 2.[1-10] Research has shown that the pincer ligand can be adapted by changing bonding atoms (P, C, N, S and O), by varying hybridizations, or by incorporating different functional groups onto the backbone.[1-10] Two common categories of pincer ligands are anionic and neutral. For anionic ligands, the two flanking arms are commonly neutral donors, while the central atom is an anionic donor (Figure 2, **1-7**).[1-8] In the neutral ligands, all three atoms act as neutral donors, and the ligands

usually include pyridine or carbene central donors (e.g., compounds **8** and **9**, Figure 2).[9,10]

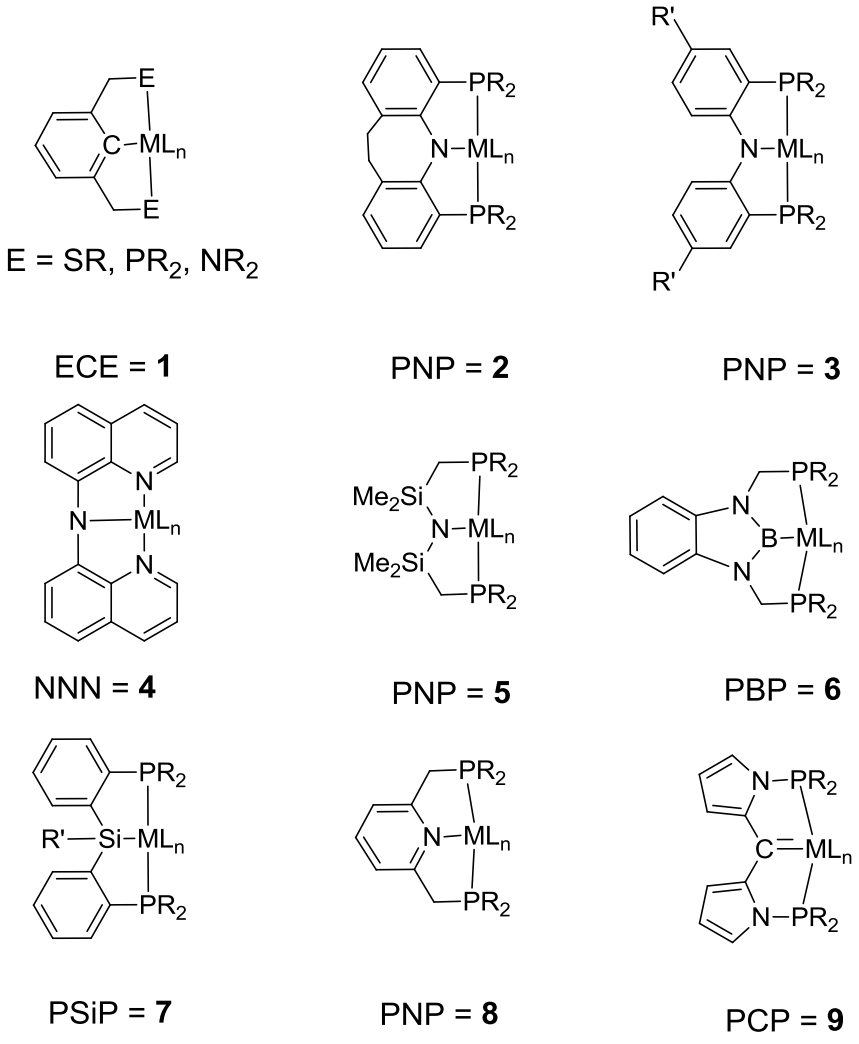

Figure 2. Metal complexes of anionic and neutral pincer ligands.[1-10]

History of Pincer Ligands

The first phosphine based pincer ligand precursor, PCP (**1**), was synthesized by Bernard Shaw in the early 1970s (Figure 2).[1] Over the years, this PCP ligand has become a valuable tool in the formation of functional nanoscale assemblies, the generation of efficient olefin dehydrogenation and Heck-type catalysts, the activation of C-O and C-C bonds, and the trapping of intermediates and unusual molecules (Scheme 1).[11]

Scheme 1. Interesting reactivity with PCP ligand.[11]

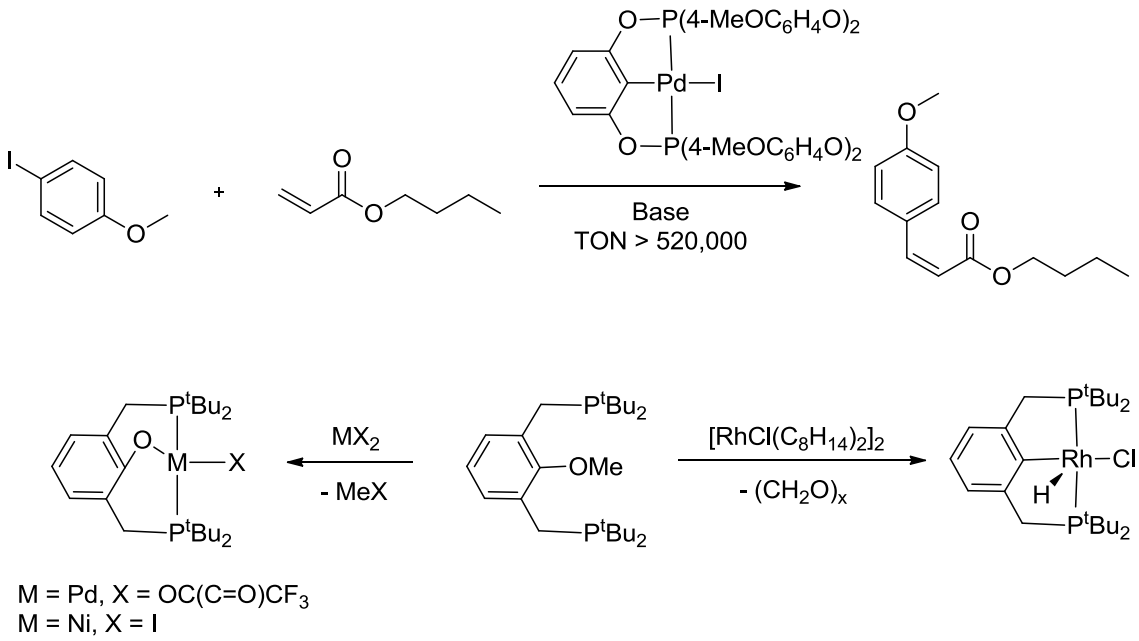

The pincer ligand family was soon expanded to include ^{Si}PNP (**5**) when a silyl linker was successfully incorporated into its scaffold (Figure 2). While **5** was capable of being installed on a variety of both early and late metals, the ligand itself was found to decompose through several pathways.[2,12-15] These included ligand dissociation,[13] ligand

rearrangement resulting in cyclometalation of the Si-CH_2-P group, as well as N-Si[14] and C-Si cleavage.[15] In order to design a more air stable and less reactive PNP ligand (**3**), the silyl linker was eliminated and sp^2 carbon atoms were incorporated into the backbone (Figure 2).[3] Studies of their PNP ligand with nickel derivatives revealed notably different chemistry compared to Fryzuk's [(^{Si}PNP)Ni] derivatives. The PNP ligand was exhibiting increased rigidity from the sp^2 carbon backbone and the elimination of the CH_2 linker was preventing unwanted β-hydrogen elimination.[3] In 2004, Ozerov et al. reported an alternative synthesis for a ^{Me}PNP ligand (Scheme 2).[4]

Scheme 2. New synthesis of a (PNP)H ligand (**12**).

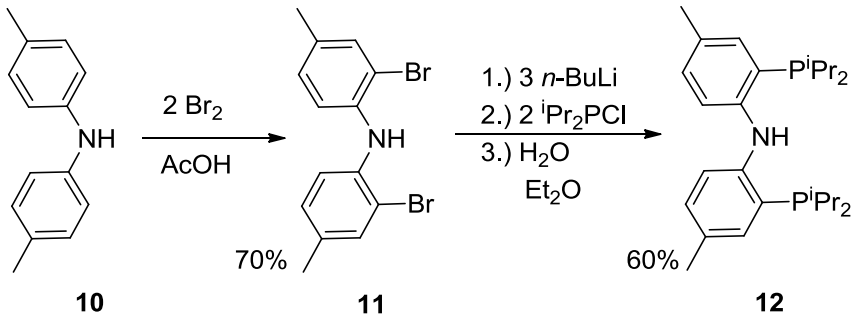

This alternative synthesis not only eliminated potential ortho-PPh metalation, showed increased solubility and enhanced electron-donating ability; it revealed ligand control in terms of stereochemistry and stoichiometry. The addition of groups with various steric and electronic features on the aryl ring and on the phosphorous atoms results in minimal changes to the overall structure and allows for the ability to modify the properties of metal centers through appropriately designed ligands (Figure 3).[3,16-27]

The incorporation of NMR active nuclei into this pincer ligand has provided a convenient spectroscopic handle. The two flanking phosphine arms allow for convenient monitoring of changes in the metal complexes by either solution or solid state ^{31}P NMR spectroscopy. Similar monitoring can be obtained by solution or solid state ^{19}F NMR spectroscopy when the methyl group on the original (PNP)H ligand is exchanged for a fluorine atom.

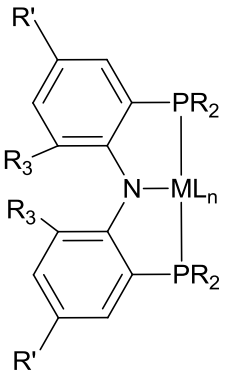

PNP

R' = Me, F, OMe

R = ^{i}Pr, Ph, OCH_2CF_3, Pyr, NMe_2, Et

R_3 = H, $-CH_2CH_2-$

M = early and late metals

Figure 3. PNP ligand design.[3,16-27]

Early and Late Metal PNP Chemistry

Overall, the development of PNP ligands has led to many catalytic applications and the development of unique chemical transformations at both early and late transition metal centers. When bound to a metal, these pincer-metal complexes are unusually robust. This was not always the case. Pincer ligands are commonly hampered by their inability to accommodate the different properties exhibited by both early and late transition metals. Late metals favor low coordinate, low oxidation states and are tolerant of many functional groups. The opposite is true for early metals, which favor high oxidation states and are intolerant of many functional groups.

Fryzuk's ^{Si}(PNP) ligand was the first PNP ligand motif to show successful coordination to both early and late metals;[12-15] however, the ligand is prone to several decomposition pathways, which were discussed above. An interesting feature of ^{Me}PNP (**12**) is its ability to accommodate the demand of both late and early transition metals by a soft-hard-soft interaction (Figure 4). Late metals, which are considered soft, have the ability to interact with the soft phosphorous pendant arms. For the hard early transition metals they can coordinate to the anionic hard amido donor comfortably through the localized electron pair of the anionic N atom. This hard-hard matchup helps stabilize the high oxidation states of the electro-positive early transition metals.[28] **12** has shown the ability to coordinate both the hard and soft matchup for early and late metals without ligand decomposition. The enforced M-P bonding from its rigid backbone that has aided in the formation of multiple (PNP)M alkylidenes using Ti,[24,29] Zr,[23] Hf[26] and Ta[25,30].

Metal complexes of **12** have also been used to activate bonds, such as C-C,[31] C-H,[32] C-O[33] and C-N[34], and various small molecules, such as NH_3,[35] CO_2[36] and CH_4.[37]

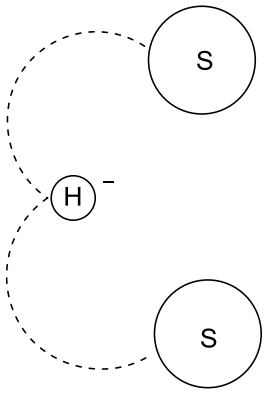

Figure 4. Soft-Hard-Soft binding motif.

CHAPTER II

EARLY METAL CHEMISTRY: HAFNIUM AND TANTALUM*

Metal Carbon Bonds

Transition metal complexes containing metal-carbon multiple bonds have been utilized extensively in catalysis.[38] Alkylidene complexes are comprised of metal-carbon double bonds, while metal alkylidynes contain metal-carbon triple bonds.[28] Complexes with metal-carbon multiple bonds are typically classified along a spectrum between Schrock carbenes and Fisher carbenes (Figure 5). The Schrock carbenes are the primary focus of this work. The first reported alkylidene complex was by Richard Schrock in 1974 (**13**, Figure 6).[39] In 2005, Richard R. Schrock, Robert H. Grubbs and Yves Chauvin were awarded the Nobel Prize in Chemistry for their work on the applications of alkylidenes and alkylidynes.[38]

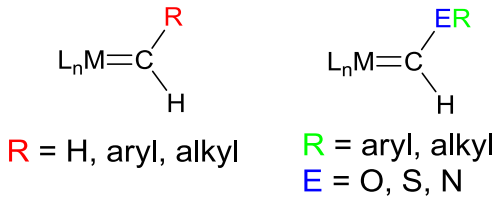

Figure 5. Example of alkylidene (left) and carbene (right).

*Reprinted with permission from "Hafnium Alkyl Complexes of the Anionic PNP Pincer Ligand and Possible Alkylidene Formation" by Brammell, C. M.; Pelton, E. J.; Chen, C.; Yakovenko, A. A.; Weng, W.; Foxman, B. M.; Ozerov, O. V. *Journal of Organometallic Chemistry*, *696*, 4132-4137 Copyright [**2011**] by Elsevier B.V.

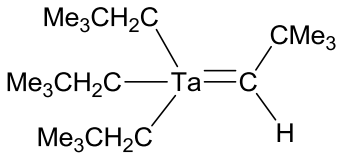

13

Figure 6. First synthesized and characterized metal alkylidene.[39]

Schrock carbenes are commonly called a metal alkylidene or alkylidene complex. Their structure consists of a metal-carbon double bond where the carbon has both a hydrogen and hydrocarbyl substituent. This α-H is acidic. Metal alkylidenes are commonly seen with high oxidation state early transition metals. In the molecular orbital diagram for a metal alkylidene, the *d*-orbital of the metal is available for π-bonding and is higher in energy than the *p*-orbital of the carbene ligand (Figure 7).[28] This generates a π-bonding orbital that is localized on the α-carbon atom, making it a nucleophilic center. In formal electron counting the ligand is viewed as a CR_2^{2-} ligand.

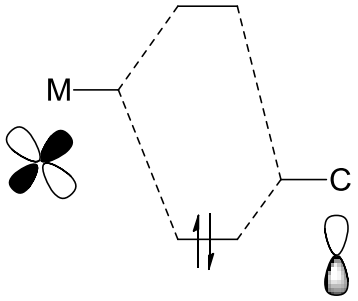

a
Alkylidene

Figure 7. Molecular orbitals of a metal alkylidene.[28]

Alpha-Abstraction, Alpha-Agostic Interactions and Characterization

Alkylidenes are often generated through α-abstraction. As shown in Scheme 3, steric congestion in metal-alkyl complexes is relieved upon abstraction of an alpha proton by an adjacent metal-alkyl group. With the elimination of the alkane, a metal-carbon double bond is formed.[28,38-41]

Scheme 3. Formation of alkylidene through α-abstraction mechanism.

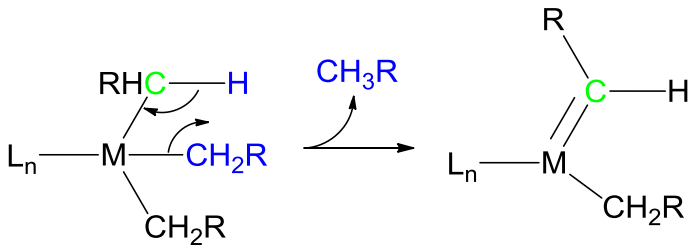

The α-abstraction can be encouraged by a variety of methods: sterics, donor ligands, donor halides.[42] The role of sterics can be seen with the use of η^5-cyclopentadienyl (Cp) ligands in neopentylidene complexes (Scheme 4).[42] When the Cp ligand is substituted onto a $Ta(CH_2CMe_3)_2$ intermediate it creates a more sterically demanding environment that results in the in the loss of a CH_2CMe_3 ligand by α-abstraction to form the tantalum alkylidene (**15**).[42]

Scheme 4. Role of sterics in the formation of an alkylidene.[42]

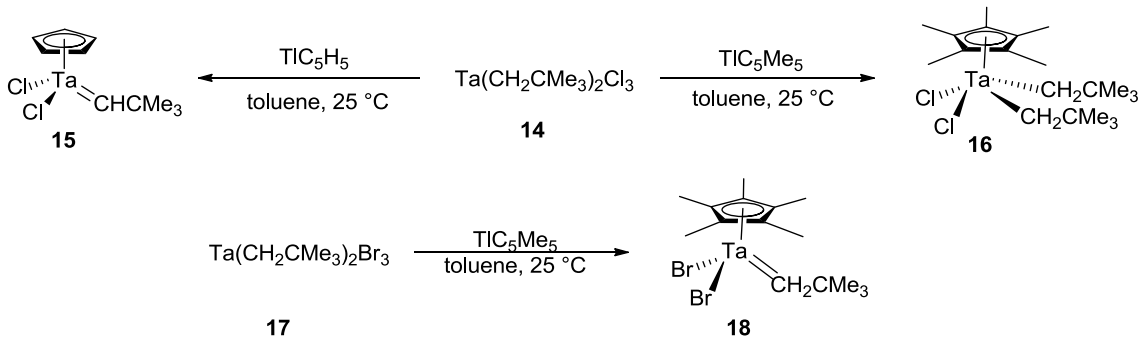

Exchanging the halide ligands can aid in the formation of alkylidenes. Bromine is a poorer π donor than chlorine and it was observed that exchanging the Cl ligand for Br resulted in the formation of an alkylidene (**18**) with the Cp* ligand (Scheme 4).[42] The addition of a neutral ligand will create a crowded coordination sphere contributing to increased electron density at the metal center.[42] Similar to the Cp ligand seen above, Scheme 5 shows the addition of PMe_3. The added electron density at the metal center will enhance the opportunity for α-abstraction to occur, but the amount of steric congestion created around the group 5 metal center is believed to be the resulting driving force for the observed α-abstraction.[42]

Scheme 5. Role of PMe_3 in the formation of an alkylidene.[42]

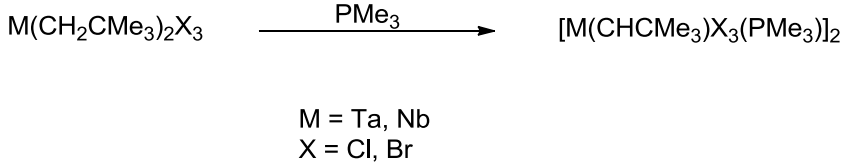

It is common for some alkylidene complexes to exhibit an alpha-agostic interaction where electron density from a carbon-hydrogen bond of a ligand donates into an empty orbital on the metal center.[28,42] In metal alkylidenes this is commonly seen between the metal and the hydrogen atom attached to the α-carbon atom (Figure 8).

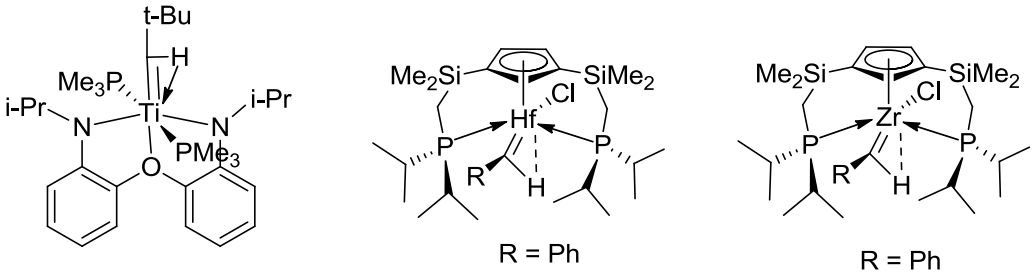

Figure 8. Alpha-agostic interaction within metal alkylidenes.[40]

The common characterization method used to determine if an alpha-agostic interaction is present is by ^1H NMR spectroscopy and crystallographic studies. For d^0 metal centers in ^1H NMR spectroscopy the M-H shifts are typically upfield between 0…+10 ppm. Using crystallographic studies to evaluating the bond lengths and angles aids in providing details about the presence of an alpha-agostic interaction. X-ray diffraction is not as reliable since its ability to locate hydrogen atoms with precise bond lengths and angles is

diminished. Utilizing neutron diffraction will provide a more accurate location of the hydrogen atom and specifically the M-C-H angle. To determine if an alpha-agostic interaction is present, the M-C_α-C_β angle is expected to be greater than 120° while the M-C_α-H angle would be less than 90°. These angles can be explained by both steric and electronic factors. The electron-deficient metal attracts the C-H_α electron pair (the electronic effect) causing the M=C_α-C_β angle to increase (the steric effect).[28,42] An additional invaluable tool in the characterization of alkylidene complexes is ^{13}C NMR spectroscopy. The C_α alkylidene resonance is found downfield of $SiMe_4$ between 220 – 260 ppm. While there are not concrete J_{CH} coupling ranges, it is common for complexes with less than 18 valence electrons, such as the aforementioned neopentylidene complexes, to display low J_{CH} values ranging from 75-100 Hz.[42] For complexes with 18 valence electrons, higher values between 105-130 Hz have been observed (Table 1).[43-45]

Table 1. J_{CH} coupling data for selected alkylidene complexes.[43-45]

Compound	$^1J_{CH\alpha}$ (Hz)
$TaCp_2(CH_2)(CH_3)$	132
$TaCp_2(CHPh)(CH_2Ph)$	127
$TaCp_2(CHCMe_3)Cl$	121

Use of the PNP Pincer Ligand in Early Transition Metal Chemistry

Alkylidene or Schrock carbene complexes are quite common for the 4d and 5d metals of groups 5 and 6.[28,40] On the other hand, examples of alkylidene complexes for their group 4 relatives, Zr and Hf, are much rarer. Examples are somewhat more numerous for the lighter group 4 element Ti.[41,46-48] The first examples of the Zr (**20**) and Hf (**23**) alkylidene complexes were reported by the Fryzuk group, utilizing a cyclopentadienyl/bis(phosphine) ligand P_2Cp (Scheme 6).[49-50]

Scheme 6. First examples of Zr and Hf alkylidenes.[49-50]

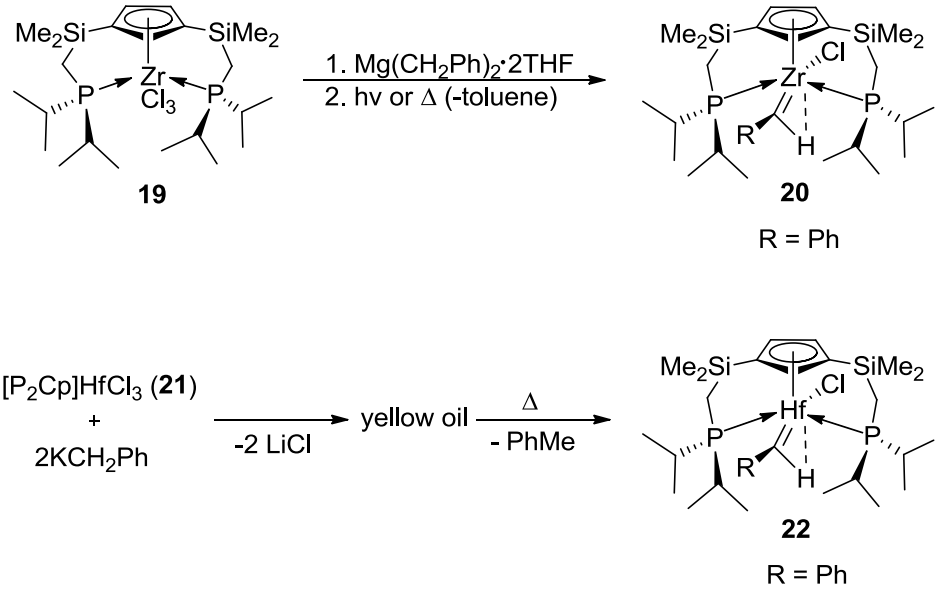

Scheme 7. Zirconium alkylidenes with the (PNP)H ligand.[3,23,27,51]

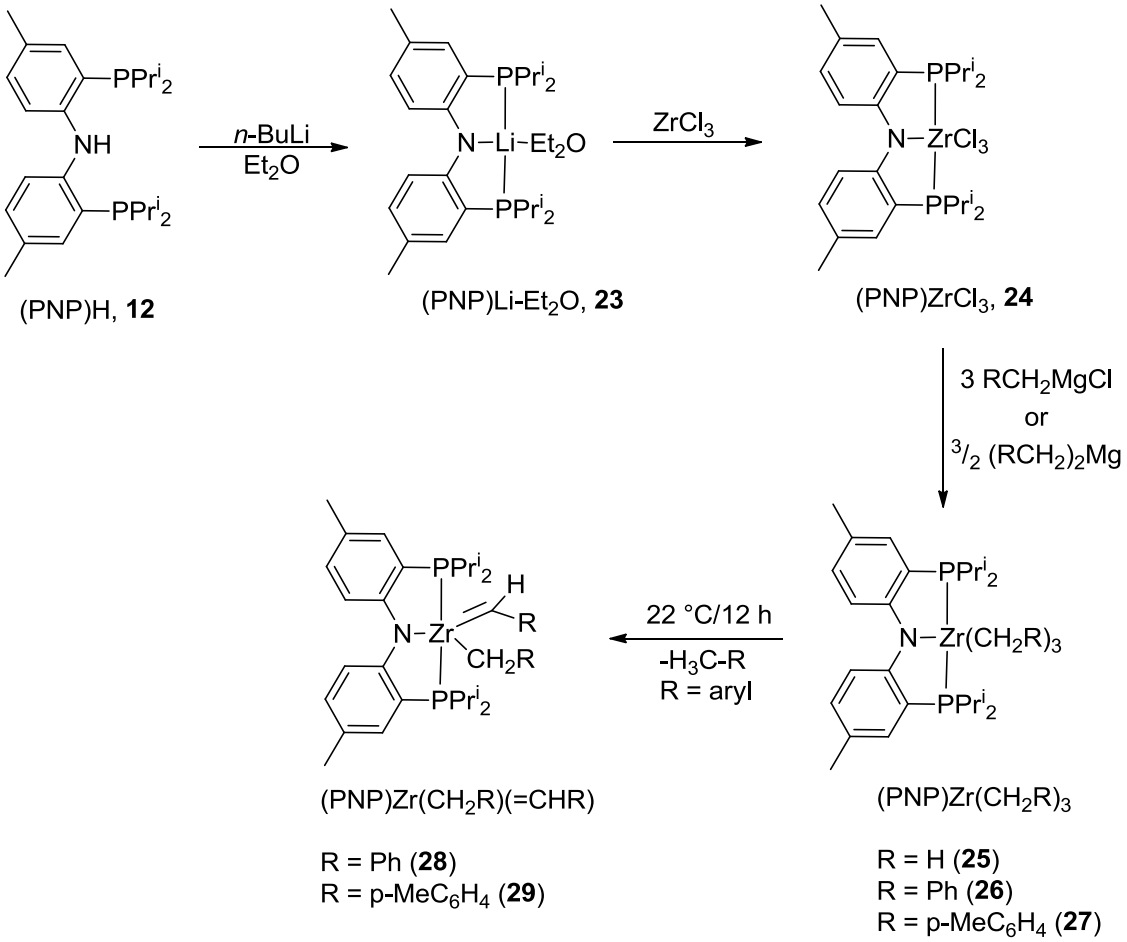

In 2004, Weng and Ozerov reported that the PNP pincer ligand[3,27,51] can support Zr alkylidene complexes (**28**-**29**, Scheme 7).[23] The viability of the PNP ligand as an excellent scaffold for exploring the reactivity of metal ligand multiple bonding in the early metal realm has been amply demonstrated through the work of Mindiola et al., especially with Ti.[52-53] The alkyl/alkylidene **28** (Scheme 8) was shown to generate a transient Ti alkylidyne that possesses rich and remarkable reactivity.[54]

Scheme 8. Ti alkylidene/yne and its remarkable reactivity.[54]

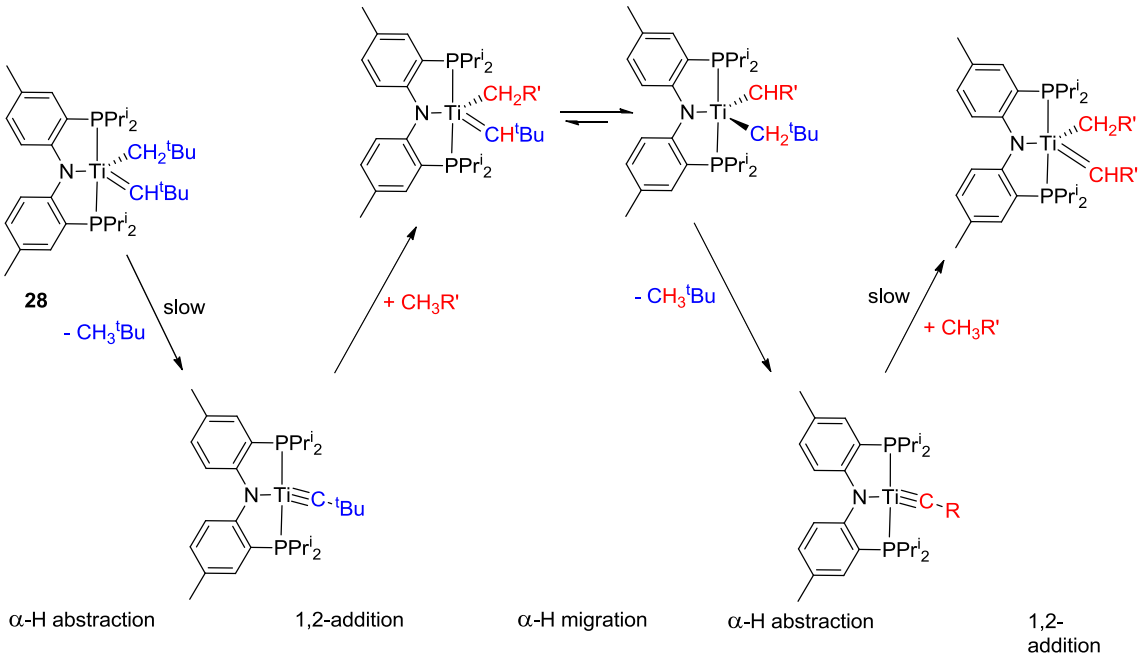

Scheme 9. ^{Si}PNP polyalkyls with M = Zr, Hf.[55]

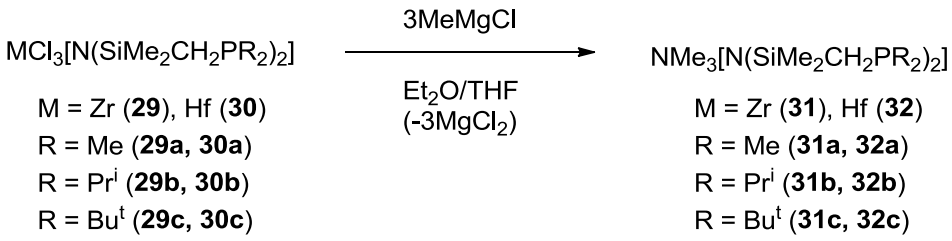

The development of the chemistry of the diarylamido/bis(phosphine) PNP ligands owes much to the history of the disilylamido/bis(phosphine) ^{Si}PNP^{R} ligands of

Fryzuk et al.,[56] more recently studied by Caulton et al.[57] Zr and Hf complexes of ^{Si}PNP have been reported, including polyalkyls (Scheme 9),[55] but not alkylidenes. Coordination number considerations ensure that stabilization of group 4 alkylidenes would probably always require neutral donor ligands coordinated to the metal center. The PNP ligand supplies two such phosphine donors. The advantage may be paradoxically in that the early metals have little affinity for phosphorus ligands and thus lack the affinity for destroying a phosphine ligand when reactive species are generated. In contrast, Mindiola showed that β-diketiminate ligands (also known as "Nacnac") are easily disassembled by Ti alkylidenes, with the Ti center forging an imido ligand out of the β-diketiminate (Scheme 10).[41] In this work, we report our exploration of the PNP chemistry of Hf with an eye on the formation of Hf alkylidenes.

Scheme 10. Rearrangement from titanium alkylidene to imide.[41]

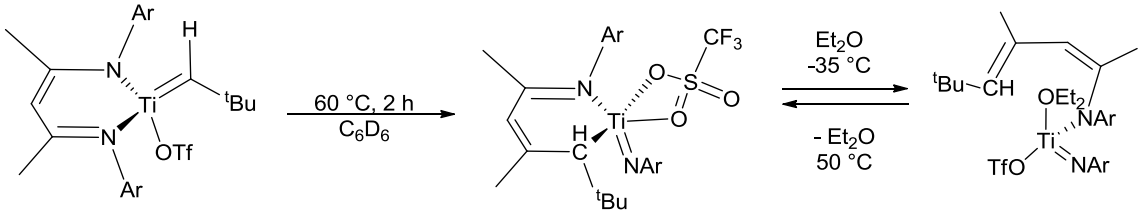

33 **34** **35**

Results and Discussion

Synthesis and Solution Characterization of (PNP)HfX$_3$ Complexes

The introduction of the PNP ligand into the coordination sphere of Hf was successfully accomplished via deprotonation of (PNP)H (**12**)[3] with n-BuLi in ether and the treatment of the resultant (PNP)Li (**23**)[23] solution with $HfCl_4(OEt_2)_2$ (Scheme 11). This reaction produced (PNP)$HfCl_3$ (**36**), which was isolated in a 69% yield as an analytically pure orange solid. (PNP)$HfCl_3$ (**36**) is only modestly soluble in aromatic hydrocarbons. Reaction of **36** with 3 equiv. of MeMgBr led to the formation of yellow trialkyl (PNP)$HfMe_3$ (**37**), isolated in a 53% yield.

On the other hand, the reaction of **36** with 2.5 equiv of Me_3SiCH_2MgCl led to the formation and isolation of the dialkyl (PNP)$Hf(CH_2SiMe_3)_2Cl$ (**38**) in a 77% yield. Utilization of a larger Me_3SiCH_2MgCl-to-3 ratio led only to the increased formation of (PNP)MgX[23] (X = halide or alkyl).

Scheme 11. Preparation of (PNP)HfX_3 complexes.

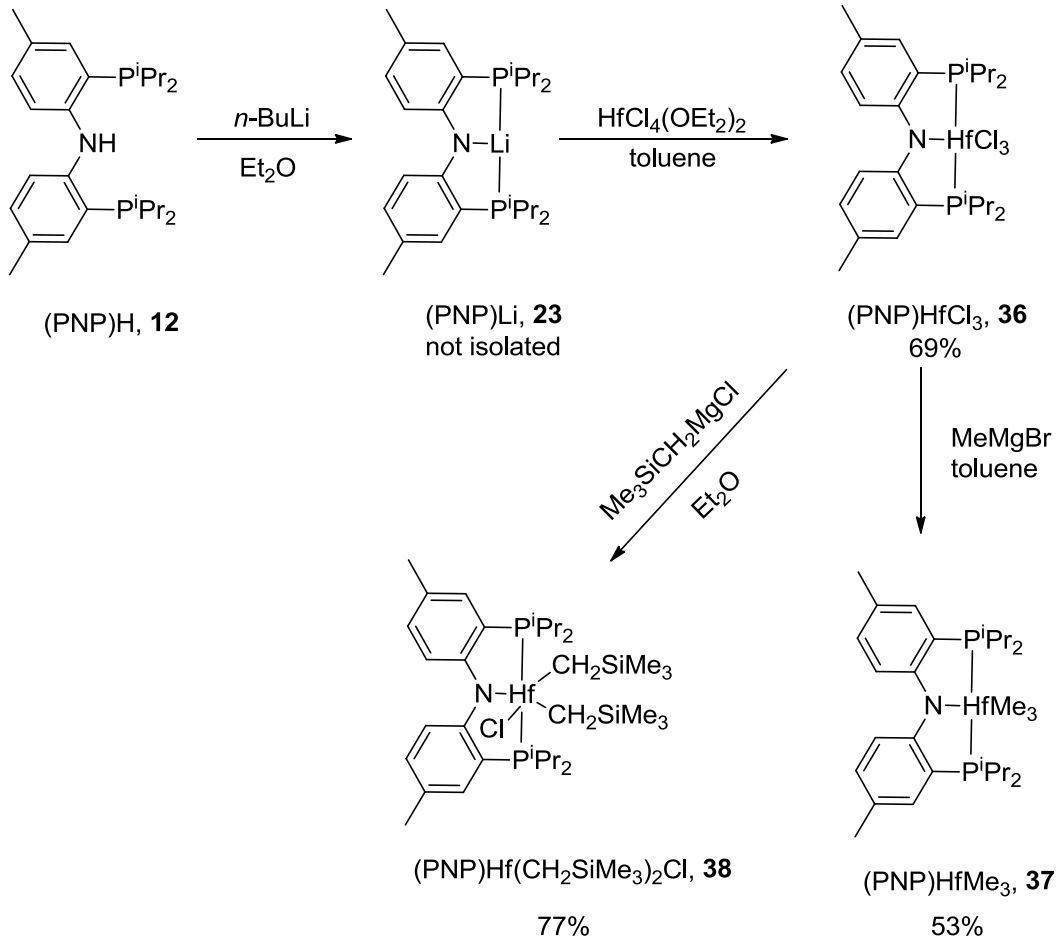

Ostensibly, the increased size of Me_3SiCH_2 vs Me prevents the installation of the third alkyl on Hf in a reaction of **36** with this larger Grignard. Ambient-temperature NMR spectra of **36** and **37** indicated either C_2 or C_s time-averaged symmetry: a lone singlet $^{31}P\{^1H\}$ resonance (δ 34.0 for **36** and 18.0 ppm for **37**), equivalent aromatic rings in the PNP ligand, as well as a pair of methine and four methyl resonances stemming from iPr groups in both ^1H and $^{13}C\{^1H\}$ NMR spectra. The Hf-bound methyl groups of **37** gave rise to one triplet resonance (δ 0.69 ppm, $^3J_{HP}$ = 4 Hz) in the ^1H NMR spectrum. In the

$^{13}C\{^{1}H\}$ NMR spectrum, a corresponding triplet resonance at 60.6 ppm (J_{PC} = 8 Hz) was observed. The equivalence of the three methyl groups on Hf is analogous to the observations for (PNP)$ZrMe_3$[23] and is indicative of exchange among the methyl group sites that is rapid on the NMR timescale at ambient temperature. No static geometry can result in equivalent methyl groups in **37**. The ^{1}H and ^{13}C chemical shifts exhibited by the Hf-Me groups in **37** are comparable to those previously reported in similar compounds. For example, Fryzuk's (SiPNP)$HfMe_3$ compounds (**22**) resonated in their ^{1}H NMR spectra in the 0.5-0.9 ppm range, depending on the nature of the alkyl group on P (no ^{13}C NMR data reported).[55] The ^{13}C NMR chemical shift of ($^{t}Bu_2C_5H_3$)$HfMe_3$ was found to be 57.3 ppm by Royo et al.[56] The ambient-temperature NMR spectra of **38** were consistent with a higher C_2v symmetry, with only one kind of methine and two methyl resonances. However, the resonances were somewhat broad, indicative of an exchange process that is only slightly faster than the NMR timescale. The $SiMe_3$ groups gave rise to singlet ^{1}H (δ 0.37 ppm) and $^{13}C\{^{1}H\}$ (δ 4.3 ppm) resonances. The methylene groups of CH_2SiMe_3 resonated as broad singlets at δ 0.64 ppm in the ^{1}H NMR spectrum and at 77.6 ppm in the $^{13}C\{^{1}H\}$ NMR spectrum. These chemical shifts are similar to those for the Hf-bound CH_2SiMe_3 groups reported in the literature.[56-59]

Thermolysis of (PNP)HfMe$_3$ (37) and (PNP)Hf(CH$_2$SiMe$_3$)$_2$Cl (38)

Thermolysis of **37** in C_6D_6 solution at 75 °C for 48 h did not result in the formation of any new products detectable by NMR spectroscopy (Scheme 12). This lack of reactivity is in line with the thermal inertness of (PNP)ZrMe$_3$,[23] but is in contrast to double α-abstraction occurring upon thermolysis of (PNP)TaMe$_4$ to give (PNP)Ta(CH$_2$)$_2$.[60]

Scheme 12. Thermolysis of **37** and **38**.

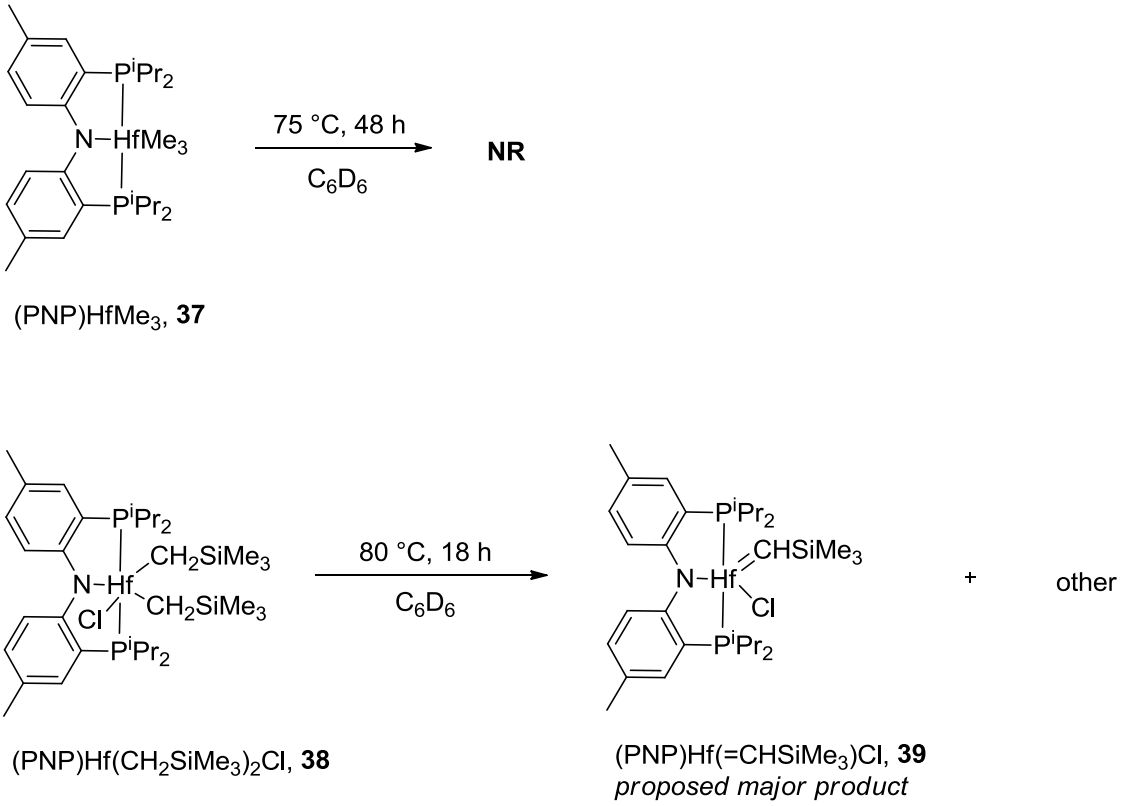

Thermolysis of (PNP)Hf(CH_2SiMe_3)$_2$Cl (**38**) at 80 °C in C_6D_6 resulted in 80% conversion overnight and gave rise to a mixture with two dominant P-containing products. In the $^{31}P\{^1H\}$ NMR spectrum of this mixture, one gave rise to a singlet at 29.4 ppm, while the other, major product, gave rise to an AB system (δ 49.0 and 39.0 ppm, $^2J_{PP}$ = 70 Hz). At the same time, a singlet resonance at δ 8.61 ppm was detected by ^1H NMR spectroscopy and a multiplet resonance at δ 248.2 ppm (identified as a CH by a DEPT experiment) by ^{13}C NMR spectroscopy in this mixture. A HSQC experiment showed correlation between the ^1H resonance at δ 8.61ppm and the ^{13}C resonance at δ 248.2 ppm. The AB system in the $^{31}P\{^1H\}$ NMR spectrum, the downfield ^1H NMR and ^{13}C NMR resonances are reminiscent of the spectra displayed by the PNP-supported alkylidenes of other group 4 metals Ti and Zr. For example, (PNP)Ti($CHCMe_3$)(OTf) displayed an AB ^{31}P NMR pattern with $^2J_{PP}$ = 55 Hz and Δδ ~ 10 ppm, an 8.42 ppm singlet ^1H NMR resonance and a 301 ppm ^{13}C NMR resonance.[24] (PNP)Zr(CHPh)(CH_2Ph) (**28**) displayed an AB ^{31}P NMR pattern with $^2J_{PP}$ = 60 Hz and Δδ ~ 2 ppm, a 7.32 ppm singlet ^1H resonance, and a 231 ppm ^{13}C resonance.[23] Likewise, Fryzuk's **20**[49] and **22**[50] gave rise to singlet ^1H NMR resonances at 7.33 and 8.1 ppm, and ^{13}C NMR resonances at 210 and 229.4 ppm, respectively. We thus hypothesized that the new unknown major component of the mixture formed in the thermolysis of **38** is (PNP)Hf($CHSiMe_3$)(Cl) (**39**, Scheme 12), the alkylidene product of α-abstraction. Indeed, the required $SiMe_4$ by-product of α-abstraction was identified by ^1H and ^{13}C NMR spectroscopy in the reaction mixture. Unfortunately, the high and apparently

similar solubility of the components of the mixture has precluded isolation of the proposed **39** in a pure state.

Single Crystal X-ray Diffraction Studies

X-ray quality single crystals of **36**, **37**, and **38** were obtained and aided in establishing their solid-state structures by X-ray diffraction methods. The individual molecular structures are depicted in Figs. 9-11. The bond distances and angles associated with the Hf immediate coordination environment are shown in Table 2, while Fig. 12 shows the immediate six-coordinate environment about the Hf center in these three molecules side by side from analogous points of view. Octahedral geometry is sterically (and often, electronically) preferred for six ligands about a metal center.

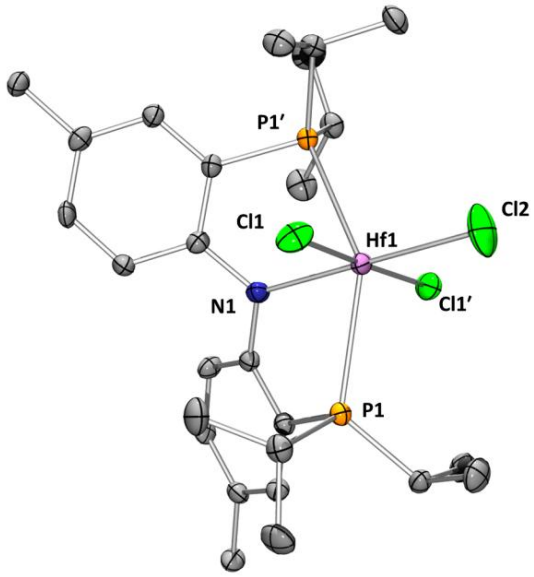

Figure 9. POV-Ray[61] rendition of an ORTEP[62] drawing (50% probability ellipsoids) of (PNP)$HfCl_3$ (**36**) with hydrogen atoms and benzene solvent molecule omitted for clarity.

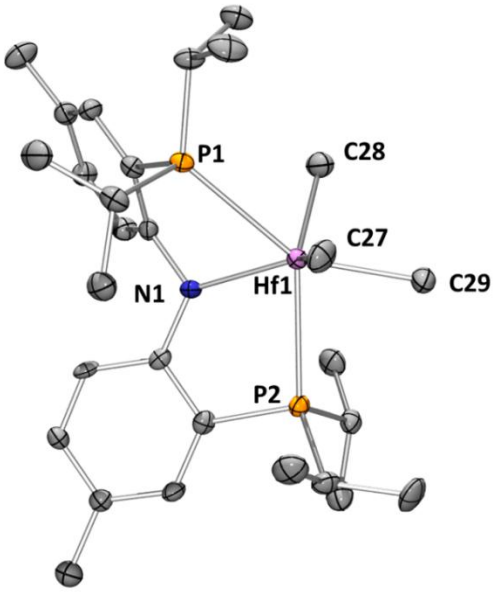

Figure 10. POV-Ray[61] rendition of an ORTEP[62] drawing (50% probability ellipsoids) of (PNP)$HfMe_3$ (**37**) with hydrogen atoms omitted for clarity.

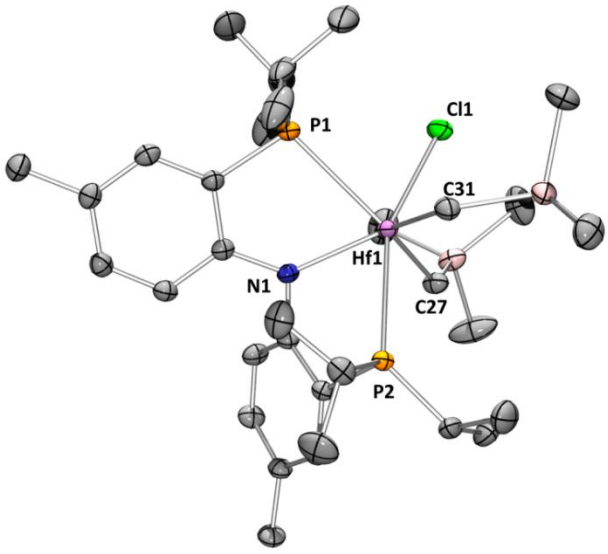

Figure 11. POV-Ray[61] rendition of an ORTEP[62] drawing (50% probability ellipsoids) of (PNP)$Hf(CH_2SiMe_3)_2Cl$ (**38**) with hydrogen atoms omitted for clarity.

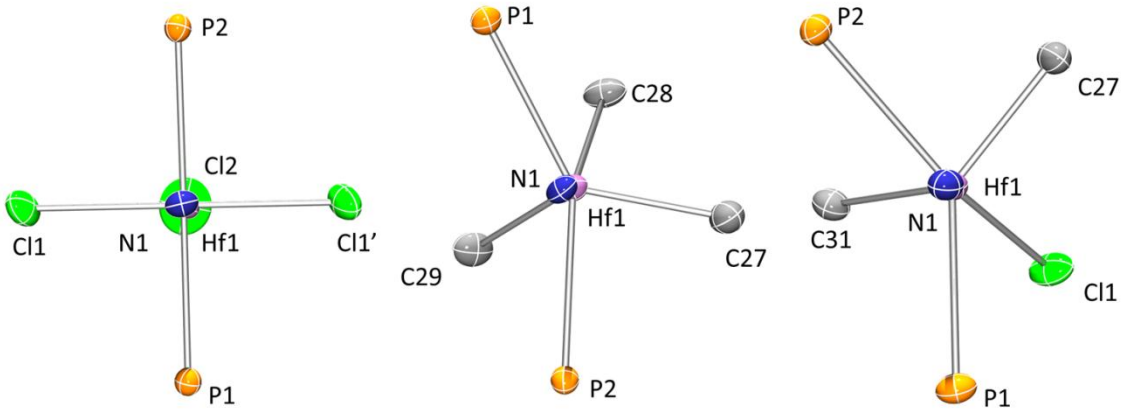

Figure 12. Views[61-62] down the N-Hf axis in (PNP)$HfCl_3$ (**36**, left), (PNP)$HfMe_3$ (**37**, center) and (PNP)$Hf(CH_2SiMe_3)_2Cl$ (**38**, right). Only the atoms directly bound to the Hf centers shown.

Table 2. Summary of select bond distances and angles in (PNP)$HfCl_3$ (**36**), (PNP)$HfMe_3$ (**37**), and (PNP)$Hf(CH_2SiMe_3)_2Cl$ (**38**).

Bond Distances (Å)	(PNP)$HfCl_3$	(PNP)$HfMe_3$	(PNP)$Hf(CH_2SiMe_3)_2Cl$
P1 – Hf1	2.6954(11)	2.7360(14)	2.7817(4)
P2 – Hf1	2.6954(11)	2.8034(14)	2.8309(4)
N1 – Hf1	2.173(5)	2.214(4)	2.1936(13)
R1-Hf1	2.4082(13)	2.234(5)	2.2478(17)
R2-Hf1	2.412(2)	2.301(5)	2.2283(16)
R3-Hf1	2.4082(13)	2.251(6)	2.4575(4)
Bond Angles (°)			
P1 – Hf1 - P2	146.32(5)	132.83(4)	124.363(13)
P1 – Hf1 - N	73.16(2)	70.78(11)	70.00(3)
P1 – Hf1 - R1	89.97(4)	126.77(15)	97.72(4)
P1 – Hf1 - R2	106.84(2)	78.50(14)	139.08(4)
P1 – Hf1 - R3	90.90(4)	104.45(16)	76.929(14)
P2 – Hf1 - N	73.16(2)	70.39(11)	69.09(3)
P2 – Hf1 - R1	90.90(4)	82.77(15)	79.94(4)
P2 – Hf1 - R2	106.84(2)	147.22(14)	82.15(4)
P2 – Hf1 - R3	89.97(4)	78.04(15)	156.209(13)
N1 – Hf1 - R1	91.50(3)	95.63(19)	128.18(5)
N1 – Hf1 - R2	180	140.63(18)	97.24(6)
N1 – Hf1 - R3	91.50(3)	125.53(19)	133.56(3)
R1 – Hf1 - R2	88.50(3)	83.3(2)	118.97(6)
R1 – Hf1 - R3	177.00(6)	123.4(2)	87.14(5)
R2 – Hf1 - R3	88.50(3)	85.2(2)	86.86(4)
R1 =	Cl1	C27	C27
R2 =	Cl2	C28	C31
R3 =	Cl1'	C29	Cl1

However, only **36** possesses a geometry about Hf that can be described as even a distorted octahedral. The only source of major deviation from the octahedron in 58 has to do with the inability of the PNP ligand to accommodate a 180° P-Hf-P angle. This angle is merely 146.32(5)°, but the N-amido and the three chlorides form a nearly perfectly square-planar "midsection" of this distorted octahedron. The low P-Hf-P angle is observed despite the strict meridionality of the PNP ligand. The P-M-P angles in meridional PNP complexes of late transition metals are typically in the 160-170° range.[27,53] Hafnium is considerably larger and the longer Hf-N bond positions it farther away from the phosphines in the PNP/Hf plane, resulting in a narrower P-Hf-P angle. The geometry about Hf in **37** and **38** is irregular and cannot be easily described in terms of simple polyhedra. The molecular structure of **37** is nearly superimposable with that of (PNP) $ZrMe_3$ we reported in 2004.[23] We described[23] the latter as having "both the PNP and the Me_3 sets of donors halfway between a facial and a meridional arrangement." This same description applies well to **37**. The coordination environment about Hf in **38** can be described similarly, although it is not superimposable with (PNP)$HfMe_3$. Fryzuk et al. analyzed the structure of the closely related (SiPNPMe)$HfMe_3$ as a bicapped tetrahedron, with the two neutral P donors capping the faces of the $NHfMe_3$ tetrahedron.[55] This description is less apt for (PNP)MMe_3 (M = Zr or Hf) because the requisite angles deviate to a significantly greater degree from the idealized bicapped tetrahedron. It is possible that the bicapped tetrahedron motif is in fact desirable for these systems, but that the greater rigidity of the diarylamido PNP causes greater distortions in the structure. Polyalkyl complexes of d^0 metals frequently deviate from the sterically

preferred geometries and it has been proposed that maximization of orbital overlap for the strongly covalent M-C bonds may be responsible.[63] The Hf-C distances in **37** and **38** are in the 2.23-2.30 Å range that is typical for Hf alkyls. The Hf-Me bond distances in Fryzuk's ($^{Si}PNP^{Me}$)$HfMe_3$[55] and (P_2N_2)$HfMe_2$[64] are in the 2.24-2.27 Å range, and the Zr-Me bond distances in our (PNP)$ZrMe_3$ are in the 2.25-2.29 Å range.[23] Scott and Lippard reported a series of Zr and Hf bis(trimethylsilylmethyl) complexes supported by N_4 dianionic tropocoronand ligands with M-C bonds ranging from 2.24 to 2.35 Å.[59] The Hf-N and Hf-Cl bond distances are unremarkable. The Hf-P distances are notably shorter in **36** (2.6954(11) Å) than in the alkyl complexes, where they range from 2.73 to 2.83 Å. That is likely a consequence of the stronger Lewis acidity of the Hf center in **36**. The longest Hf-P distances were found in **38** which probably reflects the increased steric pressure from the larger alkyl groups, as well. This trend and the approximate values are reminiscent of Fryzuk's (P_2N_2)HfX_2[64] and and (SiPNPMe)HfX_3[55,65] complexes where for X = Cl, the Hf-P distances (ca. 2.7 Å) were ca. 0.05-0.10 Å shorter than for X = Me (ca. 2.8 Å). On the other hand, the Hf-P distances in (P_2Cp)$HfCl_3$ (ca. 2.85-2.88 Å) were considerably longer,[50] despite being bound to a $HfCl_3$ center. The difference illustrates the greater donicity (and imposed electron count at Hf) of the Cp ligand vs amido. In Hf(IV) complexes, there is no possibility of back donation and the bonding between P and Hf must be of a purely Lewis acid-base adduct nature. The mismatch between soft phosphine donors and a hard Hf(IV) center probably results in a rather weak bond whose length may change considerably with minimal change in overall energy. It is worth noting that the PNP ligand resonances in the ^{1}H and ^{13}C NMR spectra of **36** displayed

virtual triplet coupling[66] to the two ^{31}P nuclei. This phenomenon is typically associated with trans-disposition of equivalent phosphines. More precisely, it stems from a large J_{PP} value that tends to be greater as the P-M-P angle approaches 180°. The coupling to the pair of ^{31}P nuclei in **37** and **38** manifested itself either simply as doublet splitting or as more complex transitional multiplets, indicative of a smaller J_{PP} value in these compounds. Our structural studies show that the P-Hf-P angle in **36** (146.32(5)°) is indeed greater than in the alkyl complexes (132.83(4)° and 124.363(13)°), although still considerable smaller than 180°. The combination of the greater P-Hf-P angle and tighter Hf-P interaction probably gives rise to a greater J_{PP} value in **36** and thus more idealized virtual triplet coupling to the pair of ^{31}P nuclei.

Synthesis and Characterization of Additional (PNP)HfX_3 Complexes

In an attempt to synthesize an alkylidene and/or an imine by alternative routes a series of J. Young NMR tube experiments were conducted. Scheme 13 shows the various routes employed with **38** including the addition of a phosphine group, external ligand and even attempts at chloride extraction. Unfortunately, each route did not yield positive results for possible alkylidene formation (See section *Experimental*).

Scheme 13. Various routes toward the synthesis of an alkylidene with (PNP)Hf(CH_2SiMe_3)$_2$Cl (**38**).

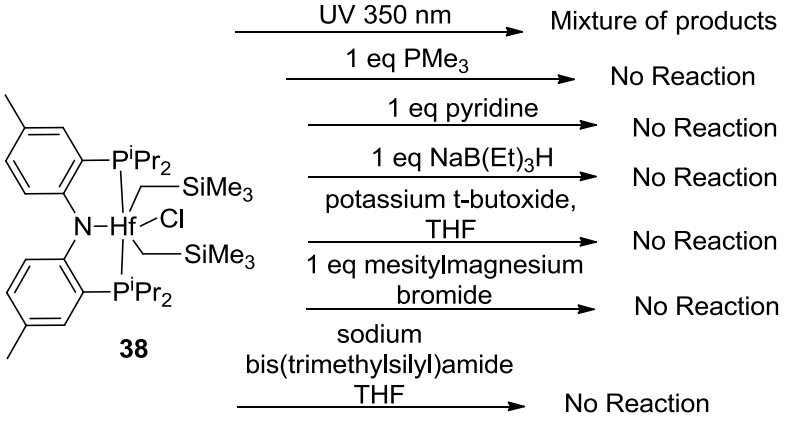

Scheme 14. Preparation of (PNP)Hf(CH_2SiMe_3)$_2$Me (**40**).

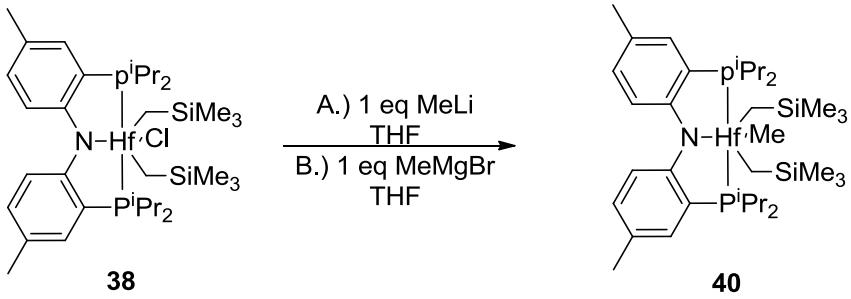

In a J. Young NMR tube **38** was dissolved in ether and 1 equiv of methyl-lithium was added (Scheme 14). After reacting overnight there were 4 new P-containing compounds observed by ^{31}P NMR spectroscopy. Pursuing the idea of synthesizing (PNP)Hf(CH_2SiMe_3)$_2$Me cleanly, **38** was dissolved in ether and 1 equiv of methylmagnesium bromide was added by syringe. Dioxane was added to help precipitate out the MgX_2 species. After 12 h, a new P-containing complex was observed at 3.4 ppm for (PNP)Hf(CH_2SiMe_3)$_2$Me (**40**). Halide exchange was ruled out by the synthesis of (PNP)Hf(CH_2SiMe_3)$_2$Br (**41**) revealing a singlet at 14.5 ppm in the $^{31}P\{^1H\}$ NMR spectrum. Thermolysis of **40** at 70 °C in C_6D_6 overnight 3 nights revealed a mixture of P-containing complexes in addition to **40**: δ 46.6 and 37.1 (J_{AB} system with $^2J_{PP}$ = 72 Hz), 21.7 (s), 14.1 (s), 3.4 (s), 1.5 (s), -13.9 (s), -19.2 (s). ^1H NMR spectroscopy in C_6D_6 revealed what looked like free $SiMe_4$ at 0.001 ppm however the integration was only 9H. The possibility of alkylidene formation during this thermolysis is plausible; however, the lack of material prohibited the repetition of this reaction.

Scheme 15. Preparation of (PNP)Hf(CH_2SiMe_3)$_2$(C_6H_5) (**42**).

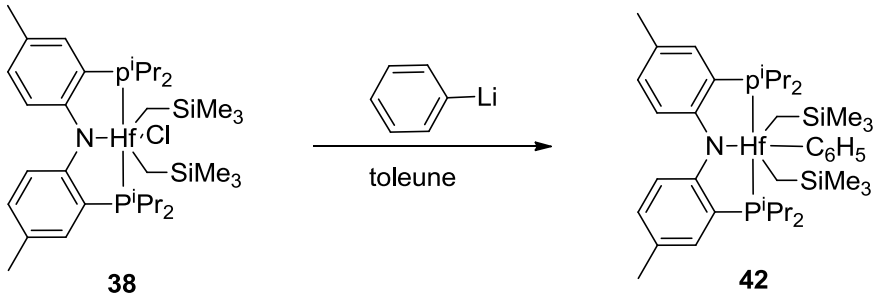

38 **42**

When **38** was reacted with 1.8 M phenyl lithium it is believed that the chloride ligand was exchanged for the phenyl with a ^{31}P singlet at -0.65 ppm (Scheme 15). This was a relatively clean reaction with a 50% yield, (PNP)Hf(CH_2SiMe_3)$_2$(C_6H_5) (**42**). Thermolysis of this sample led to a fairly clean ^{31}P spectrum with two doublets: 33.0, 27.5 (d, $^2J_{PP}$ = 32 Hz) ppm. If α-abstraction did occur it would either result in the formation of free benzene or $SiMe_4$. The ^1H NMR spectrum revealed a singlet at 0.001 ppm for free $SiMe_4$ however the integrations were below 6H.

Scheme 16. Preparation of (PNP)Hf(CH_2SiMe_3)$_2$OTf (**43**).

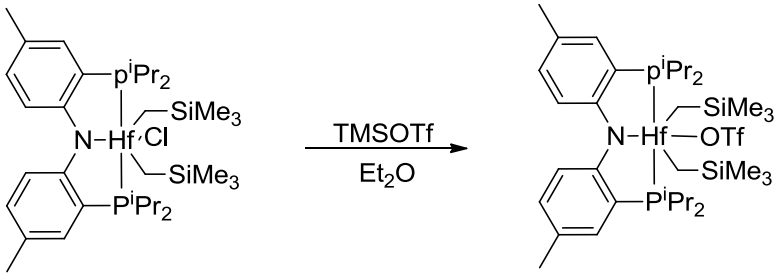

38 **43**

The addition of 5 equiv of TMSOTf to **38** resulted in (PNP)Hf(CH_2SiMe_3)$_2$OTf (**43**) (Scheme 16). $^{31}P\{^1H\}$ and ^{19}F NMR spectroscopy revealed chemical shifts of 14.7 s and -76.6 s ppm, respectively. The solid-state structure of **43** was confirmed by X-ray diffraction methods (Figure 13). The bond angles and distances associated with the immediate six-coordinate environment around the Hf center are shown in Table 3 and are in agreement with published structures.[55,59,64-65] In comparison to Figure 9, the

geometry around the metal center for **43** cannot be described as octahedral. Its distortion is more in line with **37** and **38** (Figure 14).

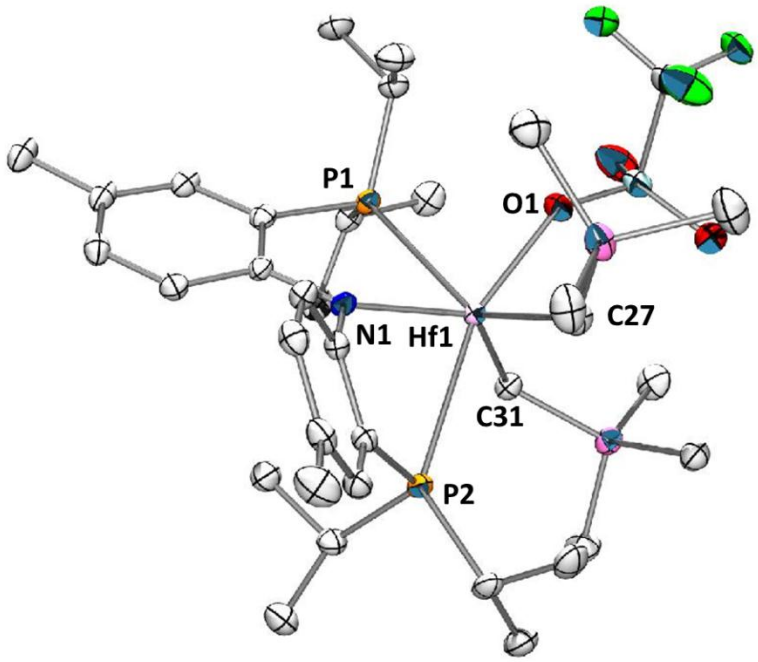

Figure 13. POV-Ray[61] rendition of an ORTEP[62] drawing (50% probability ellipsoids) of (PNP)Hf(CH_2SiMe_3)$_2$OTf (**43**) with hydrogen atoms omitted for clarity.

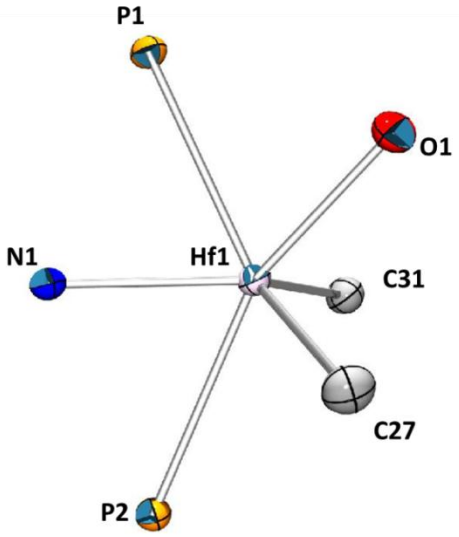

Figure 14. View[61-62] of atoms directly bound to the Hf center displayed for (PNP)Hf(CH_2SiMe_3)$_2$OTf (**43**).

Table 3. Summary of select bond distances and angles in (PNP)Hf(CH_2SiMe_3)$_2$OTf (**43**).

	Bond Length (Å)		Bond Angle (°)		Bond Angle (°)
P1 – Hf1	2.8121(6)	P1 – Hf1 – P2	124.673(18)	P1 – Hf1 – N1	70.53(5)
P2 – Hf1	2.8392(6)	N1 – Hf1 – C27	128.26(8)	P2 – Hf1 – N1	69.72(5)
N1 – Hf1	2.1674(18)	N1 – Hf1 – C31	104.56(8)	C27 – Hf1 – P1	91.80(6)
C27 – Hf1	2.218(2)	N1 – Hf1 – O1	127.08(6)	C31 – Hf1 – P1	142.24(7)
C31 – Hf1	2.216(2)	C27 – Hf1 – C31	116.77(9)	C27 – Hf1 – P2	84.03(6)
O1 – Hf1	2.1740(16)			C31 – Hf1 – P2	84.65(7)

Scheme 17. Preparation of (PNP)HfMe_2(NHC_6H_4F) (**44**).

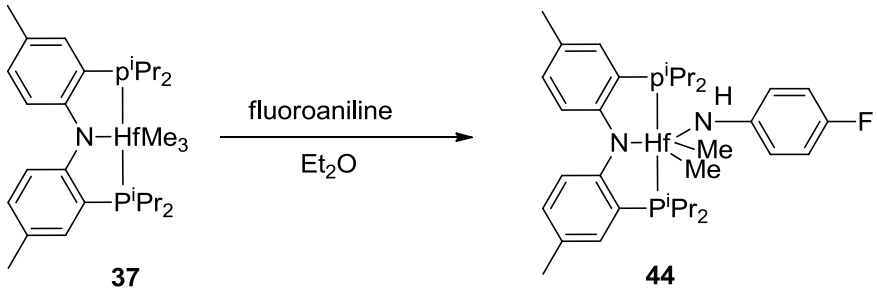

37 **44**

In an attempt to form a hafnium imide **37** was reacted with 1 equiv of fluoroaniline in a J. Young NMR tube (Scheme 17). After adding 1 equiv and letting the reaction stir overnight a new singlet was observed at 29.3 ppm in $^{31}P\{^{1}H\}$ NMR spectroscopy for (PNP)$HfMe_2(NHC_6H_4F)$ (**44**) as well as starting material **37**. A longer reaction time did not yield complete conversion to **44**. It is believed that one methyl has been replaced by one fluroaniline ligand by the δ -128.3 (t, J = 282 Hz) observed in the ^{19}F NMR spectrum.

Halide Exchange Reactions with (PNP)TaF_4

A series of new tantalum complexes using the PNP ligand scaffold were synthesized and characterized including an array of tantalum halides, polyalkyls and tantalum-carbon multiple bonds. Previously, we reported on the synthesis of (PNP)TaF_4 (**45**) (Scheme 18).[25] The properties of this complex allows for convenient ^{19}F NMR spectroscopy monitoring. The solid-state structure of **45** revealed an approximate pentagonal bipyramidal environment around tantalum (Figure 15). Two of the fluorines occupy equatorial sites as the other two occupy the axial sites. In solution, **45** displayed time-averaged C_2 symmetry with a singlet in the ^{19}F NMR spectrum at δ 71.8 and a quintet at δ 47.9 with a J_{PF} = 58 Hz in the $^{31}P\{^{1}H\}$ NMR spectrum.

Scheme 18. Synthesis of **45**.[26]

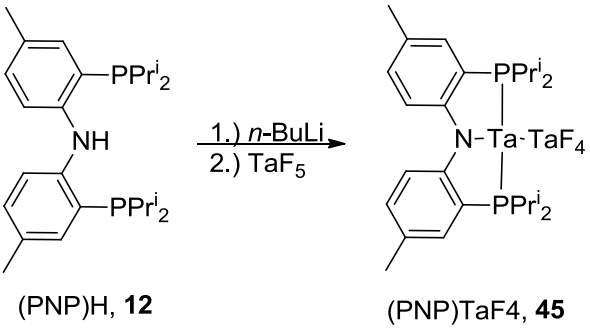

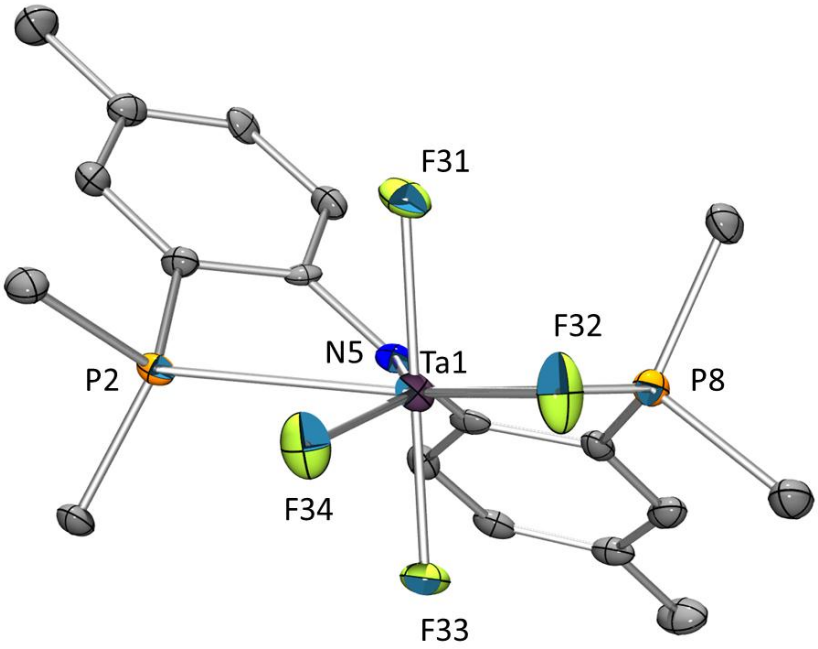

Figure 15. POV-Ray[61] rendition of an ORTEP[62] drawing (50% probability ellipsoids) of (PNP)TaF_4 (**45**)[25] with hydrogen atoms omitted for clarity.

With the coordination of four halides on the tantalum center a series of halide exchange reactions were completed with trimethylsilyl-halides (Me_3SiX, X = F, Cl, I). $(PNP)TaF_3I$ (**46**) was synthesized when 1 equivalent of iodotrimethylsilane was added to **45** (Scheme 19). In ^{19}F and ^{31}P NMR spectroscopy a broad singlet at δ 104.3 and a quartet at δ 56.6 with a J_{PF} = 43 Hz. $(PNP)TaF_2I_2$ (**47**) was synthesized when 4 equivalents of iodotrimethylsilane was added to **45**. In ^{19}F and ^{31}P NMR spectroscopy, a triplet was observed at δ 145 with a J_{PF} = 13 Hz and δ 61.5 with a J_{PF} = 31 Hz. Adding an excess of idotrimethylsilane did not result in further halide exchange.

Scheme 19. Synthesis of [(PNP)Ta] halide complexes.

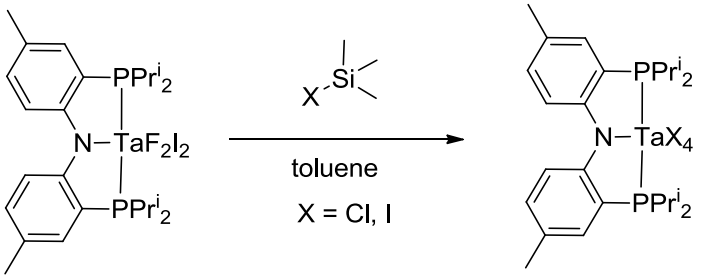

$(PNP)TaF_2I_2$, **47**

Switching halide exchange reagents to chlorotrimethylsilane revealed similar substitutions. When 1 equivalent of chlorotrimethylsilane was added to **45**, $(PNP)TaF_3Cl$ (**48**) was synthesized. A broad singlet was observed at δ 93.8 as well as a quartet at δ 54.6 with a J_{PF} = 46 Hz in both ^{19}F and $^{31}P\{^1H\}$ NMR spectra, respectively. When 4 equivalent of chlorotrimethylsilane were added to **45**, **48** was the major product. Two

new signals were also seen in both ^{19}F and ^{31}P NMR spectroscopy. (PNP)TaF_2Cl_2 (**49**) corresponds to the triplet in both ^{19}F and ^{31}P NMR spectra with shifts at δ 110.8 (J_{PF} = 29 Hz) and δ 61.4 (J_{PF} = 33 Hz). The 2nd new signal was observed to be a singlet in the ^{31}P NMR spectrum. It is postulated that all four fluorine atoms were replaced with four chlorine atoms: $^{31}P\{^1H\}$ δ 74.2 (s); ^{19}F δ 122.1 (br s).

To see if multiple halides could be exchanged in **45** in situ, 1 equiv of iodotrimethylsilane was added followed by 1 equivalent of chlorotrimethylsilane. After reacting for 12 h one product was present. It is believed to be (PNP)TaF_2ICl (**50**). The ^{31}P signal appears at δ 61.5 as a triplet with a J_{PF} = 31 Hz which is in line with the other (PNP)Ta complexes having two fluorine atoms replaced by alternative halides. The ^{19}F resonance appears at δ 144.9 as a triplet with a J_{PF} = 30 Hz. Table 4 is provided to compare all the (PNP)TaX_4 derivatives.

Table 4. Halide exchanges with (PNP)TaF_4 (**45**) and corresponding ^{31}P and ^{19}F chemical shifts.

Complex	$^{31}P\{^1H\}$ NMR (C_6D_6)	^{19}F NMR (C_6D_6)
(PNP)TaF_4 (**45**)	47.9 quintet, J = 102 Hz	71.8 s
(PNP)TaF_3I (**46**)	56.6 q, J = 43 Hz	104.3 s
(PNP)TaF_2I_2 (**47**)	61.5 t, J = 31 Hz	145 t, J = 13 Hz
(PNP)TaF_3Cl (**48**)	54.6 q, J = 46 Hz	93.8 s
(PNP)TaF_2Cl_2 (**49**)	61.4 t, J = 33 Hz	110.8 t, J = 29 Hz
(PNP)TaF_2ICl (**50**)	61.5 t, J = 31 Hz	144.9 t, J = 30 Hz

Synthesis of (PNP)Ta(alkyl) Complexes

Reacting **45** with less than 3 equiv of ethyl magnesium chloride did not result in conversion of all of the starting material (Scheme 20). Addition of 3 equiv or an excess of the ethyl magnesium chloride to **45** resulted in a $^{31}P\{^1H\}$ NMR spectroscopy triplet resonance at 37.6 ppm with a J_{PP} = 14 Hz as well as (PNP)Mg-X complexes at -16 (s) and -18 (s) ppm. There was > 90% conversion of **45** to **51**. A triplet at 57.4 ppm (^{19}F NMR: J_{PF} = 14 Hz) revealed that there were still two fluorine atoms on the metal center. ^1H NMR spectroscopy aided in the characterization of this new tantalum(V) complex, (PNP)$TaF_2(CH_2CH_3)_2$ (**51**). The CH_2 signals of Ta-CH_2CH_3 are observed at 2.14 and 2.09 ppm as quartets and the –CH_3 of the ethyl ligands are overlapping triplets at 0.91 and 0.90 ppm.

Scheme 20. Reaction of (PNP)TaF_4 (**45**) with ethyl magnesium chloride to make (PNP)$TaF_2(CH_2CH_3)_2$ (**51**).

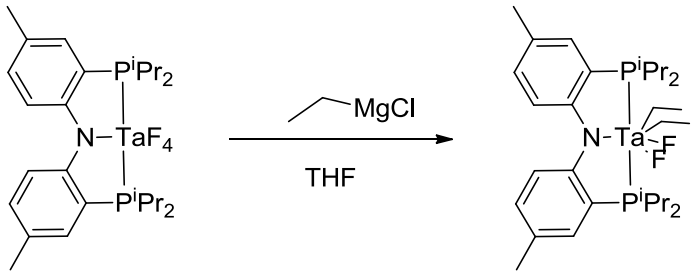

45 **51**

Dioxane was added to help precipitate out the MgX_2 species in hopes of removing halide sources from solution and encourage the alkylation of the two remaining fluoride ligands (Scheme 21). A series of J. Young NMR tube experiments were set up for 3, 4, and >8 equivalent of ethyl magnesium chloride. Dioxane was added to each one. Two doublets were observed at δ 62.1 and 59.8 ppm with a $^2J_{PP}$ = 52 Hz in addition to the triplet for **51** by the $^{31}P\{^1H\}$ NMR spectrum.

Scheme 21. Reaction of (PNP)TaF_4 (**45**) with ethyl magnesium chloride and dioxane to make (PNP)Ta($CHCH_3$)(C_2H_4) (**52**).

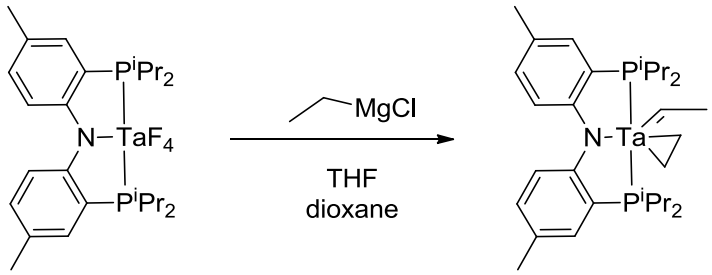

45 **52**

To isolate this new (PNP) complex the solution was placed under vacuum, extracted with fluorobenzene to yield 53 mg of orange solid. ^{1}H and ^{1}H{^{31}P} NMR spectroscopy aided in the identification of the tantalum ethylene complex, (PNP)Ta$CHCH_3$(C_2H_4) (**52**). There were no signals observed in the ^{19}F NMR spectrum for **52**, signaling that all of the fluorine atoms were exchanged. The TaCHC*H*$_3$ signal was observed as a doublet at 2.43 ppm with a $^2J_{HH}$ = 7 Hz. The Ta(C_2H_4) was observed as a multiplet at 1.15 for 4 hydrogen atoms. The characteristic C-H of the ethylidene was observed as a broad singlet at 7.31 ppm, which is in agreement with other early metal alkylidene (PNP) ligand systems.[24] The ^{13}C{^{1}H} NMR spectrum confirms an ethylidene structure with an α-carbon resonance displaying a broad singlet at 223.2 ppm, the ethylidene CH_3 at 30.8 ppm and the C_2H_4 at 19.0 ppm.

We were able to obtain an X-ray quality single crystal of **52** and confirm the solid-state structure by X-ray diffraction methods (Figure 16). The bond distances and angles associated with tantalum's coordination environment are shown in Table 5.

Figure 17 shows the immediate six-coordinate environment. The geometry here is of a distorted octahedral. The greatest distortion is seen in the P-Ta-P angle (147.85(4)°). This is most likely in part due to the chelate effect or the inability of the PNP ligand to accommodate a 180° P-Ta-P angle. It's also possible that the desire for the ethylene complex to be perpendicular in orientation to the Ta(ethylidene) results in this distortion. The Ta=C bond length, 1.909(5) Å, is in agreement with previous structures for a Ta-C double bond.[25,40a,67] The C29-C30 bond length is 1.451(7) which is longer than free C=C bond but falls within inline with other Ta(C_2H_4) systems (1.449(5)).[25,40a,67] The Ta-C bond length for C29 and C30 are 2.210(5) and 2.237(5), respectively. The C28-C27-Ta1 angle is 157.0(4)° which deviates from a linear 180° and there is no evidence by ^{1}H NMR spectroscopy of an agostic interaction with the α-carbon of the ethylidene.

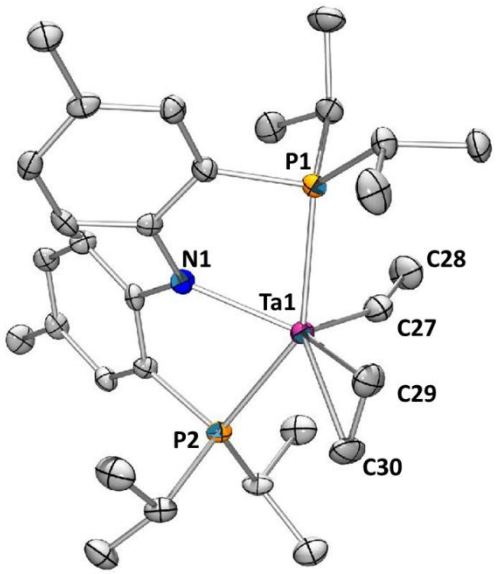

Figure 16. POV-Ray[61] rendition of an Ortep[62] drawing (50% probability ellipsoids) of (PNP)Ta($CHCH_3$)(C_2H_4) (**52**) with hydrogen atoms omitted for clarity.

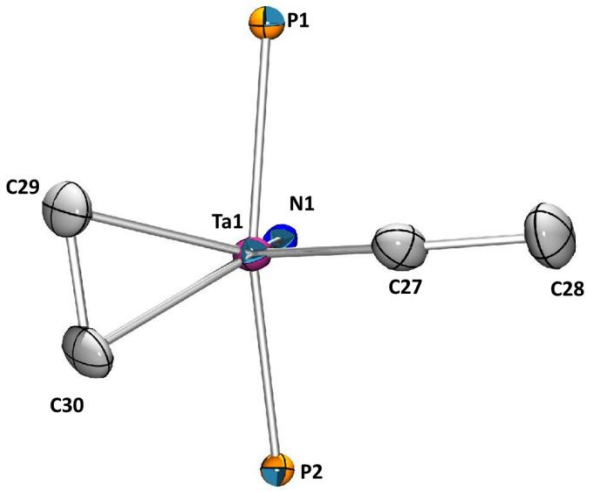

Figure 17. View[61-62] of atoms directly bound to the Ta center displayed for (PNP)Ta($CHCH_3$)(C_2H_4) (**52**).

Table 5. Summary of select bond distances and angles in (PNP)Ta($CHCH_3$)(C_2H_4) (**52**).

	Bond Lengths (Å)		Bond Angles (°)		Bond Angles (°)
P1 – Ta1	2.5650(12)	P1 – Ta1 – N1	74.27(10)	C27 – Ta1 – P1	92.15(15)
P2 – Ta1	2.5461(12)	P2 – Ta1 – N1	74.02(10)	C27 – Ta1 – P2	98.26(16)
N1 – Ta1	2.144(4)	N1 – Ta1 – C29	126.83(18)	C27 – Ta1-C29	110.1(2)
C29 – Ta 1	2.210(5)	N1 – Ta1 – C30	130.09(18)	C27 – Ta1- C30	106.1(2)
C30 – Ta1	2.237(5)	N1 – Ta1 – C27	119.68(19)	C29 – Ta1- C30	38.07(19)
C27 – Ta1	1.909(5)	Ta1 – C27 – C28	157.0(4)	C29 – Ta1 – P2	116.51(14)
C27 – C28	1.513(7)	C29 – Ta1 – P1	87.04(14)	C30 – Ta1- P1	125.09(14)
C29 – C30	1.451(7)	C30 – Ta1 – P2	80.59(14)	P2 – Ta1 – P1	147.85(4)

How **52** is formed has not been fully investigated; but a plausible route of formation is seen in Scheme 22. After successful transmetallation of two fluorine ligands the presence of dioxane aids in the precipitation of MgX_2, allowing for the remaining two fluorine atoms to undergo alkylation. This step is likely extremely fast due to the steric congestion of the four ethyl's on the tantalum center. From here the complex undergoes α-abstraction releasing ethane. With an empty site now on the metal center, β-hydride abstraction can occur to release another equivalent of ethane while forming **52**. A small singlet was observed at 0.81 before workup, however its formation is not confirmed quantitatively.

Scheme 22. Plausible mechanistic route for formation of (PNP)Ta($CHCH_3$)(C_2H_4) (**52**).

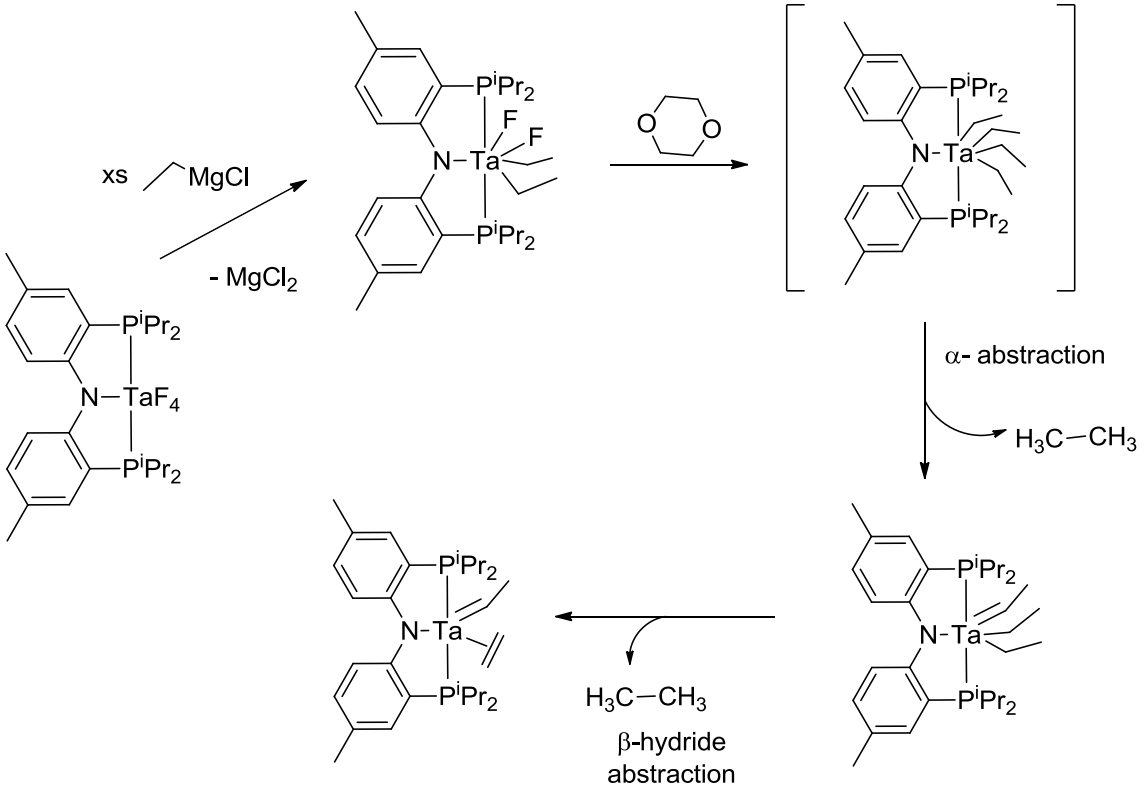

Attempted C-C Bond Cleavage Reactions

Gerber and Ozerov reported the synthesis and characterization of (PNP)Ta($=CH_2$)$_2$ (**53**).[25] If we break **53** down into its empirical composition we see the following fragments: "(PNP)Ta" and "ethylene." Previous examples have shown the ability to break C=C or X=Y bonds (Scheme 23).[68-69] To see if we could synthesize **53** by breaking the ethylene C=C bond a series of reductions were attempted (Scheme 24).

Scheme 23. Rare example of C=C bond cleavage.[68-69]

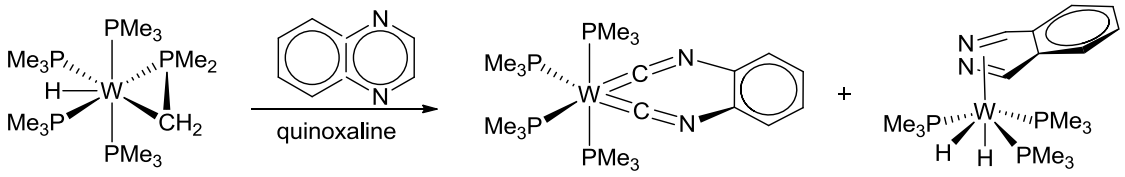

Unfortunately there was little success with isolating one major product during the reductions. When an atmosphere of ethylene was added to a mixture of activated magnesium in ether and **47,** a series of small doublets were observed in ^{31}P NMR spectroscopy after 24 h. Extended reaction time did yield conversion to one major product, the free ligand (PNP)H. Using an alternative reducing agent, such as KC_8 or Li only resulted in decomposition to free (PNP)H ligand. When an atmosphere of ethylene was added to a flask of **47** with Mg(anthracene)·THF_3, a purple solution was observed with a dark black precipitate. After stirring overnight at ambient temperature, the ^{31}P NMR spectrum revealed decomposition to (PNP)H. Repeating and heating at 65 °C the solution resulted in the formation of new complexes as observed by $^{31}P\{^{1}H\}$ NMR spectroscopy. After filtering through Celite and removing all volatiles the major product was still (PNP)H.

Scheme 24. Series of attempted C=C bond cleavage reactions.

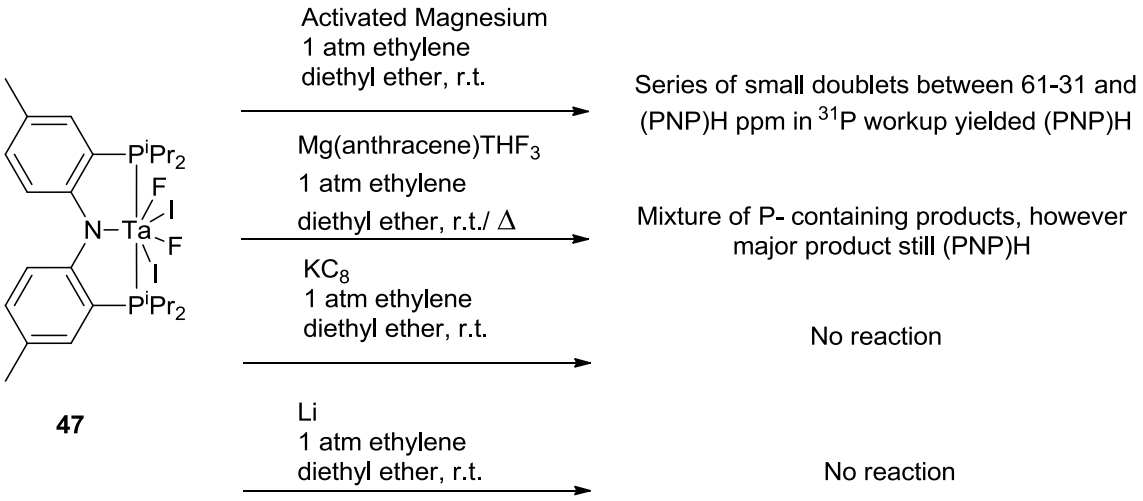

Experimental

General Considerations

Unless specified otherwise, all manipulations were performed under an argon atmosphere using standard Schlenk or glovebox techniques. Dioxane, diethyl ether, tetrahydrofuran and benzene were dried over sodium-benzophenone ketyl, distilled or vacuum transferred and stored over molecular sieves in an Ar-filled glovebox; (PNP)H (**12**) was synthesized according to published procedures,[3] $HfCl_4(OEt_2)_2$ was synthesized in a manner analogous to published procedures[70] and all other chemicals were used as received from commercial vendors. All NMR spectra were recorded on a Varian iNova 300 spectrometer (^{1}H NMR, 299.951 MHz; ^{31}P NMR, 121.425 MHz; ^{13}C NMR, 75.413 MHz), Varian Mercury 300 spectrometer (^{13}C NMR 75.426 MHz), Varian iNova 400 spectrometer (^{1}H NMR, 399.755 MHz; ^{13}C NMR, 100.518 MHz;^{31}P NMR 181.822 MHz), or a Varian iNova NMR 500 (^{1}H NMR, 499.425 MHz/499.683 MHz; ^{13}C NMR, 75.424 MHz/125.580 MHz; ^{31}P NMR, 202.171 MHz) spectrometer. Chemical shifts are reported in δ/ppm. For ^{1}H and ^{13}C NMR spectra, the residual solvent peak was used as an internal reference. ^{31}P NMR spectra were referenced externally using 85% H_3PO_4 at δ 0 ppm. Elemental analysis was performed by CALI Labs, Parsippany, NJ, USA. UV experiments were performed in a Rayonet-type photochemical reactor, which contained 19 light sources at 350 nm. Samples were hung in the center of the reaction chamber for a specified amount of time.

(PNP)$HfCl_3$ (36). (PNP)H (**12**) (4.39 g, 10.2 mmol) was suspended in diethyl ether at −35 °C. In a slow dropwise fashion *n*-butyllithium (4.1 mL of a 2.5 M solution in hexanes, 10.2 mmol) was added to the suspension. The reaction was left to stir for 30 min and then placed under vacuum to remove all volatiles. The oily residue (presumed to contain **23**) was dissolved in toluene. $HfCl_4 \cdot Et_2O$ (4.80 g, 10.2 mmol) was added to the solution. After stirring overnight a deep orange solution was observed with a precipitate (LiCl). The solution was stripped down and CH_2Cl_2 was added and the solution was passed through a plug of Celite. $^{31}P\{^1H\}$ NMR spectroscopic analysis revealed >98% content of **36**. The filtrate was recrystallized from pentane at −35 °C. The collected crystals were washed with cold pentane and dried under vacuum (69% yield). ^1H NMR (C_6D_6): δ 6.94 (dvt, 2H, J_{HH} = 8 Hz, J_{PH} = 8 Hz, Ar–*H*), 6.89 (ddd, 2H, J_{HH} = 2 Hz, J_{HH} = 8 Hz, Ar–*H*), 6.86 (br, 2H, Ar–*H*), 2.36 (m, 2H, *CH*Me_2), 2.12 (m, 2H, *CH*Me_2), 2.09 (s, 6H, Ar–*CH_3*), 1.40 (app. q, 6H, J_{HH} = 7 Hz, CH*Me_2*), 1.21 (dd overlapping with 1.18, 6H, J_{HH} = 7 Hz, CH*Me_2*), 1.18 (dd overlapping with 1.21, 6H, J_{HH} = 7 Hz, CH*Me_2*), 0.93 (app. q, 6H, J_{HH} = 7 Hz, CH*Me_2*). $^1H\{^{31}P\}$ NMR (C_6D_6): δ 6.94 (br d, 2H,J_{HH} = 8 Hz, Ar–*H*), 6.90 (dd, 2H, J_{HH} = 2, 7 Hz, Ar–*H*), 6.86 (br d, 2H, J_{HH} = 2 Hz, Ar–*H*), 2.36 (m, 2H,*CH*Me_2), 2.12 (m, 2H, *CH*Me_2), 2.09 (s, 6H, Ar–*CH_3*), 1.40 (d, 6H, J_{HH} = 7 Hz, CH*Me_2*), 1.21 (d overlapping with 1.18, 6H, J_{HH} = 7 Hz, CH*Me_2*), 1.18 (d overlapping with 1.21, 6H, J_{HH} = 7 Hz, CH*Me_2*), 0.93 (d, 6H,J_{HH} = 7 Hz, CH*Me_2*). $^{31}P\{^1H\}$ NMR (C_6D_6): δ 34.0 (s). $^{13}C\{^1H\}$ ($CDCl_3$): δ 157.9 (vt, J_{PC} = 11 Hz), 133.4 (s), 132.1 (s), 131.4 (s), 121.0 (vt, J_{PC} = 17 Hz), 120.0 (s), 26.4 (br s, *C*HMe_2), 21.7 (vt, J_{PC} = 9 Hz, *C*HMe_2), 21.1 (s, Ar–*Me*), 21.0 (s, CH*Me_2*), 19.1 (s,

CH*Me*$_2$), 18.9 (s, CH*Me*$_2$), 17.6 (s, CH*Me*$_2$). Elem. Anal., Calculated for $C_{26}H_{40}Cl_3HfNP_2$: C, 43.75; H, 5.65; Cl, 14.71. Found, batch 1: C, 43.73; H, 5.62 and batch 2: C, 43.49; H, 5.57; Cl, 14.64.

(PNP)HfMe$_3$ (**37**). **36** (0.31 g, 0.44 mmol) was suspended in 75 mL of toluene. CH_3MgBr (0.44 mL, 3 M solution in diethyl ether, 1.3 mmol) was added dropwise. The orange solution turned lime yellow. 50 μL of dioxane was added to precipitate out the $MgBr_2$ and $MgCl_2$. The reaction was stirred overnight. The volatiles were removed from the solution under vacuum and then approximately 5 mL of isooctane was added to help precipitate magnesium halides. The volatiles were then removed under vacuum and the residue was dissolved in toluene. The solution was passed through a pad of Celite and the volatiles were again removed under vacuum. Approximately 4 mL of pentane was added to dissolve the yellow residue and the flask was placed in the freezer at −35 °C for recrystallization. Yellow crystals of **37** were collected, washed with cold pentane and the solid was placed under vacuum to dry (53% yield). ^{1}H NMR (C_6D_6): δ 6.96 (dd, 2H, J_{HH} = 8 Hz, J_{PH} = 5 Hz, Ar–*H*), 6.92 (br d, 2H, J_{HH} = 8 Hz, Ar–*H*), 6.88 (br d, 2H, J_{HH} = 8 Hz, Ar–*H*), 2.37 (m, 2H, C*H*Me$_2$), 2.21 (m, 2H, C*H*Me$_2$), 2.11 (s, 6H, Ar–*Me*), 1.22 (dd, 6H, J_{HH} = 7 Hz, J_{PH} = 14 Hz, CH*Me*$_2$), 1.13 (app. t overlapping with 1.10, 6H, J_{HH} = 7 Hz, J_{PH} = 17 Hz, CH*Me*$_2$), 1.10 (app. t overlapping with 1.10, 6H, J_{HH} = 7 Hz, J_{PH} = 17 Hz, CH*Me*$_2$), 0.94 (app. t, 6H, J_{HH} = 8 Hz, CH*Me*$_2$), 0.69 (t, 9H, J_{PH} = 4, Hf*Me*$_3$). ^{31}P{^{1}H} NMR (C_6D_6): δ 18.4 (s). ^{31}P{^{1}H} NMR (toluene): δ 17.7. ^{13}C{^{1}H} NMR (C_6D_6): δ 161.0 (d, J_{PC} = 23 Hz), 133.3 (s), 132.7 (s),

122.2 (s), 121.8 (s), 121.7 (d, J_{PC} = 8 Hz), 60.6 (t, J_{PC} = 8 Hz, Hf*Me*$_3$), 25.0 (br s, *C*HMe$_2$), 21.6 (m, *C*HMe$_2$), 21.1 (s, Ar*C*H$_3$), 20.0 (br s, CH*Me*$_2$), 19.6 (br s, CH*Me*$_2$), 18.7 (br s, CH*Me*$_2$), 17.6 (br s, CH*Me*$_2$). Elem. Anal., found(calc) for $C_{29}H_{49}HfNP_2$: C, 53.29(53.27); H, 7.47(7.56).

(PNP)Hf(CH$_2$SiMe$_3$)$_2$Cl (38). (PNP)HfCl$_3$ (**36**) (500 mg, 0.708 mmol) was dissolved in 11 mL of diethyl ether. To this was added 62 μL of dioxane and Me$_3$SiCH$_2$MgCl (1.75 mL, 1.0 M in Et$_2$O, 1.75 mmol). The color of the solution changed from yellow to faint green. The mixture was stirred until no starting material was present by $^{31}P\{^1H\}$ NMR spectroscopy. After that, the solution was passed through a pad of Celite. The filtrate was placed under vacuum to remove all volatiles. Twice, pentane was added to the yellow residue and placed under vacuum to remove volatiles. The product was recrystallized from pentane at −35 °C. The yellow crystalline solid was washed twice with cold pentane and dried under vacuum. (446 mg, 77% yield). ^1H NMR (C_6D_6): δ 6.98 (br dd, 2H, J_{HH} = 2 Hz, J_{PH} = 5 Hz, Ar–*H*), 6.90 (br dd, 2H, J_{HH} = 2 Hz, J_{HH} = 8 Hz, Ar–*H*), 6.79 (dd, 2H, J_{HH} = 8 Hz, J_{PH} = 5 Hz, Ar–*H*), 2.35 (br m, 4H, *CH*Me$_2$), 2.10 (s, 6H, Ar–*CH*$_3$), 1.16 (dd, 12H, J_{HH} = 7 Hz, J_{PH} = 13 Hz CH*Me*$_2$), 1.05 (br, 12H, CH*Me*$_2$), 0.64 (br s, 4H, Hf*CH*$_2$SiMe$_3$), 0.37 (s, 18H, Si*Me*$_3$). $^{31}P\{^1H\}$ NMR (Et$_2$O): δ 11.2 (s).$^{31}P\{^1H\}$ NMR (C_6D_6): δ 12.0 (s). $^{31}P\{^1H\}$ NMR (THF): δ 12.4 (s). $^{13}C\{^1H\}$ NMR (C_6D_6): δ 158.7 (d, J_{PC} = 16 Hz), 133.2 (s), 131.1 (s), 128.3 (additional aromatic signal overlapping with internal standard), 124.6 (d, J_{PC} = 14 Hz), 123.5 (s), 77. 6 (t, J_{PC} = 6 Hz, Hf*C*H$_2$), 24.3 (br s, *C*HMe$_2$), 21.3 (s,

Ar*C*H_3), 20.2 (br s, CH*Me*$_2$), 19.3 (br s, CH*Me*$_2$), 4.5 (s, Si*Me*$_3$). Elem. Anal., found(calc) for $C_{34}H_{62}ClHfNP_2Si_2$: C, 49.88(49.92); H, 7.53(7.65).

Thermolysis of (PNP)HfMe$_3$ (37). was dissolved in C_6D_6, forming a yellow solution, and was placed into a 75 °C oil bath for 48 h, during which time it became a dark reddish brown solution. The $^{31}P\{^1H\}$ NMR spectrum revealed no new resonances. Only the resonance of **12** was observed at 18.2 (s) ppm.

Thermolysis of (PNP)Hf(CH$_2$SiMe$_3$)$_2$Cl (38). (48.0 mg, 0.612 mmol) was dissolved in C_6D_6 in a J-Young NMR tube yielding a yellow solution. The NMR tube was placed into an 80 °C oil bath overnight, during which time it became a dark orange solution. $^{31}P\{^1H\}$ NMR spectrum revealed 80% conversion of **38** and the appearance of a major new product (**39**) displaying an AB system (two doublets at 49.0 ppm and 39.0 ppm, J_{PP} = 70 Hz) and another, lesser product displaying a singlet resonance at 29.4 ppm. In the ^1H NMR spectrum, a new singlet downfield resonance (δ 8.61 ppm) was detected. In the $^{13}C\{^1H\}$ NMR spectrum, a new resonance at 248.2 ppm (br m) was detected. ^1H and ^{13}C NMR spectroscopic analysis also indicated the presence of substantial amount of $SiMe_4$ (0 ppm in both).

Photolysis of (PNP)Hf(CH$_2$SiMe$_3$)$_2$Cl . (PNP)Hf(CH_2SiMe_3)$_2$Cl was dissolved in C_6D_6 and placed into the UV box in increments of ten minutes for a total of 30 minutes. $^{31}P\{^1H\}$ NMR spectrum revealed twelve new signals: δ 48.9, 48.4, 39.0, 38.6, 36.4, 34.2,

29.72, 27.8, 21.6, 12.0, -2.0, -19.0 ppm. However, each time the amount of (PNP)Hf(CH_2SiMe_3)$_2$Cl did not decrease.

Addition of PMe_3 to (PNP)Hf(CH_2SiMe_3)$_2$Cl. (PNP)Hf(CH_2SiMe_3)$_2$Cl (21 mg, 0.0257 mmol) was suspended in 1 mL of C_6D_6. To this suspension was added (2.8 μL 0.0283 mmol) PMe_3 to result in gradual dissolution of (PNP)Hf(CH_2SiMe_3)$_2$Cl. No coordination was observed: $^{31}P\{^1H\}$ NMR (Et_2O): δ 12.1 s, -18 s, -61.8 s. The NMR tube was placed into an oil bath at 35 ºC overnight with no new coordination and then increased to 55 ºC with no new coordination.

Addition of Pyridine to (PNP)Hf(CH_2SiMe_3)$_2$Cl. (PNP)Hf(CH_2SiMe_3)$_2$Cl (21 mg, 0.0234 mmol) was suspended in 1 mL of C_6D_6. To this suspension 2.0 μL of pyridine to result in gradual dissolution of (PNP)Hf(CH_2SiMe_3)$_2$Cl. The color of the solution remained a lime yellow. The mixture showed no coordination. $^{31}P\{^1H\}$ NMR (C_6D_6): δ 11.94 s.

Addition of $Na(Et)_3BH$ to (PNP)Hf(CH_2SiMe_3)$_2$Cl. (PNP)Hf(CH_2SiMe_3)$_2$Cl (15 mg, 0.0183 mmol) was suspended in 1 mL of Et_2O. To this suspension (2.64 μL, 0.0193 mmol) $Na(Et)_3BH$ was added. The color of the solution became a cloudy lime yellow with a white precipitate on the bottom (NaCl). $^{31}P\{^1H\}$ NMR (C_6D_6): δ 21.6, 12.0, -13.0, -19.1. The solution was placed into an oil bath at 55 ºC. No evident coordination had occurred, in fact, the starting material and (PNP)H were still present in a higher

percentage than any new resonance signals. $^{31}P\{^{1}H\}$ NMR (C_6D_6): δ 35.3, 31.5, 29.2, 28.9, 28.7, 23.0, 12.0, -10.4, -13.0, -18.7.

Addition of potassium *t*-butoxide to (PNP)Hf(CH_2SiMe_3)$_2$Cl. (PNP)Hf(CH_2SiMe_3)$_2$Cl (20 mg, 0.0244 mmol) was suspended in 1 mL of C_6D_6. This C_6D_6 had been combined with 1.2 equivalent of potassium *t*-butoxide and filtered through a plug of Celite to remove all inorganic matter. $^{31}P\{^{1}H\}$ NMR (C_6D_6): δ 12.0 s. There was some observance of TMS at 0 ppm by both ^{1}H and ^{13}C NMR spectra, but there was no other change in the spectrum to show the formation of a new hafnium complex.

Addition of mesitylmagnesium bromide to (PNP)Hf(CH_2SiMe_3)$_2$Cl. (PNP)Hf(CH_2SiMe_3)$_2$Cl (20 mg, 0.0244 mmol) was suspended in 1 mL of C_6D_6. 1.0 M mesitylmagnesium bromide in ether (30.6 μL, 0.0244 mmol) was added by syringe. An excess of dioxane was added. $^{31}P\{^{1}H\}$ NMR spectrum revealed only starting material.

Addition of sodium (bistrimethylsilyl)amide. (PNP)Hf(CH_2SiMe_3)$_2$Cl (20 mg, 0.0244 mmol) was suspended in 1 mL of THF. Sodium (bistrimethylsilyl)amide (4.94 mg, 0.0269 mmol) was added to J. Young NMR tube. $^{31}P\{^{1}H\}$ NMR (C_6D_6): δ 12.0 s after 2 h, overnight, and heating overnight.

(PNP)Hf(CH_2SiMe_3)$_2$Me from CH_3Li (40). 38 (16 mg, 0.0183 mmol) was suspended in 1 mL of ether. To this suspension (8.7 μL, 0.0206 mmol) CH_3Li (2.2 M in Et_2O) to

result in gradual dissolution of (PNP)Hf(CH_2SiMe_3)$_2$Cl. The mixture was left to react overnight. The solution was passed through a pad of celite with Et_2O. The filtrate was placed under vacuo to remove volatiles. A yellow oil was collected. $^{31}P\{^1H\}$ NMR (C_6D_6): δ 18 s, 14.1 s, 3.4 s.

Thermolysis of (PNP)Hf(CH_2SiMe_3)$_2$Me (40). Addition of heat by an oil bath at 55 ºC for 2 h $^{31}P\{^1H\}$ NMR (C_6D_6): δ 17.5 s, 14.0 s, 3.4 s, -23.2 s. There was no significant signal observed (4 μL, 0.00947 mmol) MeLi were added to the NMR tube. $^{31}P\{^1H\}$ NMR (C_6D_6): δ 14.1, 3.4, -13.0, -23.2 ppm. The reaction was left in an oil bath at 55 ºC overnight and (PNP)Li was observed by $^{31}P\{^1H\}$ NMR (C_6D_6): δ 18.1 s, 14.0 s, -5.3 m, -19 s.

(PNP)Hf(CH_2SiMe_3)$_2$Me from MeMgBr (40). (PNP)Hf(CH_2SiMe_3)$_2$Cl (15 mg, 0.0183 mmol) was suspended in 1 ml of Et_2O. (21.4 μL, 0.0214 mmol) 3.0 M MeMgBr in diethyl ether was added dropwise. To this suspension 10 μL of dioxane was added. The reaction was left to react. $^{31}P\{^1H\}$ NMR (C_6D_6): δ 3.4 s, -12.9 s. ^1H NMR (C_6D_6): δ 7.03 (d, 2H, J_{HH} = 4 Hz, Ar–*H*), 6.94 (br d, 2H, J_{HH} = 8 Hz, Ar–*H*), 6.73 (dd, 2H, J_{HH} = 8 Hz, J_{PH} = 4 Hz, Ar–*H*), 2.20 (br s, 4H, *CH*Me_2), 2.14 (s, 6H, Ar–*CH*$_3$), 1.10 (dd, 12H, J_{HH} = 7 Hz, J_{PH} = 13 Hz CH*Me*$_2$), 1.05 (br, 12H, CH*Me*$_2$), 0.83 (t, J_{HH} = 3 Hz, 3H, HfC*H*$_3$), 0.61 (br s, 4H, Hf*CH*$_2$SiMe$_3$), 0.33 (s, 18H, Si*Me*$_3$).

Thermolysis of (PNP)Hf(CH_2SiMe_3)$_2$Me (40). When the J. Young NMR tube was heated at 70 C overnight a $^{31}P\{^1H\}$ NMR revealed: δ 14.0 br s, 3.4 s, -14 s. Heating overnight again yielded δ 21.5 s, 14.1 s, 3.4 s, -14.0 s, -19.2 s by $^{31}P\{^1H\}$ NMR. Heating again overnight yielded δ 46.6 & 37.1 (d, $^2J_{PP}$ = 72 Hz), 21.7 (s), 14.1 (s), 3.4 (s), 1.5 (s), -13.9 (s), -19.2 (s). Heating again to see if conversion to the two doublets would happen resulted with the major product still be the 3.4 s for (PNP)Hf(CH_2SiMe_3)$_2$Me in addition to δ 46.6 d & 37.1 (d, $^2J_{PP}$ = 72 Hz), 21.7 (s), 1.5 (s), -13.9 (s), -19.2 (s). The ^{1}H NMR spectrum showed an increase in a signal at 0.001 ppm for free $SiMe_4$; however the integrations for a free molecule of TMS was not accurate.

(PNP)Hf(CH_2SiMe_3)$_2$Br (41). (15.0 mg, 0.0183 mmol) **38** was dissolved in ether in a J. Young NMR tube. $MgBr_2$ (8.0 mg, 0.0275 mmol) and dioxane were added to the NMR tube. $^{31}P\{^1H\}$ NMR (Et_2O): δ 14.5 s.

(PNP)Hf(CH_2SiMe_3)$_2$(C_6H_5) (42). (PNP)Hf(CH_2SiMe_3)$_2$Cl (331 mg, 0.405 mmol) was suspended in toluene. 1.8 M phenyl lithium in dibutyl ether (247.6 mL, 0.446 mmol) was added by syringe. The reaction was left to react overnight. The solution was placed under vacuum. The residue was extracted with pentane and passed through a plug of Celite. The solution was concentrated and recrystallized. Yield: 166.6 mg (50 %) $^{31}P\{^1H\}$ NMR (C_6D_6): δ -0.65 s. ^{1}H NMR (C_6D_6): δ 7.89 (d, J_{HH} = 6 Hz, Ar–*H*), 7.34 (t, J_{HH} = 8 Hz, Ar–*H*), 7.17 (d, J_{HH} = 7 Hz, Ar–*H*), 7.05 (d, J_{HH} = 4 Hz, Ar–*H*), 6.99 (dd, J_{PH} = 8 Hz, J_{HH} = 2 Hz, Ar–*H*), 6.90 (dd, J_{PH} = 8 Hz, J_{HH} = 4 Hz, Ar–*H*), 2.13 (s,

6H, Ar–CH_3), 2.06 (m, 4H, CHMe$_2$), 1.04 (br s, 24H, CHMe_2), 0.30 (s, 4H, HfCH_2SiMe$_3$), 0.22 (s, 18H, SiMe_3).

Thermolysis of (PNP)Hf(CH_2SiMe_3)$_2$(C_6H_5) (42). (PNP)Hf(CH_2SiMe_3)$_2$(C_6H_5) (166 mg, 0.193 mmol) was added to a J. Young NMR tube and dissolved in C_6D_6. The tube was placed in an oil bath at 80 °C for 11 days. $^{31}P\{^1H\}$ NMR (C_6D_6): δ 33.0 & 27.5 (d, $^2J_{PP}$ = 32 Hz).

(PNP)Hf(CH_2SiMe_3)$_2$(OTf) (43). 38 (122 mg, 0.149 mmol) was dissolved in toluene. (135 μL, 0.747 mmol) TMSOTf was added by syringe. After stirring overnight only 70% of **38** had converted to **43**. To drive this reaction further the solution was stripped down to remove the TMSCl being formed and additional (135 μL, 0.747 mmol) TMSOTf was added and the reaction was left to stir. $^{31}P\{^1H\}$ NMR spectrum revealed > 90% conversion of the starting material, **43**. Removing all solvent and then passing through a plug of celite with pentane the filtrate was concentrated. X-ray quality crystals were obtained. $^{31}P\{^1H\}$ NMR (C_6D_6): δ 14.4 s .^{19}F NMR (C_6D_6): δ -76.6 s. ^{1}H NMR (C_6D_6): δ 6.97 (br d, 2H, J_{HH} = 8 Hz, Ar–H), 6.89 (br d, 2H, J_{HH} = 8 Hz, Ar–H), 6.69 (dd, 2H, J_{PH} = 8 Hz, J_{HH} = 4 Hz, Ar–H), 2.37 (m, 4H, CHMe$_2$), 2.11 (s, 6H, Ar–CH_3), 1.14 (dd, 12H, J_{HH} = 7 Hz, J_{PH} = 14 Hz, CHMe_2), 1.01 (dd, 12H, J_{HH} = 7 Hz, J_{PH} = 14 Hz, CHMe_2), 0.24 (s, 18H, SiMe_3), 0.21 (s, 4H, HfCH_2SiMe$_3$).

(PNP)HfMe$_2$(NHC$_6$H$_4$F) (44). (PNP)HfMe$_3$ (300 mg, 0.469 mmol) was suspended in 3 mL of E$_2$O. To this suspension (44.1 μL, 0.469 mmol) of fluoroaniline was added dropwise. After reacting overnight a new P-containing signal was observed by ^{31}P{^{1}H} NMR (C$_6$D$_6$): δ 29.3 s and ^{19}F (C$_6$D$_6$): δ -128.3 (t, J_{CF} = 282 Hz). Starting material was present as well as a resonance at -19.7 ppm in ^{31}P{^{1}H} NMR. Attempts at recrystallization were unsuccessful for isolating pure product.

(PNP)TaF$_4$ (45). Dissolved (1.5146 g, 3.846 mmol) (PNP)H in Et$_2$O in a 250 mL flask. (1.33 mL, 3.65 mmol) n-butyl lithium solution added by syringe. Solution turned from clear to yellow. ^{31}P{^{1}H} NMR showed < 1% (PNP)H. (0.978 g, 3.54 mmol) TaF$_5$ added to the suspension. An immediate white smoke was observed as the solution turned red. The reaction was left to stir overnight. Upon arrival the orange solution was stripped down to remove all volatiles. The mixture was then dissolved in CH$_2$Cl$_2$ and filtered a plug of Celite in a "C" frit. The filtrate was then placed under vacuum. The dried solid was washed three times with diethyl ether and three times with pentane. Final NMR revealed < 8% (PNP)H. Yield: 2.1115 g (87.5%). ^{31}P{^{1}H} NMR (C$_6$D$_6$): δ 47.9 (quintet, J_{PF} = 58 Hz). ^{19}F NMR (C$_6$D$_6$): δ 71.8 (br s). ^{1}H NMR (C$_6$D$_6$): δ 6.86 (br s, 4H Ar-*H*), 6.81 (s, 2H, Ar-*H*), 2.50 (septet, 2H, C*H*Me$_2$) 2.18 (m, 2H, C*H*Me$_2$), 2.08 (s, 6H, ArC*H*$_3$), 1.33 (dd, 6H, J_{HH} = 7 Hz, J_{PH} = 15 Hz, HC*Me$_2$*), 1.23 (m, 12H, HC*Me$_2$*), 0.902 (dd, 6H, J_{HH} = 7 Hz, J_{PH} = 11 Hz, HC*Me$_2$*). ^{13}C{^{1}H} NMR (CD$_2$Cl$_2$): δ 162.8 (vt, J_{CN} = 13 Hz), 133.5, 132.4, 131.4, 121.2, 119.2 (vt, J_{PC} = 20 Hz), 25.6 (vt, J_{PC} = 7 Hz,

*C*HMe$_2$), 21.7 (vt, J_{PC} = 10 Hz, *C*HMe$_2$), 20.8 (s, CH*Me$_2$*), 18.5 (s, CH*Me$_2$*), 18.0 (s, CH*Me$_2$*), 17.4 (s, CH*Me$_2$*), 17.1 (s, CH*Me$_2$*).

(PNP)TaF$_3$I (46). (PNP)TaF$_4$ (20.0 mg, 0.0292 mmol) was dissolved in C_6D_6 in a J. Young NMR tube. 1 equivalent of iodotrimethylsilane (4.15 μL, 0.0292 mmol) was added by syringe. After letting the reaction sit for 40 min: $^{31}P\{^1H\}$ NMR (C_6D_6): δ 56.6 (q, J_{PF} = 43 Hz) and (PNP)H. ^{19}F NMR (C_6D_6): δ 104.3 (br s).

(PNP)TaF$_2$I$_2$ (47). (PNP)TaF$_4$ (300.0 mg, 0.438 mmol) was dissolved in toluene. (17.0 μL, 1.75 mmol) iodotrimethylsilane was added by syringe. The solution turned from orange to deep red. After 7 h complete conversion. Removed volatiles, washed solid with pentane to remove (PNP)H. Dried solid and the recrystallized from fluorobenzene. Yield: 281.5 mg (71%). ^{19}F NMR (C_6D_6): δ 145 (t, J_{PF} = 13 Hz). $^{31}P\{^1H\}$ NMR (C_6D_6): δ 61.5 (t, J_{PF} = 31 Hz). ^1H NMR (C_6D_6): δ 6.98 (br s, 2H, Ar-*H*), 6.80 (d, 2H, J_{HH} = 8 Hz, Ar-*H*), 6.57 (d, 2H, J_{HH} = 8 Hz, Ar-*H*), 3.23 (m, 2H, C*H*Me$_2$), 2.80 (m, 2H, C*H*Me$_2$), 2.04 (s, 6H, Ar-C*H$_3$*), 1.46 (app q, 6H, J_{HH} = 7 Hz, CH*Me$_2$*), 1.25 (br d, 12, J_{HH} = 4H, CH*Me$_2$*), 1.04 (app q, 6H, J_{HH} = Hz, CH*Me$_2$*).

(PNP)TaF$_3$Cl (48). (PNP)TaF$_4$ (20.0 mg, 0.0292 mmol) was dissolved in C_6D_6 in a J. Young NMR tube. (15.4 μL, 0.117 mmol) chlorotrimethylsilane was added by syringe. Reaction after 1 h shows 87% (PNP)TaF$_4$, 7% (PNP)TaF$_3$Cl and 6% (PNP)H by $^{31}P\{^1H\}$ NMR. ^{19}F NMR (C_6D_6): δ 93.8 (br s). $^{31}P\{^1H\}$ NMR (C_6D_6): δ 54.6 (q, J_{PF} = 46 Hz).

(PNP)TaF_2Cl_2 (49) + excess chlorotrimethylsilane. Adding additional (15.4 μL, 0.117 mmol) chlorotrimethylsilane revealed only a 17% yield in desired product, 77% (PNP)TaF_4 and 6% (PNP)H by $^{31}P\{^1H\}$ NMR spectroscopy after reacting overnight. Leaving over 48 h revealed two new signals and a loss of the original (PNP)H observed by the $^{31}P\{^1H\}$ NMR spectrum. $^{31}P\{^1H\}$ NMR (C_6D_6): δ 74.2 s, 61.4 (t, J_{PF} = 33 Hz). ^{19}F NMR (C_6D_6): δ 122.1 (br s), 110.8 (t, J_{PF} = 29 Hz). Believe sample was oxidized or that water got into the NMR tube over the weekend.

(PNP)TaF_2ICl (50). (PNP)TaF_4 (20.0 mg, 0.0292 mmol) was dissolved in C_6D_6 in a J. Young NMR tube. 1 equivalent of iodotrimethylsilane (4.15 μL, 0.0292 mmol), 1 equivalent of chlorotrimethylsilane (3.70 μL, 0.0292 mmol) was added by syringe. After letting the reaction sit for 12 h one product was observed. $^{31}P\{^1H\}$ NMR (C_6D_6): δ 61.5 (t, J_{PF} = 31 Hz) and (PNP)H. ^{19}F NMR (C_6D_6): δ 144.9 (t, J_{PF} = 30 Hz).

(PNP)TaF_4 + reducing agent + substrate studies. (PNP)TaF_2I_2 (116.1 mg, 0.129 mmol) and activated magnesium (27.1 mg, 1.11 mmol) was added to a flask. Ether was added to dissolve the solid. The flask was brought out and degassed. Ethylene (1 atm) was added and the reaction was allowed to stir overnight. $^{31}P\{^1H\}$ NMR spectrum revealed decomposition to (PNP)H and the ^{19}F NMR spectrum was silent.

(PNP)TaF_2I_2 (60.0 mg, 0.0666 mmol) and Mg(anthracene)THF_3 (71.0 mg, 0.170 mmol) was dissolved in a Teflon flask with ether. The flask was then degassed and 1 atm of

ethylene was added. The solution became a brown color with a black precipitate. After stirring overnight the $^{31}P\{^{1}H\}$ NMR spectrum revealed (PNP)H. Allowing the flask to stir overnight again showed a mixture of products between 43 – 27 ppm. Stirring longer did not see any full conversion, just further decomposition to (PNP)H. Added methanol to see how many products were being formed. The ^{19}F NMR spectrum did not reveal any significant signals, however the base line was rather noisy.

(PNP)TaF_2I_2 (60.0 mg, 0.0666 mmol) and KC_8 (22.5 mg, 0.166 mmol) was dissolved in a Teflon flask with toluene. The flask was then degassed and 1 atm of ethylene was added. The solution was a deep purple color with a black precipitate. After stirring overnight the $^{31}P\{^{1}H\}$ NMR spectrum revealed decomposition to (PNP)H. The flask was allowed to stir longer (overnight) and was placed into an oil bath at 65 °C. Added methanol to see how many products were being formed. Results revealed (PNP)H as the major product.

(PNP)TaF_2I_2 (65.0 mg, 0.0721 mmol) and Li granules (7.0 mg, 1.01 mmol) was added to a Teflon flask with ether. The flask was then degassed and 1 atm of ethylene was added. After stirring overnight the $^{31}P\{^{1}H\}$ NMR spectrum revealed starting material and (PNP)H. Allowing to react another 12 h revealed same starting material and (PNP)H signals and the ^{19}F NMR spectrum was silent.

Equivalent ratio study: (20.0 mg, 0.0292 mmol) (PNP)TaF_4 dissolved in a J. Young NMR tube with THF. 2.0 M ethyl magnesium chloride (14.6 μL, 0.0292 mmol; 29.2 μL, 0.0584 mmol; 43.7 μL, 0.0876 mmol; 58.0 μL, 0.117 mmol) was added by syringe. **1 equiv**: $^{31}P\{^1H\}$ NMR (Et_2O): δ 47.9 (quintet, J_{PF} = 102 Hz), 37.7 (t, J_{PF} = 14 Hz), -12.0 (s, free (PNP)H). ^{19}F NMR (Et_2O): δ 71.8 (br s), 57.4 (t, J_{PF} = 14 Hz). **2 equiv**: $^{31}P\{^1H\}$ NMR (Et_2O): δ 51.0 (br s), 47.9 (quintet, J_{PF} = 102 Hz), 37.7 (t, J_{PF} = 14 Hz), 34.9 (d, J_{PF} = 60 Hz), 30.6 (d, J_{PP} = 60 Hz), -11.9 (s), -18.6 (s). ^{19}F NMR (Et_2O): δ 71.8 (br s), 57.4 (t, J_{PF} = 14 Hz), 49.8 (s). **3 equiv**: $^{31}P\{^1H\}$ NMR (Et_2O): δ 37.7 (t, J_{PF} = 14 Hz), -16.5 (s), -18.6 (s). ^{19}F NMR (Et_2O): δ 57.4 (t, J_{PF} = 14 Hz). **4 equiv**: $^{31}P\{^1H\}$ NMR (Et_2O): δ 37.7 (t, J_{PF} = 14 Hz), -16.5 (s). ^{19}F NMR (Et_2O): δ 57.4 (t, J_{PF} = 14 Hz). **Excess amount (>8 equiv)**: $^{31}P\{^1H\}$ NMR (Et_2O): δ 37.7 (t, J_{PF} = 14 Hz), -16.5 (s). ^{19}F NMR (Et_2O): δ 57.4 (t, J_{PF} = 14 Hz).

Addition of dioxane. An excess amount of dioxane was added to the equivalent J. Young NMR tubes. After sitting overnight $^{31}P\{^1H\}$ NMR and ^{19}F NMR spectra revealed the following: **2 equiv**: $^{31}P\{^1H\}$ NMR (Et_2O): δ 37.7 (t, J_{PF} = 14 Hz), 37.1 (d, J_{PP} = 11 Hz), 36.6 (d, J_{PP} = 12 Hz), -13.0 s. ^{19}F NMR (Et_2O): δ 71.8 (br s), 57.6 (s), 57.4 (t, J_{PF} =14 Hz). **3 equiv**: $^{31}P\{^1H\}$ NMR (Et_2O): δ 62.1 (d, J_{PP} = 52 Hz), 59.8 (d, J_{PP} = 59.8 Hz), 37.7 (t, J_{PF} = 14 Hz), -18.6 s. ^{19}F NMR (Et_2O): δ 57.4 (t, J_{PF} = 14 Hz) ppm. **4 equiv**: $^{31}P\{^1H\}$ NMR (Et_2O): δ 62.1 (d, J_{PP} = 52 Hz), 59.8 (d, J_{PP} = 52 Hz), 37.7 (t, J_{PF} = 14 Hz), -16.5 (s), -18.6 (s). ^{19}F NMR (Et_2O): δ 57.4 (t, J_{PF} = 14 Hz). **Excess amount (>8**

equiv): $^{31}P\{^{1}H\}$ NMR (Et_2O): δ 62.1 (d, J_{PP} = 52 Hz), 59.8 (d, J_{PP} = 59.8 Hz), 37.7 (t, J_{PF} = 14 Hz), -16.5 (s), -18.6 (s). ^{19}F NMR (Et_2O): δ 57.4 (t, J_{PF} = 14 Hz).

(PNP)Ta(CH_2CH_3)$_2F_2$ (51). (PNP)TaF_4 (96.0 mg, 0.140 mmol), 2.0 M ethyl magnesium chloride (280 μL, 0.560 mmol) and dixoane (80 μL, 0.945 mmol) was dissolved in a flask with toluene. After stirring overnight the sample was filtered through a plug of Celite, volatiles removed and dissolved in C_6D_6 (sample not isolated). ^{1}H NMR (C_6D_6): δ 7.47 (dvt, 2H, Ar-*H*), 7.02 (br d, 2H, J_{HH} = 3 Hz, Ar-*H*), 6.91 (dd, 2H, J_{HH} = 2 J_{PH} = 8 Hz, Ar-*H*), 2.63 (m, 2H, C*H*Me_2), 2.47 (m, 2H, C*H*Me_2), 2.17 (s, 6H, Ar-CH_3), 2.14 (q, 2H, J_{HH} = 4Hz, TaC$H_2$$CH_3$), 2.09 (q, 2H, J_{HH} = 4Hz, TaC$H_2$$CH_3$), 1.38 (app. q, 6H, J_{HH} = 7, J_{PH} = 15 Hz, CHMe_2), 1.21 (app. q, 6H, J_{HH} = 7, J_{PH} = 15 Hz, CHMe_2), 1.05 (app. q, 6H, J_{HH} = 7, J_{PH} = 15 Hz, CHMe_2), 0.99 (app. q, 6H, J_{HH} = 7, J_{PH} = 15 Hz, CHMe_2), 0.91 and 0.90 (overlapping triplets, 6H, $TaCH_2C$$H_3$). $^{31}P\{^{1}H\}$ NMR (C_6D_6): δ 37.3 (t, J_{PF} = 14 Hz). ^{19}F NMR (C_6D_6): δ 57.4 (t, J_{PF} =14 Hz).

(PNP)Ta(C_2H_4)$CHCH_3$ (52). (PNP)TaF_4 (22.0 mg, 0.0321 mmol), 2.0 M ethyl magnesium chloride (58 μL, 0.128 mmol) and dixoane (20 μL, 0.225 mmol) was dissolved in a flask with THF. After stirring overnight the $^{31}P\{^{1}H\}$ NMR spectrum revealed: 62.2 and 60.0 d ($^{2}J_{PP}$ = 52 Hz), 37.6 (t, J_{PF} = 14 Hz), -16.4 (s), -18.5 (s). Sample was placed under vacuum, extracted with fluorobenzene and filtered through a plug of Celite. Recrystallization from fluorobenzene yielded X-ray quality crystals: 0.053 g (57% yield) X-ray Diffraction: OZ307. $^{1}H\{^{31}P\}$ NMR (C_6D_6): δ 7.31 (br s,

Ta=C*H*CH_3), 7.11 (d, 1H, J_{HH} = 8 Hz, Ar-*H*), 7.01 (d, 1H, J_{HH} = 6 Hz, Ar-*H*), 7.00 (d, 1H, J_{HH} = 8 Hz, Ar-*H*), 6.95 (d, 1H, J_{HH} = 6 Hz, Ar-*H*), 6.84 (d, 1H, J_{HH} = 8 Hz, Ar-*H*), 6.74 (d, 1H, J_{HH} = 8 Hz, Ar-*H*), 2.71 (m, 1H, C*H*Me_2), 2.56 (m, 1H, C*H*Me_2), 2.43 (d, 3H, J_{HH} = 7 Hz, Ta=CHC*H*$_3$), 2.34 (m, 1H, C*H*Me_2), 2.24 (m, 1H, C*H*Me_2), 2.13 (s, 3H, Ar-C*H*$_3$), 2.11 (s, 3H, Ar-C*H*$_3$), 1.45 (d, 3H, J_{HH} = 7 Hz, CH*Me*$_2$), 1.32 (d, 3H, J_{HH} = 7 Hz, CH*Me*$_2$), 1.22 (d, 6H, J_{HH} = 7 Hz, CH*Me*$_2$), 1.15 (m, 4H, Ta(C_2*H*$_4$)), 1.13 (d, 3H, J_{HH} = 7 Hz, CH*Me*$_2$), 1.02 (d, 3H, J_{HH} = 7 Hz, CH*Me*$_2$), 0.98 (d, 3H, J_{HH} = 7 Hz, CH*Me*$_2$), 0.65 (d, 3H, J_{HH} = 7 Hz, CH*Me*$_2$), (impurities include: toluene, grease, pentane, small signals at: 0.43 m, 0.26 m, 0.10 q unidentified, but observed as impurities in the 2.0 M ethyl magnesium chloride). $^{31}P\{^1H\}$ NMR (C_6D_6): δ 62.0 and 59.6 (d, $^2J_{PP}$ = 52 Hz). $^{13}C\{^1H\}$ NMR (C_6D_6): δ 223.2 (br s, Ta=*C*H), 162.3 (d, C-N), 162.1 (d, C-N), 159.9 (d, Ar), 159.7 (d, Ar), 132.3 (d, Ar), 132.1 (d, Ar), 128.5 (d-overlapping with benzene, Ar), 126.2 (d, Ar), 122.3 (d, Ar), 121.4 (d, Ar), 120.0 (d, Ar), 117.2 (d, Ar), 30.8 (s, TaCH_2*C*H_3), 27.8 (d, *C*HMe_2), 25.1 (d, *C*HMe_2), 24.3 (d, *C*HMe_2), 22.0 (d, *C*HMe_2), 21.4 (d, CH*Me*$_2$), 20.7 (d, CH*Me*$_2$), 20.6 (d, *C*HMe_2), 19 (s, Ta(*C*$_2$H$_4$)), 18.6 (d, CH*Me*$_2$), 18.2 (d, CH*Me*$_2$), 18.1 (d, CH*Me*$_2$), 17.2 (d, CH*Me*$_2$), 16.4 (d, CH*Me*$_2$) (small impurities of pentane, toluene, grease).

CHAPTER III

A REDUCTIVE ELIMINATION STUDY: UNTIED VS TIED PNP LIGANDS

Reductive Elimination / Oxidative Addition

The 2010 Nobel Prize in Chemistry was awarded for the development of palladium-catalyzed cross-coupling reactions. At the heart of these cross-coupling reactions is carbon-carbon (C-C) reductive elimination. Despite the importance of this bond forming step, little is known about the kinetics of C-C reductive elimination.[35] Reductive elimination is a type of organometallic reaction in which a covalent X-Y bond is formed as X and Y are extruded from the metal center, M, decreasing the coordination number, oxidation state and electron count of the metal by two units (Scheme 25).[28]

Scheme 25. Reductive elimination and oxidative addition.

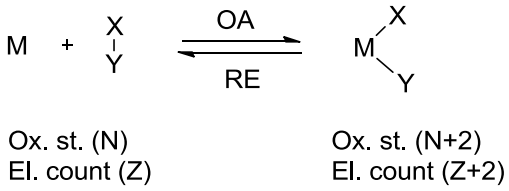

The opposite of reductive elimination is oxidative addition. Here, a metal center is inserted into a covalent bond, X-Y. The X-Y bond is cleaved and new M-X and M-Y bonds are formed, increasing the coordination number, oxidation state and electron count of the metal by two units (Scheme 25). For oxidative addition to occur, the metal center must be unsaturated and have two energetically accessible oxidation states. According to

the principle of microscopic reversibility, both oxidative addition and reductive elimination will follow the same lowest energy pathway for a given system, so information about one mechanism will directly contribute to understanding of the other.[28]

Carbon-carbon reductive elimination from d^6 Pt^{IV} centers have been studied in detail and have been shown to proceed via five-coordinate intermediates.[8,71] In complexes of the type *fac*-[$(L_2)PtMe_3X$], ligand dissociation first occurs from the six-coordinate Pt prior to the actual reductive coupling from a five-coordinate intermediate (Scheme 26).[71-72]

Scheme 26. An example of ligand dissociation prior to reductive elimination.

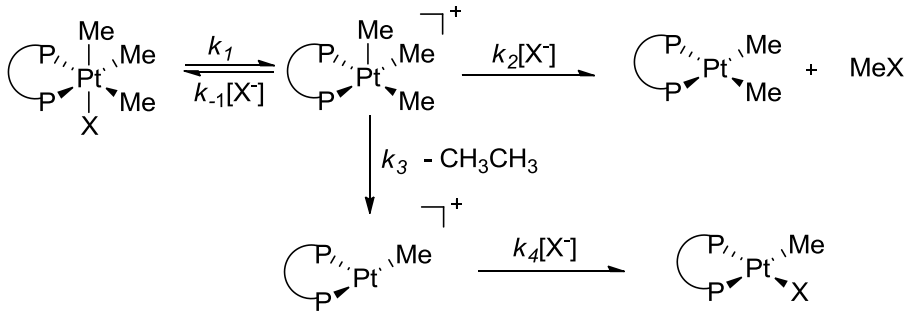

A theoretical study exploring the kinetics for reductive elimination in a Pd(II)/Pd(0) system highlighted the impact sterics can have on the rate of C-C reductive elimination. The use of bulkier phosphines resulted in faster rates for C-C reductive elimination (L = PCy_3 > PPh_3 > PH_3 > PMe_3) in three-coordinate Pd^{II} complexes (Scheme 27).[73] The cone angles for these phosphines are in agreement with this trend revealing that the larger the cone angle the faster the rate for C-C reductive elimination in the Pd(II)/Pd(0) system.[73]

Scheme 27. Reductive elimination from a Pd(II)/Pd(0) three-coordinate system.

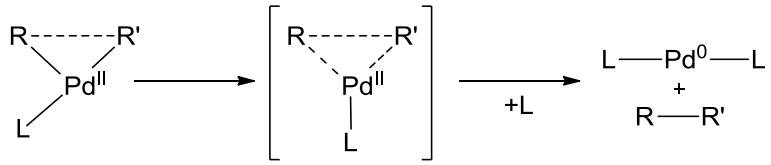

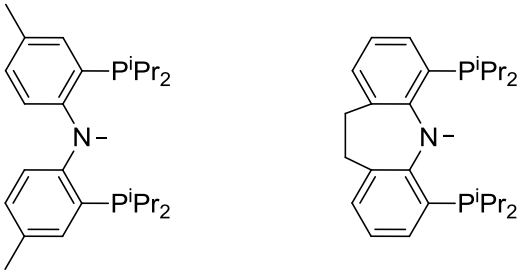

^{Me}(PNP)
53

TH(PNP)
54

Figure 18. Untied ^{Me}(PNP) and tied TH(PNP) ligands.

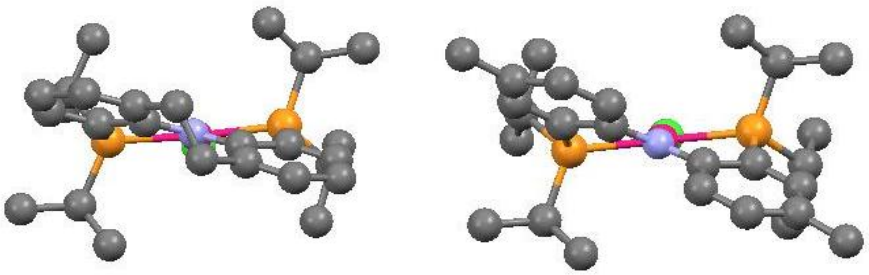

Figure 19. Untied ^{Me}(PNP)PdCl (left) and tied TH(PNP)PdCl (right) complexes.

Ozerov et al. have previously reported on the synthesis of a tied PNP ligand,

TH(PNP)Me, (Figure 18) and its successful installation on metal centers, M = Rh, Ir, Pd.[19] When palladium derivatives of both the tied and untied ligand were compared, they found the tied ligand provided a more rigid and bulkier environment at the metal center (Figure 19).[19] Coordinating rhodium to both ligands yielded insight into subsequent N-C cleavage. The rigidity of the tied TH(PNP) ligand (**54**), a result of the –CH_2CH_2– linker, accelerated N-C cleavage in the synthesis of TH(PNP)RhMeCl (**55**) in comparison to ^{Me}(PNP)RhMeCl (**56**).[19] Additionally, the [Rh]H_2 derivatives of both ligands are active as alkyne dimerization catalysts.[8] However, despite their electronically similar structures, the tied ligand was found to be more active and more selective in catalyzing the formation of trans-enynes. The high selectivity observed with the TH(PNP)RhH_2 catalyst was unprecedented for enyne formation reactions which are otherwise complicated by reduced chemo- and regioselectivity.[8] While the mechanism for this catalyst has not been fully investigated, it has been postulated that the bulky nature of the tied ligand is a critical factor.

While **53** and **54** are electronically quite similar, each has one alkyl substituent per aromatic ring and they both have the same substituents on phosphorus. Since the tied ligand serves as a bulkier PNP scaffold, it was hypothesized that the tied ligand, TH(PNP), could enforce additional steric congestion at the metal center resulting in an increased rate for C-C reductive elimination. A series of C-C reductive elimination studies for both the untied and tied ligand were investigated. To provide an additional spectroscopic handle, the desired five-coordinate Rh^{III} precursor will have fluorine atoms incorporated into the R group. This was accomplished by the use of *p*-

trifluoromethylphenyl chloride, which provided the ability to track the amount of product consumed and the amount of byproduct formed by ^{19}F NMR spectroscopy. To ensure accurate ratios, an internal standard of 1-fluorooctane was used.

Synthesis of the Untied PNP Ligand

To compare the effects of the different ligands on the process of reductive elimination, the untied PNP ligand was synthesized according to published procedures.[18-19] From there, oxidative addition over the N-C bond resulted in the formation of ^{Me}(PNP)RhMeCl (**56**).[19] Two routes are possible for the synthesis of the five-coordinate Rh^{III} oxidative addition precursor (Scheme 28).

The first method requires the synthesis of (PNP)RhH_2 (**57**), which when stirred with tert-butylethylene results in the formation of the (PNP)Rh(TBE) adduct (**58**).[8] When this solid was isolated and then stirred in a solution of *p*-trifluoromethylphenyl chloride, complete conversion to the desired precursor (PNP)Rh($C_6H_4CF_3$)(Cl) (**59**) was observed after 7 h. The alternative synthesis involved adding an organolithium reagent such as PhLi to release the toluene byproduct via reductive elimination before oxidatively adding *p*-trifluoromethylphenyl chloride at room temperature. The solution characterization of **59** was in agreement with previously reported data.[8] A singlet was observed in the ^{19}F NMR spectrum at δ -62.3 corresponding to the CF_3 group. In the $^{31}P\{^1H\}$ NMR spectrum, a doublet was observed at δ 38.0 with J_{Rh-P} = 105 Hz.

Scheme 28. Synthesis of untied ^{Me}(PNP)Rh($C_6H_4CF_3$)Cl, **59**.

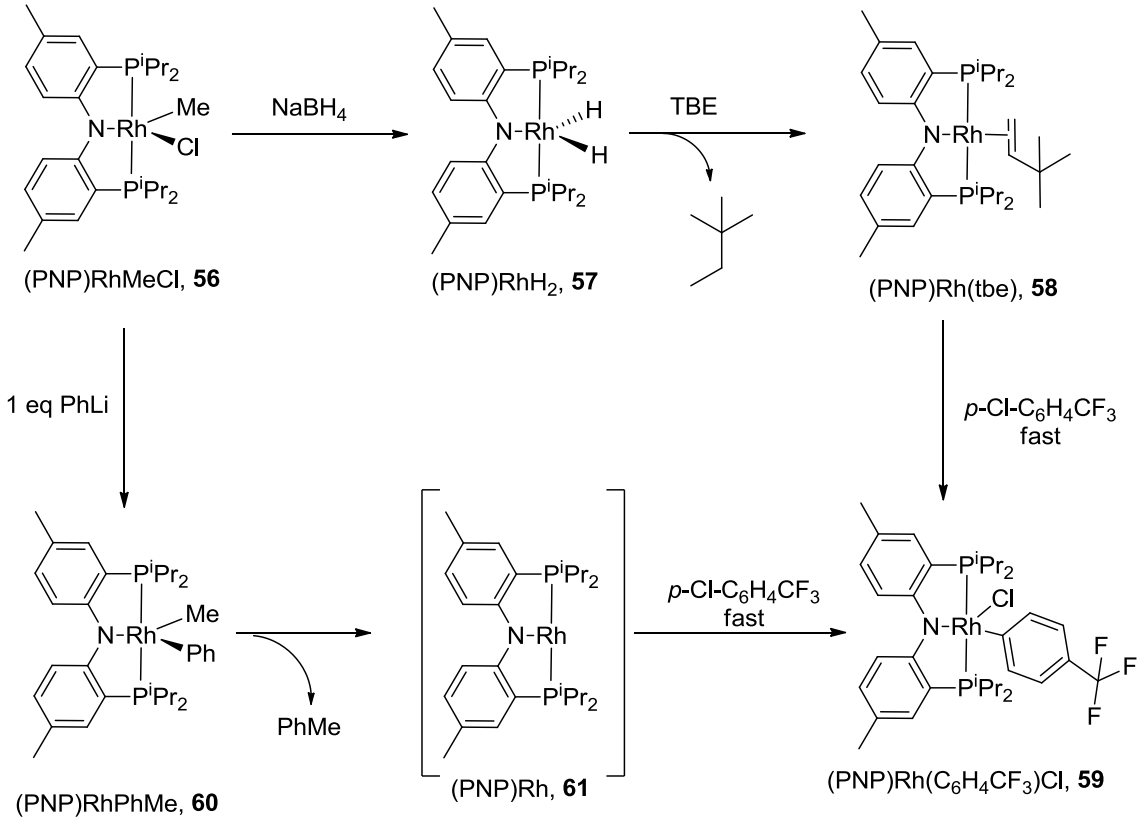

Synthesis of the Tied PNP Ligand

Ozerov et al. previously reported on the synthesis of the tied TH(PNP)Me ligand (**66**).[9] The synthesis is lengthy, and a "one-pot like" reaction has been developed to simplify its production (Scheme 29). Without the need for recrystallization after each step, the overall ligand can be successfully synthesized in a shorter amount of time.

Scheme 29. Simplified synthesis of TH(PNP)Me (**66**).

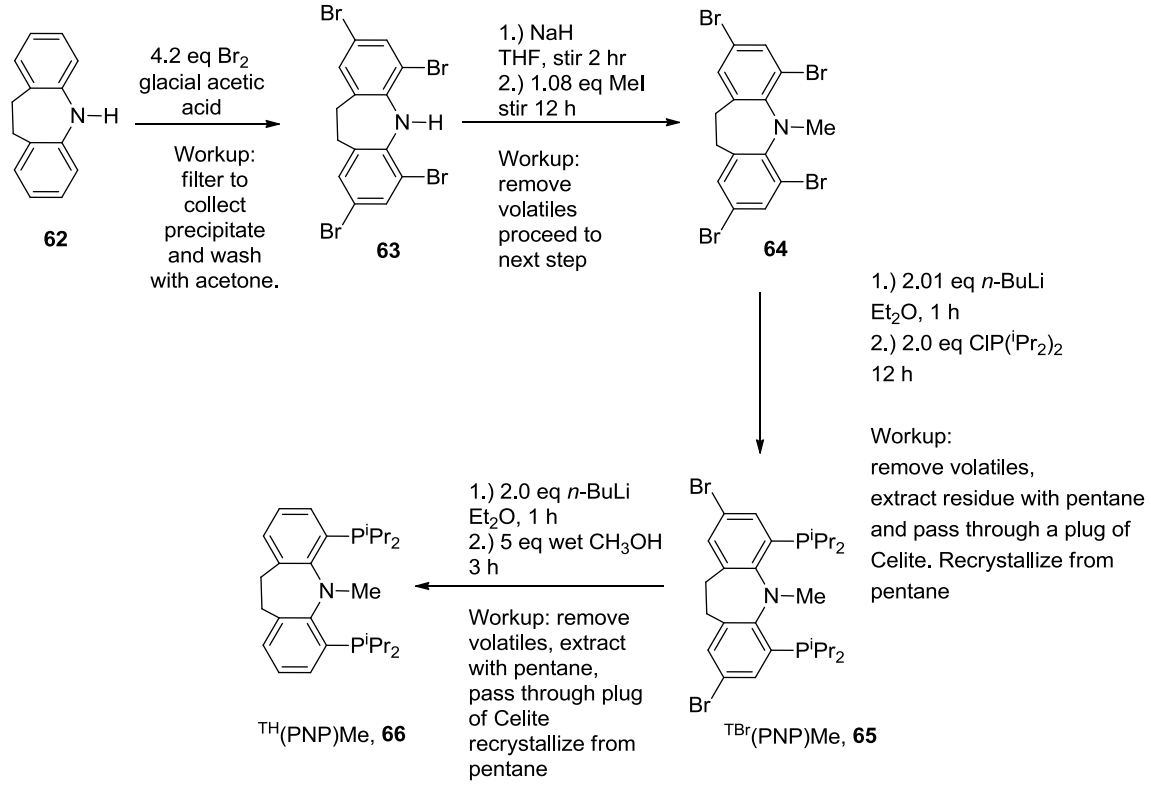

Addition of PhLi to TH(PNP)Rh(Me)(Cl) in the presence of *p*-trifluoromethylphenyl chloride does not cleanly produce TH(PNP)Rh($C_6H_4CF_3$)(Cl) (**69**), which is different from the analogous reaction on the untied (PNP)Me ligand system. In an attempt to synthesize the desired Rh^{III} complex by an alternative route, an excess of $NaBH_4$ was added to **55**, and TH(PNP)RhH_2 (**67**) was cleanly produced (Scheme 30). From there, an excess of *t*-butylethylene was added to form the Rh^{I} adduct, which after 48 h in neat *p*-trifluoromethylphenyl chloride was completely converted to TH(PNP)Rh($C_6H_4CF_3$)(Cl) (**69**) (Scheme 30).

Scheme 30. Synthesis of tied TH(PNP)Rh($C_6H_4CF_3$)Cl, **69**.

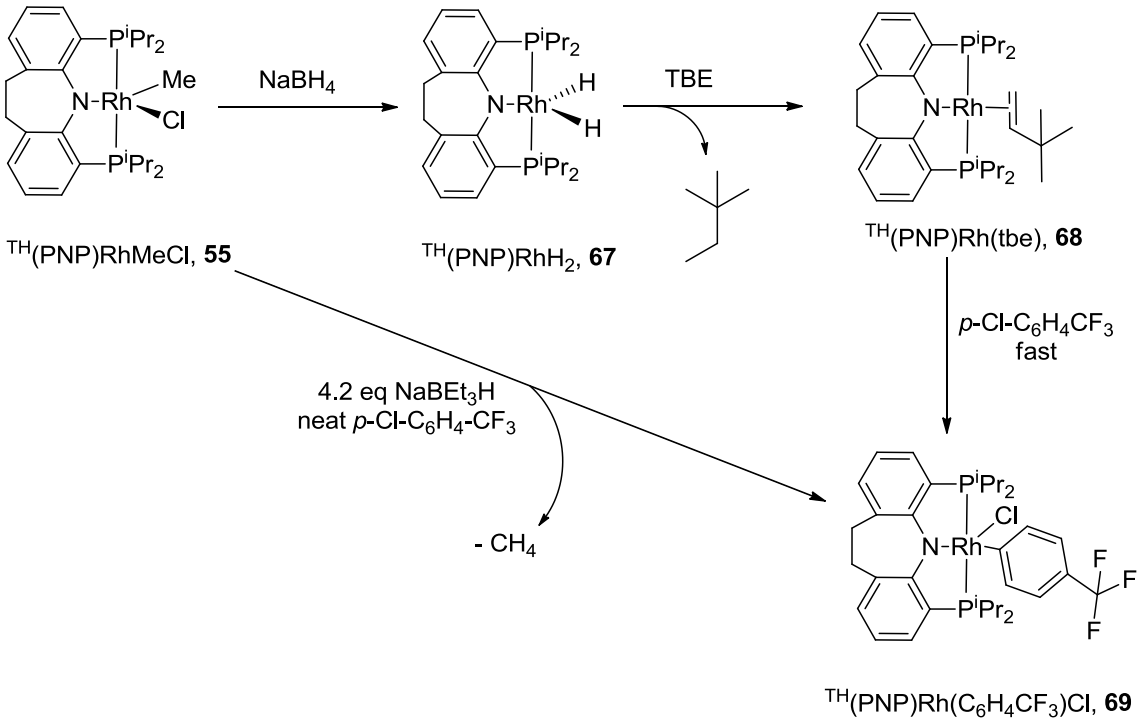

To see if the desired compound **69** could be synthesized in other ways, **55** was dissolved in neat *p*-trifluoromethylphenyl chloride. 4.2 eq of $NaBEt_3H$ was added, and the reaction was left to stir overnight (Scheme 30). When fewer equivalents of $NaBEt_3H$ were used, the result was a mixture of **55** and **69**. Removal of volatiles followed by workup yielded one apparent singlet at δ -62.32 and a very broad doublet at δ 40.0 by ^{19}F NMR and $^{31}P\{^1H\}$ NMR spectra, respectively. The ^1H NMR spectrum revealed four inequivalent Ar-H resonances consistent with the coordination of $C_6H_4CF_3$ to the rhodium center. The broadness that was observed is most likely a result of slow rotation about the Rh-Ar bond at ambient temperature (Figure 20).

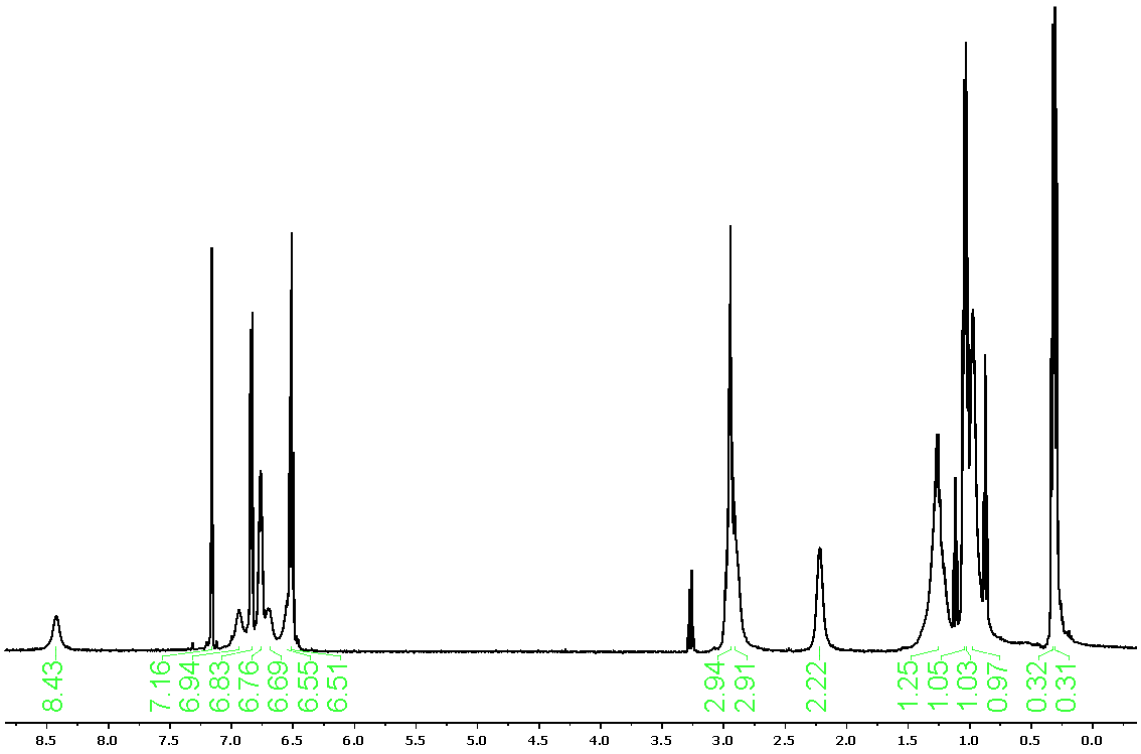

Figure 20. ^1H NMR spectrum of $^{TH}(PNP)Rh(C_6H_4CF_3)Cl$ (**69**) in C_6D_6 with residual ether and pentane.

Results of the C-C Reductive Elimination Study

The kinetics of C-C reductive elimination from the untied **70** and tied **72** ligand complexes in the presence of chlorobenzene were investigated by ^{19}F NMR spectroscopy (Scheme 31). Both reactions exhibited clean first-order kinetics. The rate of elimination of *p*-$PhC_6H_4CF_3$ from the untied ligand ($t_{1/2}$ = 15.5 min at 38 °C) was significantly faster than the rate using the tied ligand ($t_{1/2}$ = 7.7 h at 64 °C and $t_{1/2}$ = 2.13 h at 75 °C) (Figure 21 and 22 for the untied ligand Figure 23 and 24 for the tied ligand).

Scheme 31. Reductive elimination study comparing the untied and tied PNP ligands with a rhodium center.

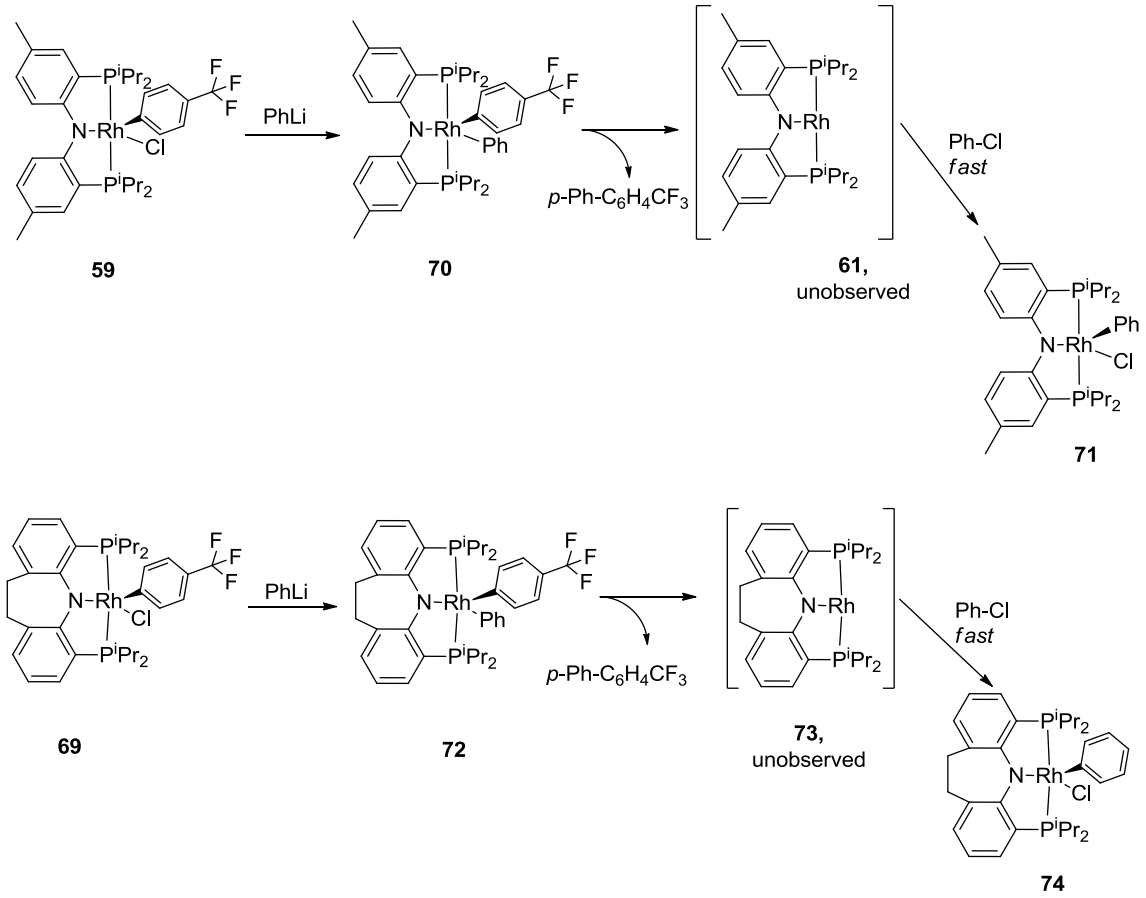

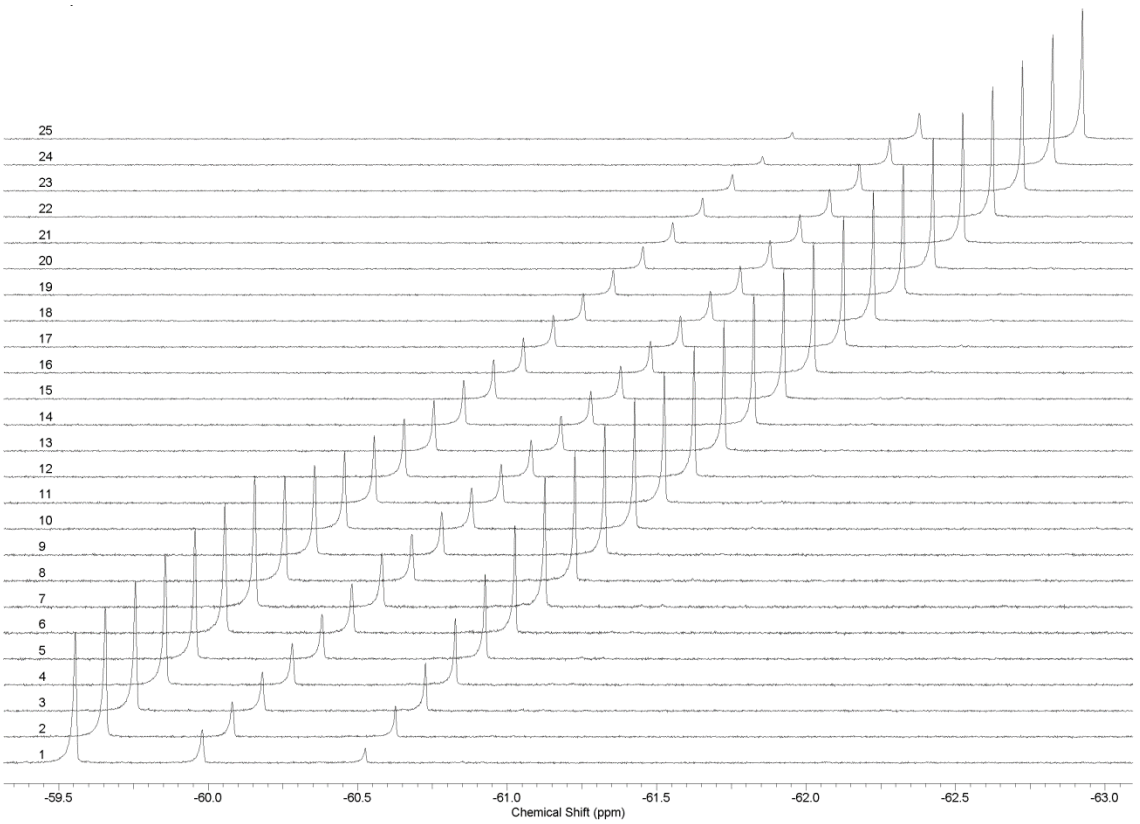

Figure 21. Reductive elimination study at 38 °C. Peaks from left to right: *p*-$PhC_6H_4CF_3$, ^{Me}(PNP)Rh(C_6H_5)($C_6H_4CF_3$) (**70**), ^{Me}(PNP)Rh($C_6H_4CF_3$)Cl (**59**).

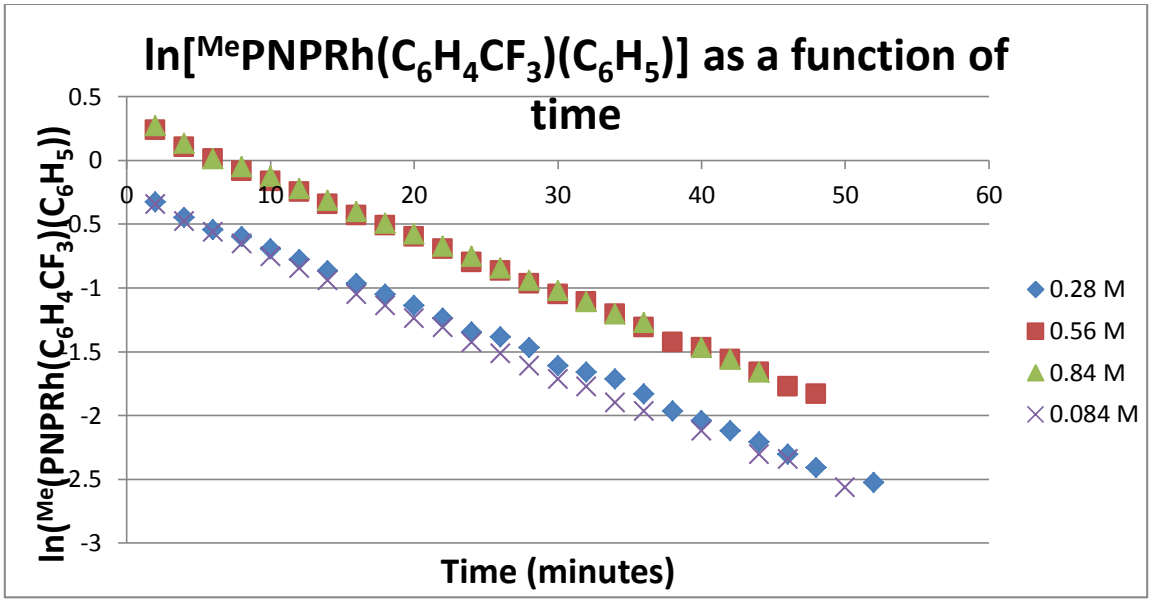

Figure 22. Plot illustrating the first-order reductive elimination of *p*-$PhC_6H_4CF_3$ from **70** at different concentrations of PhCl.

Repeating these experiments with the tied ligand complex, TH(PNP)Rh($C_6H_4CF_3$)Cl (**69**), revealed interesting results. After 7 hours at 38 °C, **72** saw very little elimination of *p*-$PhC_6H_4CF_3$ (< 4%), with > 90% of the material present as TH(PNP)Rh(C_6H_5)($C_6H_4CF_3$) (**72**). Raising the temperature to 64 °C revealed an increase in the rate of *p*-$PhC_6H_4CF_3$ elimination (> 85%), with $t_{1/2}$ = 7.7 h. A further increase to 75 °C produced an even faster rate of elimination, with $t_{1/2}$ = 2.13 h (Figure 23 and 24). The rates of both reactions were independent of the concentration of PhCl (tested at 0.140, 0.281, 0.421 and 0.042 mmol). These results are consistent with the rate-limiting step likely being the C-C elimination to generate the 14-electron (PNP)Rh/ TH(PNP)Rh fragments (or their kinetic equivalents) followed by rapid C-X oxidative addition.

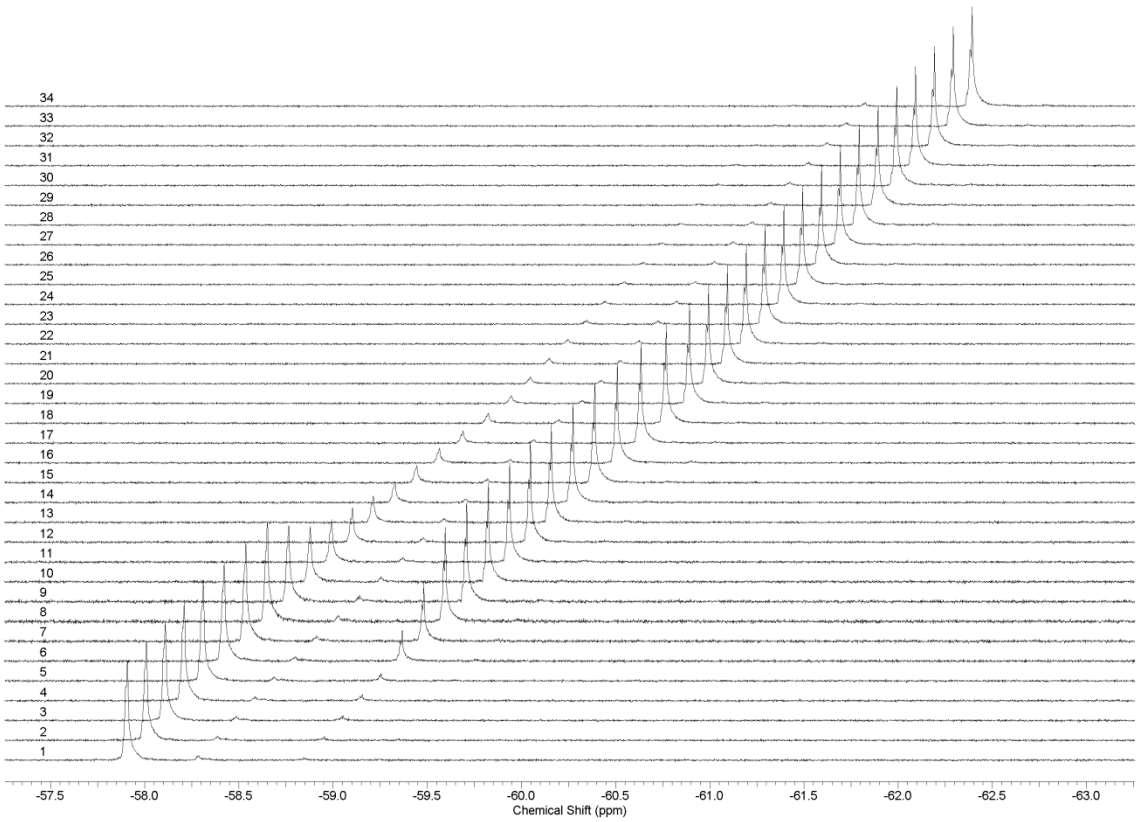

Figure 23. C-C reductive elimination at 75 °C. Peaks from left to right: TH(PNP)Rh(C_6H_5)($C_6H_4CF_3$) (**72**), TH(PNP)Rh($C_6H_4CF_3$)Cl (**69**), and *p*-Ph$C_6H_4CF_3$.

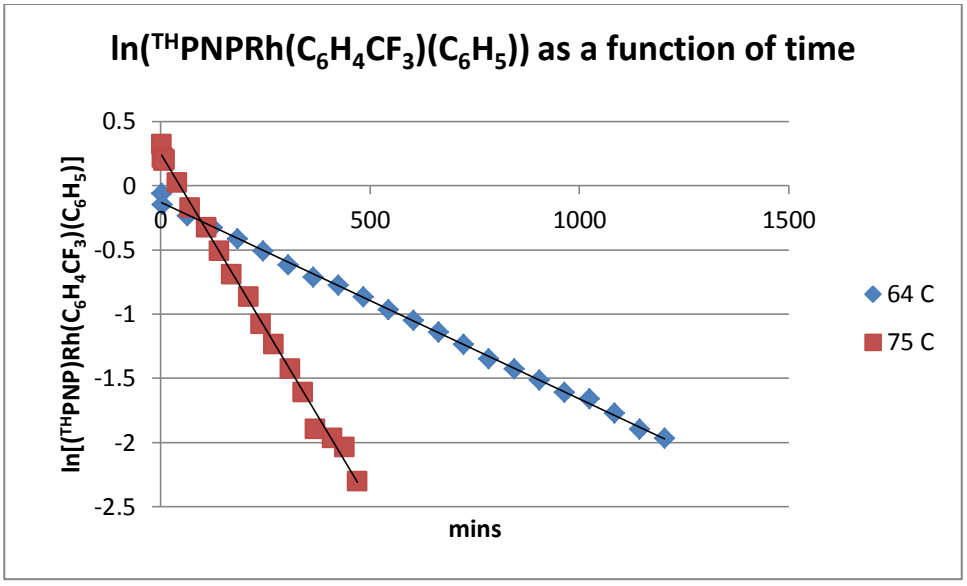

Figure 24. Plot illustrating the first-order reductive elimination of *p*-$PhC_6H_4CF_3$ from **72** (red) 64 °C, $t_{1/2}$ = 7.7 h (blue) 75 °C, $t_{1/2}$ = 2.13 h.

These results reveal that the reductive elimination is slower for the tied PNP ligand. This is contrary to studied Pd(II)/Pd(0) systems.[74] Normally, the increased bulk in the ancillary ligands promotes the rotation of the aryl groups out of the C-M-C plane to allow for reductive elimination. One possible explanation for this opposite observation is that there is too much bulk above and below the C-M-C plane in the tied PNP ligand system. This would cause both aryl groups to be coplanar, hindering the ease of the groups rotating for reductive elimination of *p*-$PhC_6H_4CF_3$ (Figure 25). This has been observed previously in (PCP)IrR_2 systems.[74]

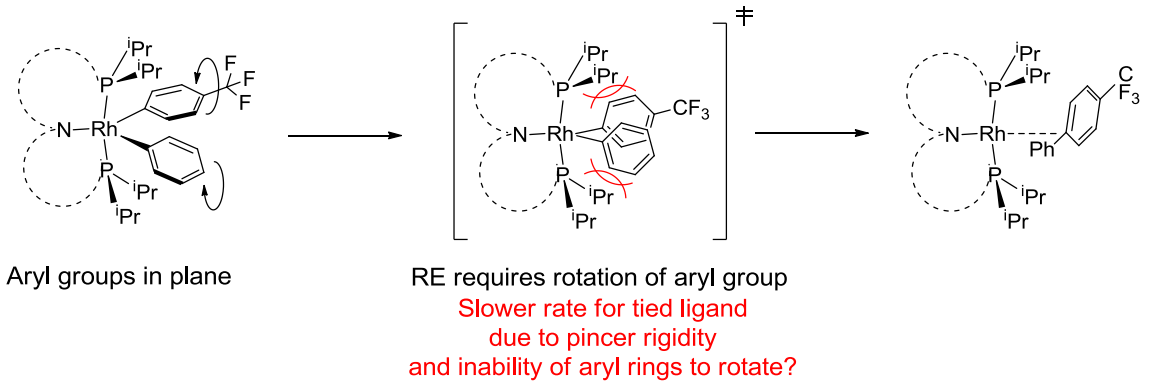

Figure 25. Possible coplanarity of **72** at the transition state.

Comparing the solid-state structures of these two ligand systems reveals many similarities and no clear explanation of the observed C-C reductive elimination results. The crystal structure of the tied ligand, TH(PNP)Rh(C_6H_4Me)Cl (**75**, Figure 26), is rather similar to the untied (PNP)Rh(Ph)Br (**76**, Figure 27), and both are comparable to the structures of (PNP)Ir(Ph)Cl and **76**.[75] The geometry of the rhodium(III) complexes **75** and **76** can best be described as square pyramidal, with the strongest trans influence group (C_6H_5 or *p*-MeC_6H_4) trans to the empty site (Figure 28). This is very typical for group 9 five-coordinate metal complexes with one strong trans influencing ligand (Table 6).[75] Evaluating the electronics between these two systems by the carbonyl stretching still does not yield significant insight into the difference between these two systems (TH(PNP)RhCO, IR ν_{CO} (toluene): 1943 cm^{-1}; ^{Me}(PNP)RhCO IR, ν_{CO} (toluene): 1945 cm^{-1}). To evaluate this unexpected result, further additional investigations will be necessary to determine what is causing the decreased rate of C-C reductive elimination in the tied ligand system in the transition state structure of both the untied and tied PNP systems.

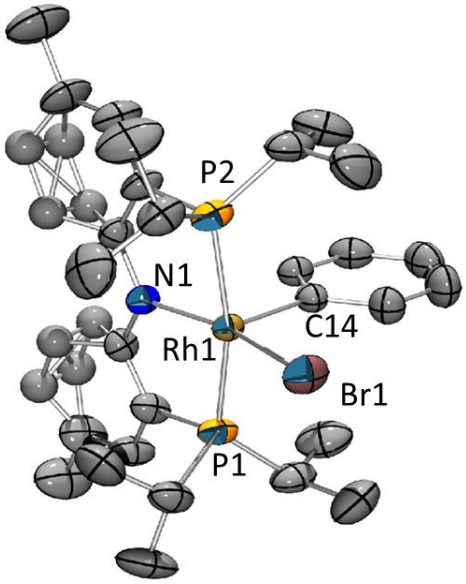

Figure 26. POV-Ray[61] rendition of an ORTEP[62] drawing (50% probability ellipsoids) of (PNP)Rh(Ph)Br (7**6**) with hydrogen atoms omitted for clarity.

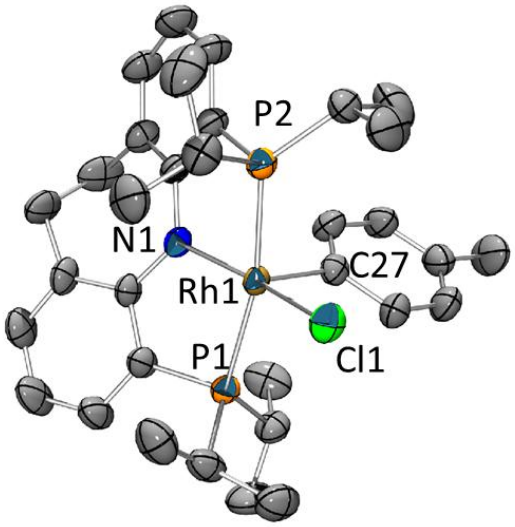

Figure 27. POV-Ray[61] rendition of an ORTEP[62] drawing (50% probability ellipsoids) of TH(PNP)Rh(C_6H_4Me)Cl (**75**) with hydrogen atoms omitted for clarity.

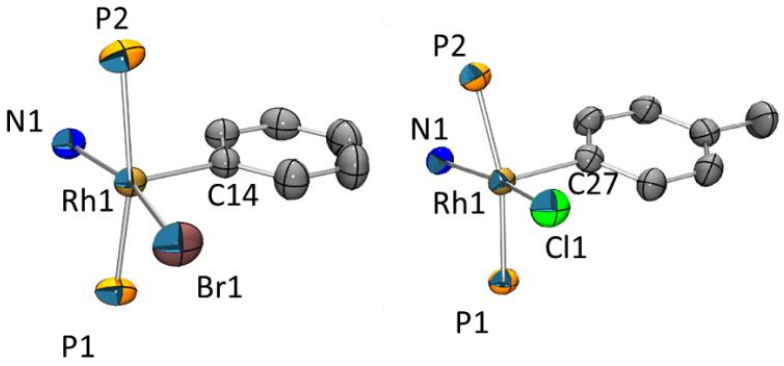

Figure 28. Views[61-62] down the N-Rh axis in (PNP)Rh(Ph)Br (**76**, left) and TH(PNP)Rh(C_6H_4Me)Cl (**75**, right)**.** Only the atoms directly bound to the Rh centers are shown.

Table 6. Comparison of the crystal structures for the tied and untied ligands.

Å/°	(PNP)Rh(Ph)Br (**76**)	TH(PNP)Rh(C_6H_4Me)Cl (**75**)
Rh1 – P1	2.3040(11)	2.3143(15)
Rh1 – P2	2.3040(11)	2.2765(14)
Rh1 – C(14/27)	2.006(6)	2.000(4)
Rh1 – N1	2.048(5)	2.086(3)
Rh1 – X	2.5015(8)	2.36600(13)
P2 – Rh1 – C(14/27)	92.75(4)	95.51(13)
P2 – Rh1 – N1	84.50(3)	84.51(11)
C(14/27) – Rh1 – N1	94.9(2)	96.45(16)
P2 – Rh1 – P1	168.08(6)	167.48(4)
C(14/27) – Rh1 – P1	92.75(4)	92.48(13)
N1 – Rh1 – P1	84.50(3)	85.03(11)
P2 – Rh1 – X	94.60(3)	90.12(6)
C(14/27) – Rh1 – X	101.93(19)	98.81(13)
N1 – Rh1 – X	163.17(14)	164.25(11)
P1 – Rh1 – X	94.60(3)	98.17(5)

Experimental

General Considerations

Unless specified otherwise, all manipulations were performed under an argon atmosphere using standard Schlenk or glovebox techniques. Dioxane, diethyl ether, tetrahydrofuran and benzene were dried over sodium-benzophenone ketyl, distilled or vacuum transferred and stored over molecular sieves in an Ar-filled glovebox. ^{Me}(PNP)Me (**66**) was synthesized according to published procedures,[3] TH(PNP)Rh(Me)Cl (**55**) was synthesized according to published procedures[19] and all other chemicals were used as received from commercial vendors. All NMR spectra were recorded on a Varian iNova 300 spectrometer (^{1}H NMR, 299.951 MHz; ^{31}P NMR, 121.425 MHz; ^{13}C NMR, 75.413 MHz), Varian Mercury 300 spectrometer (^{13}C NMR, 75.426 MHz), Varian iNova 400 spectrometer (^{1}H NMR, 399.755 MHz; ^{13}C NMR, 100.518 MHz; ^{31}P NMR, 181.822 MHz), or Varian iNova NMR 500 spectrometer (^{1}H NMR, 499.425 or 499.683 MHz; ^{13}C NMR, 75.424 MHz/125.580 MHz; ^{31}P NMR, 202.171 MHz). Chemical shifts are reported in δ/ppm. For ^{1}H and ^{13}C NMR spectra, the residual solvent peak was used as an internal reference. ^{31}P NMR spectra were referenced externally using 85% H_3PO_4 at δ 0 ppm. ^{19}F NMR spectra were referenced externally at δ -78.5 ppm. Elemental analysis was performed by CALI Labs, Parsippany, NJ, USA.

^{Me}(PNP)Rh($C_6H_4CF_3$)Cl (59). ^{Me}(PNP)Rh(Me)Cl (**56**) (0.100 g, 0.172 mmol) was dissolved in *p*-chlorobenzotrifluoride (68.8 μL, 0.516 mmol) in a flask, and PhLi (129 μL, 0.258 mmol) was added to the solution. The reaction was monitored by NMR over 7

h. Yield: 0.099 g (81%). $^{31}P\{^{1}H\}$ NMR (C_6D_6): δ 38.0 (d, J_{RhP} = 105 Hz). ^{19}F NMR (C_6D_6): δ -62.3 (s, CF_3). $^{13}C\{^{1}H\}$ NMR (C_6D_6): δ 161.6 (vt, J_{CRh} = 10 Hz, *C*-N), 146.2 (dt, J_{CP} = 9 Hz, J_{CRh} = 38 Hz, *i*-$C_6H_4CF_3$), 139.8 (br s, $C_6H_4CF_3$), 134.2 (br s, $C_6H_4CF_3$), 133.2, 131.9 (s, 2C, C_{Ar} of PNP), 126.8 (vt, J_{CP} = 3 Hz, C_{Ar} of PNP), 125.5 (q, J_{CF} = 32 Hz, *p*-$C_6H_4CF_3$), 125.3 (q, J_{CF} = 270 Hz, CF_3), 123.3 (br s, $C_6H_4CF_3$), 122.3 (s, $C_6H_4CF_3$), 118.7 (vt, J_{CP} = 19 Hz, C_{Ar} of PNP), 118.7 (vt, J_{CP} = 6 Hz, C_{Ar} of PNP), 25.9 (vt, J_{CP} = 12 Hz, CHMe$_2$), 24.2 (vt, J_{CP} = 12 Hz, CHMe$_2$), 20.2 (s, Ar-CH_3 of PNP), 18.9 (s, CHMe_2), 17.4 (s, CHMe_2) 17.3 (s, CHMe_2) 17.3 (s, CHMe_2). ^{1}H NMR (C_6D_6): δ 8.57 (br d, 1H, $C_6H_4CF_3$), 7.94 (d, 2H, J_{HH} = 9 Hz, Ar-*H*), 6.96 (br d, 1H, J_{HH} = 8 Hz, $C_6H_4CF_3$), 6.87 (br d, 1H, $C_6H_4CF_3$), 6.83 (br d (two overlapping signals), 4H, J_{HH} = 8 Hz, Ar-*H*), 6.65 (br d, 1H, $C_6H_4CF_3$), 2.91 (m, 2H, C*H*Me$_2$), 2.20 (m, 2H, C*H*Me$_2$), 2.13 (s, 6H, Ar-CH_3), 1.33 (app q, 6H, J_{HH} = 7 Hz, CHMe_2), 1.01 (app q, 6H, J_{HH} = 7 Hz, CHMe_2), 0.95 (app q, 6H, J_{HH} = 7 Hz, CHMe_2), 0.27 (app q, 6H, J_{HH} = 7 Hz, CHMe_2). Elem. Anal. Found (Calculated) for $C_{33}H_{44}NP_2ClF_3Rh(Et_2O)_{0.5}$ (derived from the integration of the ^{1}H NMR spectrum): C 55.88 (56.14); H 6.33 (6.54).

Tetrabromoiminodibenzyl (63). A solution of bromine (12.7 g, 0.080 mol) in 100 mL of glacial acetic acid was slowly added to a solution of iminodibenzyl (**62**) (3.69 g, 0.019 mol) in 250 mL of glacial acetic acid. The mixture was stirred at ambient temperature for 1 h and then passed through an "M" frit to collect the solid precipitate. The collected solid was washed with acetone and dried. The remaining filtrate was placed under vacuum, and the residue was recrystallized from acetone. Yield: 8.5 g (89%). ^{1}H NMR

(C_6D_6): δ 7.46 (s, 1H, N-*H*), 7.36 (d, 2H, J_{HH} = 7, Ar-*H*), 6.67 (d, 2H, J_{HH} = 7, Ar-*H*), 2.17 (s, 4H, CH_2CH_2). $^{13}C\{^1H\}$ NMR (C_6D_6): δ 137.9 (s), 133.1 (s), 132.5 (s), 131.6 (s), 114.0 (s), 111.9 (s), 34.3 (s, -*C*H_2*C*H_2-).

***N*-Methyl-tetrabromoiminodibenzyl (64)**. NaH (0.29 g, 12 mmol) and **63** (5.14 g, 10 mmol) were dissolved in ca. 35 mL of THF. The mixture was stirred for 2 h, and then MeI (747 μL, 12 mmol) was added. The resulting mixture was stirred for another 12 h, and the volatiles were removed under vacuum. The residue was extracted with 30 mL of diethyl ether and then used directly in the next step. ^1H NMR (C_6D_6): δ 7.52 (d, 2H, J_{HH} = 2 Hz, Ar-*H*), 6.74 (d, 2H, J_{HH} = 2 Hz, Ar-*H*), 2.83 (s, 3H, N-*Me*), 2.47 (m, 2H, CH_aH$_b$CH_aH$_b$), 1.92 (m, 2H, CH$_a$$H_bCH_a$$H_b$). ^{13}C NMR (C_6D_6): δ 145.2 (s), 141.5 (s), 134.5 (s), 132.0 (s), 125.6 (s), 119.0 (s), 43.8 (s, N-*Me*), 31.9 (s, -*C*H_2*C*H_2-).

^{TBr}PN(Me)P^{iPr} (65). *n*-BuLi (3.76 mL of a 2.5 M solution in hexanes, 9.40 mmol) was slowly added to a solution of **64** in diethyl ether at ambient temperature. The mixture was stirred for 1 h, and then chlorodiisopropylphosphine (1.50 mL, 9.40 mmol) was added to the mixture. After stirring for an additional 12 h, the volatiles were removed in vacuo. The residue was dissolved in pentane and filtered through a plug of Celite. The filtrate was treated with silica gel and left to stir for 30 min, and then the solids were filtered off. The resulting filtrate was concentrated and placed into the freezer for recrystallization. A white solid was collected. Yield: 1.7 g (65%). ^1H NMR (C_6D_6): δ 7.54 (d, 2H, J_{HH} = 2 Hz, Ar-*H*), 7.00 (d, 2H, J_{HH} = 2 Hz, Ar-*H*), 3.25 (s, 3H, N-*Me*), 2.68

(dd, 2H, CH_aH$_b$CH_aH$_b$, J_{HH} = 16 Hz, J_{HH} = 10 Hz), 2.16 (dd, 2H, CH$_a$$H_bCH_a$$H_b$, J_{HH} = 16 Hz, J_{HH} = 10 Hz), 1.80 (m, 4H, C*H*Me$_2$), 1.13 (app. q (dvt), 12H, CH*Me*$_2$), 1.03 (app. quartet (dvt), 6H, CH*Me*$_2$), 0.92 (app. quartet (dvt), 6H, CH*Me*$_2$). ^{31}P{^{1}H} NMR (C_6D_6): δ –7.7 (s). ^{13}C NMR (C_6D_6): δ 153.6 (t, J_{CRh} = 11 Hz), 142.1 (t, J_{CP} = 13 Hz), 141.7 (s), 134.3 (s), 133.7 (s), 119.0 (s), 50.9 (t, J_{CRh} = 10 Hz, N-*Me*), 32.8 (s, *C*H$_2$*C*H$_2$), 27.3 (t, J_{CP} = 7 Hz, *C*HMe$_2$), 26.0 (t, J_{CP} = 8 Hz, *C*HMe$_2$), 21.5 (app. quartet (dvt), CH*Me*$_2$), 20.2 (app. quartet (dvt), CH*Me*$_2$). Selected ^{1}H NMR spectroscopy data that were collected while decoupling the ^{31}P signal at –7.7 ppm include the following: 7.53 (d, 2H, $^4J_{HH}$ = 2 Hz, Ar-*H*), 7.01 (d, 2H, $^4J_{H\text{-}H}$ = 2 Hz, Ar-*H*), 1.13 (d, 12H, J_{HH} = 7 Hz, CH*Me*$_2$), 1.03 (d, 6H, J_{HH} = 7 Hz, CH*Me*$_2$), 0.92 (d, 6H, J_{HH} = 7 Hz, CH*Me*$_2$).

THPN(Me)P^{iPr} (66). ^{TBr}PN(Me)P^{iPr} (**65**) (1.7 g, 2.84 mmol) was dissolved in 25 mL of diethyl ether, and the flask was placed into the freezer for ca. 30 min. *n*-BuLi (2.27 mL of a 2.5 M solution in hexanes, 5.67 mmol) was slowly added to the cooled solution. The mixture was allowed to warm to room temperature and stirred for 1 h. Then, 6 mL of methanol was added to the mixture, and it was stirred for an additional 30 min. The volatiles were removed in vacuo, and the residue was dissolved in pentane and passed through a pad of silica gel. The resulting solution was concentrated for recrystallization. The precipitate was collected the next day and dried under vacuum. Yield: 1.01 g (81%). ^{1}H NMR (C_6D_6): δ 7.30 (d, 2H, $^3J_{HH}$ = 7 Hz, Ar-*H*), 6.98 (t, 2H, $^3J_{HH}$ = 7 Hz, Ar-*H*), 6.90 (d, 2H, $^3J_{H\text{-}H}$ = 7 Hz, Ar-*H*), 3.46 (s, 3H, N-*Me*), 3.05 (dd, 2H, J_{HH} = 14 Hz, J_{HH} = 8 Hz, CH_aH$_b$CH_aH$_b$), 2.53 (dd, 2H, J_{HH} = 14 Hz, J_{HH} = 8 Hz, CH$_a$$H_bCH_a$$H_b$), 1.99 (m, 4H,

C*H*Me$_2$), 1.27 (app. quartet (dvt), 12H, CH*Me$_2$*), 1.16 (app. quartet (dvt), 6H, CH*Me$_2$*), 1.06 (app. quartet (dvt), 6H, CH*Me$_2$*). ^{31}P{^{1}H} NMR (C_6D_6): δ –8.8 (s). ^{13}C NMR (C_6D_6): δ 155.2 (t, J_{CRh} = 11 Hz), 139.7 (s), 138.8 (t, J_{CP} = 11 Hz), 131.8 (s), 131.0 (s), 125.0 (s), 51.3 (t, J_{CP} = 11 Hz, N-*Me*), 33.8 (s, -*C*H$_2$*C*H$_2$-), 27.3 (t, J_{CP} = 8 Hz, *C*HMe$_2$), 26.1 (t, J_{CP} = 8 Hz, *C*HMe$_2$), 21.7 (app. quartet (dvt), CH*Me$_2$*), 20.5 (app. quartet (dvt), CH*Me$_2$*). Elem. Anal. Calcd. for $C_{27}H_{41}NP_2$: C, 73.44; H, 9.36. Found: C, 73.28; H, 9.49.

TH(PNP)Rh($C_6H_4CF_3$)Cl (69). TH(PNP)Rh(Me)Cl (0.0916 g, 0.158 mmol) was dissolved in *p*-chlorobenzotrifluoride in a 25 mL flask. A 1.0 M solution of $NaBEt_3H$ in toluene (474 μL, 0.474 mmol) was added to the mixture by syringe. The reaction was left to stir for 12 h, and the volatiles were removed. Pentane was used to extract the residue, and it was passed through a plug of Celite. The filtrate was concentrated and placed into the freezer. A bright green solid was collected. Yield: 0.0734 g (65%). ^{1}H NMR (C_6D_6): δ 8.43 (br s, 1H, $C_6H_4CF_3$), 6.94 (br d, 1H, $C_6H_4CF_3$), 6.84 (d, 2H, J_{HH} = 7 Hz, Ar-*H*), 6.77 (dd, 2H, J_{HH} = 9 Hz, Ar-*H*), 6.69 (br s, 1H $C_6H_4CF_3$), 6.54 (br s, 1H, $C_6H_4CF_3$), 6.51 (vt, 2H, J_{HH} = 7 Hz, Ar-*H*), 2.94 (s, 4H, -C*H$_2$*C*H$_2$*-), 2.93 (m, 2H, C*H*Me$_2$), 2.21 (m, 2H, C*H*Me$_2$), 1.25 (app q, 6H, J_{HH} = 7 Hz, CH*Me$_2$*), 1.01 (app q, 6H, J_{HH} = 7 Hz, CH*Me$_2$*), 0.97 (br m, 6H, CH*Me$_2$*), 0.31 (app q, 6H, J_{HH} = 7 Hz, CH*Me$_2$*). ^{13}C{^{1}H} NMR (C_6D_6): δ 161.4 (vt, J_{CRh} = 10 Hz, *C*-N), 146.4 (dt, J_{CP} = 8 Hz, $J_{C\text{-}Rh}$ = 40 Hz, *i*-$C_6H_4CF_3$), 140.0 (br s, $C_6H_4CF_3$), 134.4 (br s, $C_6H_4CF_3$), 133.4 (s, 2C_{Ar} of PNP), 132.1 (s, 2C_{Ar} of PNP), 127.0 (vt, J_{CP} = 4 Hz, C_{Ar} of PNP), 125.8 (q, J_{CF} = 30 Hz, *p*-$C_6H_4CF_3$), 125.5 (q, J_{CF} = 270 Hz, CF_3), 123.5 (br s, $C_6H_4CF_3$), 122.6 (br s, $C_6H_4CF_3$),

26.1 (vt, J_{CP} = 8 Hz, *C*HMe$_2$), 24.4 (vt, J_{CP} = 8 Hz, *C*HMe$_2$), 20.4 (s, 2C, -*C*H$_2$*C*H$_2$-) 19.2 (s, CH*Me$_2$*), 17.7 (s, CH*Me$_2$*), 17.6 (s, CH*Me$_2$*), 17.4 (s, Ar-*C*H$_3$). ^{31}P{^{1}H} NMR (C_6D_6): δ 43.7, J_{RhP} = 178 Hz ^{19}F NMR (C_6D_6): δ -62.3 (s, CF_3). Elem. Anal. Found (Calculated) for $C_{33}H_{42}ClF_3NP_2Rh$: C 55.81 (55.82); H 5.88 (5.96).

Kinetic study of the C-C elimination of *p*-Ph-$C_6H_4CF_3$ from 70. ^{Me}(PNP)Rh($C_6H_4CF_3$)Cl (**59**) was added to a J. Young NMR tube and treated with chlorobenzene (four different experiments using four different concentrations of chlorobenzene: 14.2 μL, 0.140 mmol; 28.5 μL, 0.281 mmol; 42.7 μL, 0.421 mmol; 4.27 μL, 0.042 mmol) in C_6D_6. Phenyllithium (8.6 μL, 1.8 M in toluene, 0.0154 mmol) was added to the NMR tube along with 1-fluorooctane (4.6 μL, 0.0281 mmol) as an internal standard. The sample was inserted into the NMR probe, which was preheated to 38 °C. The disappearance of ^{Me}(PNP)Rh($C_6H_4CF_3$)Cl was integrated against the internal 1-fluorooctane standard by monitoring the ^{19}F NMR spectrum at regular intervals of 120 seconds for at least 3 half-lives. The ^{19}F NMR spectra were referenced externally to CF_3CO_2H at δ -78.5. The sum of the integrals for ^{Me}(PNP)Rh($C_6H_4CF_3$)Cl, ^{Me}(PNP)Rh($C_6H_4CF_3$)(C_6H_5), *p*-Ph$C_6H_4CF_3$ and the internal 1-fluorooctane standard remained constant throughout the experiment (Figure 29).

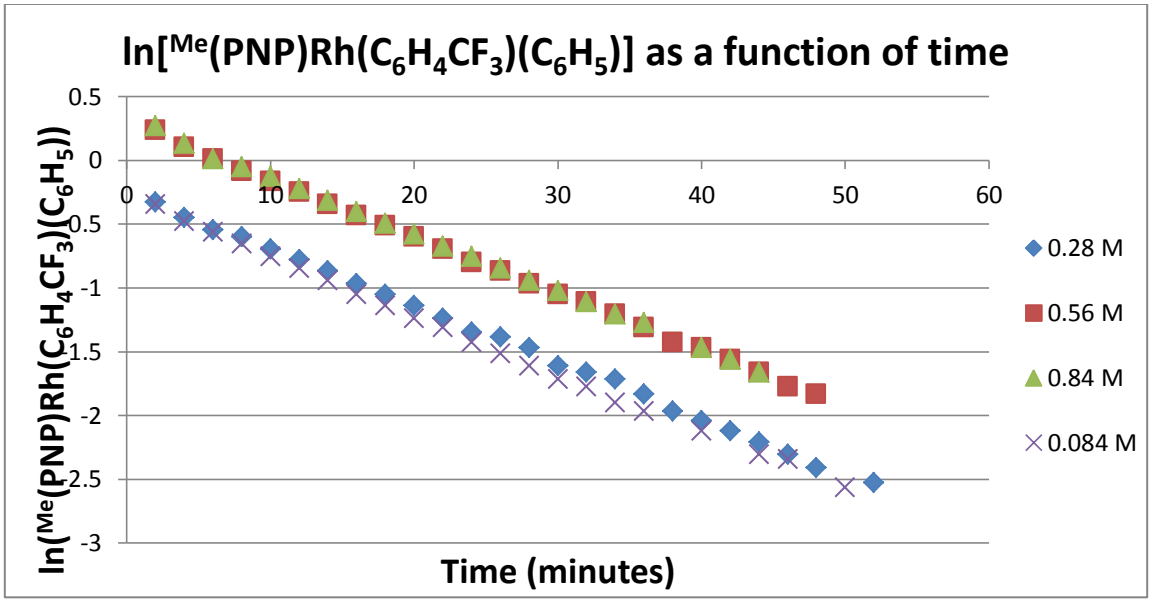

Rate Constants:

$4.43(3)\times10^{-2}$ for 0.28 M, $t_{1/2}$ = 15.6 min

$4.43(3)\times10^{-2}$ for 0.56 M, $t_{1/2}$ = 15.6 min

$4.47(2)\times10^{-2}$ for 0.84 M, $t_{1/2}$ = 15.5 min

$4.48(5)\times10^{-2}$ for 0.084 M, $t_{1/2}$ = 15.5 min

Averaged

$t_{1/2}$ = 15.6 min

Figure 29. Plot illustrating the first-order reductive elimination of *p*-$PhC_6H_4CF_3$ from **70** at different concentrations of PhCl with rate constants.

Kinetic study of the C-C elimination of *p*-Ph-$C_6H_4CF_3$ from 72. TH(PNP)Rh($C_6H_4CF_3$)Cl (**69**) was added to a J. Young NMR tube and treated with chlorobenzene (a series of different experiments with varying concentrations of chlorobenzene: 57.0 μL, 0.562 mmol; 42.7 μL, 0.421 mmol; 4.27 μL, 0.042 mmol) in C_6D_6. Phenyllithium (8.6 μL, 1.8 M in toluene, 0.0154 mmol) was added to the NMR tube along with 1-fluorooctane (4.6 μL, 0.0281 mmol) as an internal standard. The sample was inserted into the NMR probe, which was preheated to 38 °C, 64 °C or 75 °C. The disappearance of TH(PNP)Rh($C_6H_4CF_3$)Cl was integrated against the internal 1-fluorooctane standard by monitoring the ^{19}F NMR spectrum at regular intervals of 120 (for 38 °C), 1,800 (for 75 °C) or 3,600 (for 64 °C) seconds for at least 3 half-lives. The ^{19}F NMR spectra were referenced externally to CF_3CO_2H at δ -78.5. The sum of the integrals for TH(PNP)Rh($C_6H_4CF_3$)Cl, TH(PNP)Rh($C_6H_4CF_3$)(C_6H_5), *p*-Ph$C_6H_4CF_3$ and the internal 1-fluorooctane standard remained constant throughout the experiment.

Rate Constants:

$1.53(1)x10^{-3}$ for 0.84 M for 64 °C, $t_{1/2}$ = 7.7 h

$5.44(7)x10^{-3}$ for 0.84 M for 75 °C, $t_{1/2}$ = 2.13 h

Note on error calculation. The errors listed in the values of the rate constants are twice the standard deviations (s) (averaged over all four trials for Me(PNP)Rh($C_6H_4CF_3$)(C_6H_5)) that were calculated in the statistical analysis (LINEST) using MS Excel.

- Minutes Averaged: 0.000325 x2 = 0.00065
- Seconds Averaged: 0.0000054 x2 = 0.000011

Note on the measurement of temperature. The temperature inside the NMR probe was determined to be 38.7 °C, 64.4 °C and 75.5 °C via a chemical shift thermometer (neat ethylene glycol). We habitually assumed an uncertainty of ±1 °C for such temperature measurements.

CHAPTER IV

CONCLUSION: PNP PINCER LIGAND CHEMISTRY

Conclusion

In summary, we have synthesized and characterized Hf(IV) complexes of the diarylamido-based PNP ligand. The structure of (PNP)$HfCl_3$ displays deviations from octahedral geometry about Hf that can be simply explained by the constraint of the PNP ligand. The deviations from octahedral geometry about Hf in (PNP)$HfMe_3$, (PNP)$Hf(CH_2SiMe_3)_2Cl$ and (PNP)$Hf(CH_2SiMe_3)_2OTf$ are much more severe and stem from a combination of the effect of the chelate constraint and from the preference for accommodating stronger bonds to anionic ligands. Thermolysis of (PNP)$Hf(CH_2SiMe_3)_2Cl$ led to the formation of a new compound that displays spectroscopic characteristics consistent with a Hf alkylidene; however, attempts at isolation and full characterization have not proven successful. Alternative attempts at synthesis and isolation of an alkylidene with (PNP)$Hf(CH_2SiMe_3)_2CH_3$ and (PNP)$Hf(CH_2SiMe_3)_2(C_6H_5)$ were inconclusive even though free $SiMe_4$ was observed by the ^1H NMR spectrum. The attempts at isolation of a (PNP)Hf imide were also unsuccessful, but it is believed that (PNP)$HfMe_2(NHC_6H_4F)$ can be synthesized in situ.

A series of tantalum(V) halide complexes and an ethylene complex have been characterized with the diarylamido-based PNP ligand. The structure of (PNP)$TaCHCH_3(C_2H_4)$ displays deviations from an octahedral geometry around the tantalum center as a result of the constraint of the PNP ligand itself. The synthesis of

(PNP)TaCHCH$_3$(C_2H_4) is only seen after addition of dioxane to help precipitate out the MgX_2 species when ethyl magnesium chloride is used.

Rhodium complexes of the tied and untied PNP ligands were compared. The fundamental steps of aryl halide coupling reactions, C-X oxidative addition and C-C reductive elimination, were observed at ambient (untied ligand) and slightly elevated temperatures (tied ligand). The oxidative addition of *p*-Cl-C_6H_4-CF_3 is thermodynamically favored, which is in agreement with previous studies on (PNP)Rh and (PNP)Ir.[32b,76-77] While the tied PNP ligand was shown to exhibit faster N-C cleavage[19] and be more selective for alkyne dimerization,[8] it is not ideal for the reductive elimination of aryl-aryl products at ambient temperatures when compared to the untied PNP ligand system.

REFERENCES

1. Moulton, C. J.; Shaw, B. L. *J. Chem. Soc., Dalton Trans*. **1976**, 1020. (b) van Koten, G. *Pure Appl. Chem.* **1989**, *61*, 1681.
2. Liang, L. C.; Lin, J. M.; Hung, C. H. *Organometallics* **2003**, *22*, 3007.
3. Fan, L.; Foxman, B. M.; Ozerov, O. V. *Organometallics* **2004**, *23*, 326.
4. Langer, R.; Leitus, G.; Ben-David, Y.; Milstein, D. *Angew. Chem. Int. Ed.* **2011**, *50*, 2120.
5. Fryzuk, M. D.; MacNeil, P. A. *J. Am. Chem. Soc.* **1981**, *103*, 3592.
6. Segawa, Y.; Yamashita, M.; Nozaki, K. *J. Am. Chem. Soc.* **2009**, *131*, 9201.
7. Mitton, S. J.; McDonald, R.; Turculet, L. *Organometallics* **2009**, *28*, 5122.
8. Weng, W.; Guo, C.; Celenligil-Cetin, R.; Foxman, B. M.; Ozerov, O. V. *Chem. Commun.* **2006**, 197.
9. Weng, W.; Chen, C. H.; Foxman, B. M.; Ozerov, O. V. *Organometallics* **2007**, *26*, 3315.
10. Peters, J. C.; Harkins, S. B.; Brown, S. D.; Day, M. W. *Inorg. Chem.* **2001**, *40*, 5083.
11. Boom, M. E. van D.; Milstein, D. *Chem. Rev.* **2003**, 1759.
12. Fryzuk, M. D.; MacNeil, P. A. *Organometallics* **1982**, *1*, 1540.
13. (a) Fryzuk, M. D.; Rettig, S. J.; Westerhaus, A.; Williams, H. D. *Inorg. Chem.* **1985**, *24*, 4316. (b) Fryzuk, M. D.; Haddad, T. S.; Rettig, S. J. *Organometallics* **1989**, *8*, 1723. (c) Fryzuk, M. D.; Haddad, T. S.; Rettig, S. J. *J. Am. Chem. Soc.* **1990**, *112*, 8185.

14. Fryzuk, M. D.; Haddad, T. S.; Rettig, S. J. *Organometallics* **1991**, *10*, 2026.

15. Fryzuk, M. D.; MacNeil, P. A. *J. Am. Chem. Soc.* **1984**, *106*, 6993.

16. Ozerov, O. V.; Guo, C.; Papkov, V. A.; Foxman, B. M. *J. Am. Chem. Soc.* **2004**, *126*, 4792.

17. Fan, L.; Yang, L.; Guo, C.; Foxman, B. M.; Ozerov, O. V. *Organometallics* **2004**, *23*, 4778.

18. Ozerov, O. V.; Guo, C.; Fan, L.; Foxman, B. M. *Organometallics* **2004**, *23*, 5573.

19. Weng, W.; Guo, C.; Moura, C. P.; Ozerov, O. V. *Organometallics* **2005**, *24*, 3487.

20. DeMott, J. C.; Basuli, F.; Kilgore, U. J.; Foxman, B. M.; Huffman, J. C.; Ozerov, O. V.; Mindiola, D. J. *Inorg. Chem.* **2007**, *46*, 6271.

21. DeMott, J. C.; Guo, C.; Foxman, B. M.; Yandulov, D. V.; Ozerov, O. V. *Mendeleev Commun.* **2007**, *17*, 63.

22. This is not a complete list.

23. Weng, W.; Tang, L.; Foxman, B. M.; Ozerov, O. V. *Organometallics* **2004**, *23*, 4700.

24. Bailey, B. C.; Huffman, J. C.; Mindiola, D. J.; Weng, W.; Ozerov, O. V. *Organometallics* **2005**, *24*, 1390.

25. Gerber, L. C. H.; Watson, L. A.; Parkin, S.; Weng, W.; Foxman, B. M.; Ozerov, O. V. *Organometallics* **2007**, *26*, 4866.

26. Brammell, C. M.; Pelton, E. J.; Chen, C. H.; Yakovenko, A. A.; Weng, W.; Foxman, B. M.; Ozerov, O. V. *J. Organomet. Chem.* **2011**, *696*, 4132.

27. Ozerov, O. V. Rigid PNP pincer ligands and their transition metal complexes in Morales-Morales, D. and Jensen, C. M. (Eds.) *The Chemistry of Pincer Compounds* (ISBN-10: 0-444-53138-6), Oxford, UK, Elsevier, 2007.

28. Hartwig, J. F. *Organotransition Metal Chemistry: From Bonding to Catalysis*; University Science Books: Sausalito, CA, 2009, pp 41-45.

29. Baumann, R.; Stumpf, R.; Davis, W. M.; Liang, L. C.; Schrock, R. *J. Am. Chem. Soc.* **1999**, *121*, 7822.

30. (a) Abbenhuis, H. C. L.; Feiken, N.; Haarman, H. F.; Grove, D. M.; Horn, E.; Kooijman, H.; Spek, A. L.; can Koten, G. *Angew. Chem., Int. Ed. Engl.* **1991**, *30*, 996. (b) Abbenhuis, H. C. L.; Feiken, N.l Haarman, H. F.; Grove, D. M.; Horn, E.; Spek, A. L.; Pfeffer, M.; van Koten, G. *Organometallics* **1993**, *12*, 2227.

31. (a) Sundermann, A.; Uzan, O.; Martin, J. M. L. *Organometallics* **2001**, *20*, 1783. (b) Cohen, R.; van der Boom, M. E.; Shimon, L. J. W.; Rozenberg, H.; Milstein, D. *J. Am. Chem. Soc.* **2000**, *122*, 7723. (c) Sundermann, A.; Uzan, D.; Milstein, D. *J. Am. Chem. Soc*. **2000**, *122*, 7095. (d) Rybtchinski, B.; Oevers, S.; Montag, M.; Vigalok, A.; Rozenberg, H.; Martin, J. M. L.; Milstein, D. *J. Am. Chem. Soc*. **2001**, *123*, 9064.

32. (a) Choi, J.; MacArthur, A. H. R.; Brookhart, M.; Goldman, A. S. *Chem. Rev.* **2011**, *111*, 1761. (b) Fan, L.; Parkin, S.; Ozerov, O. V. *J. Am. Chem. Soc.* **2005**, *127*, 16772. (c) Ben-Ari, E.; Gandelman, M.; Rozenberg, H.; Shimon, L. J. W.; Milstein, D. *J. Am. Chem. Soc*. **2003**, *125*, 4714.

33. (a) Choi, J.; Choliy, Y.; Zhang, X.; Emge, T. J.; Krogh-Jespersen, K.; Goldman, A. S. *J. Am. Chem. Soc.* **2009**, *131*, 15627. (b) van der Boom, M. E.; Liou, S. Y.; Ben-David, Y.; Shimon, L. J. W.; Milstein, D. *J. Am. Chem. Soc.* **1998**, *120*, 6531.

34. (a) Gandelman, M.; Milstein, D. *Chem. Commun.* **2000**, 1603. (b) Ozerov, O. V.; Guo, C.; Papkov, V. A.; Foxman, B. M. *J. Am. Chem. Soc.* **2004**, *126*, 4792.

35. (a) Morgan, E.; MacLean, D. F.; McDonald, R.; Turculet, L. *J. Am. Chem. Soc.* **2009**, *131*, 14234. (b) Zhao, J.; Goldman, A. S.; Hartwig, J. F. *Science* **2005**, *307*, 1080. (c) Kanzelberger, M.; Zhang, X.; Emge, T. J.; Goldman, A. S.; Zhao, J.; Incarvito, C.; Hartwig, J. F. *J. Am. Chem. Soc*. **2003**, *125*, 13644.

36. (a) Tanaka, R.; Yamashita, M.; Nozaki, K. *J. Am. Chem. Soc.* **2009**, *131*, 14168. (b) Lee, D. W.; Jensen, C. M.; Morales-Morales, D. *Organometallics* **2003**, *22*, 4744.

37. Young, K. J. H.; Oxgaard, J.; Ess, D. H.; Meier, S. K.; Stewart, T.; Goddard, W. A.; Periana, R. A. *Chem. Commun.* **2009**, 3270.

38. "The Nobel Prize in Chemistry 2005". Nobelprize.org. 12 Jul 2012 http://www.nobelprize.org/nobel_prizes/chemistry/laureates/2005/.

39. Schrock, R. R. *J. Am. Chem. Soc.* **1974**, *96*, 6796.

40. (a) Schrock, R. R. *Chem. Rev*. **2002**, *102*, 145. (b) Schrock, R. R. In *Reactions of Coordinated Ligands*; Braterman, P. R., Ed.; Plenum: New York, **1986**. (c) Feldman, J.; Schrock, R. R. *Prog. Inorg. Chem*. **1991**, *39*, 1. (d) Schrock, R. R. *Pure Appl. Chem*. **1994**, *66*, 1447. (e) Beckhaus, R.; Santamaria, C. *J. Organomet. Chem*. **2001**, *617-618*, 81.

41. Basuli, F.; Bailey, B. C.; Tomaszewski, J.; Huffman, J. C.; Mindiola, D. J. *J. Am. Chem. Soc*. **2003**, *125*, 326.

42. Schrock, R. R. *Accounts of Chemical Research* **1979**, *12*, 98.

43. Guggenberger, L. J.; Schrock, R. R. *J. Am. Chem. Soc.* **1975**, *97*, 6578.

44. Schrock, R. R.; Messerle, L. W.; Wood, C. D.; Guggenberger, L. J. *J. Am. Chem. Soc.* **1978**, *100*, 3793.

45. (a) Churchill, M. R.; Hollander, F. J.; Schrock, R. R. *J. Am. Chem. Soc*. **1978**, *100*, 647. (b) Churchill, M. R.; Hollander, F. J. *Inorg, Chem.* **1978**, *17*, 1957.

46. (a) van der Heijden, H.; Hessen, B. *J. Chem. Soc. Chem. Commun.* **1995**, 145. (b) Sinnema, P.-J.; van der Veen, L., Spek, A. L.; Veldman, N.; Teuben, J. H. *Organometallics* **1997**, *16*, 4245. (c) Kahlert, S.; Goerls, H.; Scholz, J. *Angew. Chem., Int. Ed.* **1998**, *37*, 1857. (d) Kruger, C.; Mynott, R.; Siedenbiedel, C.; Stehling, L.; Wilke, G. *Angew. Chem. Int. Ed. Engl.* **1991**, *30*, 1668. (e) See also Tebbe's reagent: Tebbe, F. N.; Parshall, G. W.; Reddy, G. S. *J. Am. Chem. Soc.* **1978**, *100*, 3611. (f) For

studies of the thermal decomposition of $Ti(CH_2CMe_3)_4$, see: Cheon, J.; Rogers, D. M.; Girolami, G. S. *J. Am. Chem. Soc.* **1997**, *119*, 6804.

47. (a) Van Doorn, J. A.; van der Heijden, H.; Orpen, A. G. *Organometallics*, **1994**, *13*, 4271. (b) Doorn, J. A.; van der Heijden, H.; Orpen, A. G. *Organometallics*, **1995**, *14*, 1278. (c) Baumann, R.; Stumpf, R.; Davis, W. M.; Liang, C. C.; Schrock, R. R. *J. Am. Chem. Soc.* **1999**, *121*, 7822. (d) Coville et al. described a series of bis(iminophosphorano)methanediide complexes of the group 4 metals that resemble metal alkylidenes Babu, R. P. K.; McDonald, R.; Cavell, R. G. *Organometallics* **2000**, *19*, 3462.

48. Andrews et al. have studied reactions of group 4 metal atoms with CX4 molecules that give $M{=}CX_2$ products: (a) Lyone, J. T.; Andrews, L. *Organometallics* **2007**, *26*, 332. (b) Cho, H. G.; Kim, T. H.; Andrews, L. *Chem. Asian J.* **2006**, *1*, 404. (c) Cho, H. G.; Wang, X. Andrews, L. *Organometallics* **2005**, *24*, 2854. (d) Cho, H. G.; Andrews, L. *Organometallics* **2004**, *24*, 4357.

49. (a) Fryzuk, M. D.; Mao, S. S. H.; Zaworotko, M. J.; MacGillivray, L. R. *J. Am. Chem. Soc*. **1993**, *115*, 5336. (b) Fryzuk, M. D.; Duval, P. B., Mao, S. S. H.; Zaworotko, M. J.; MacGillivray, L. R. *J. Am. Chem. Soc.* **1999**, *121*, 2478. (c) Fryzuk, M. D.; Duval, P. B.; Mao, S. S. H., Rettig, S. J.; Zaworotko, M. J.; MacGillivray, L. R. *J. Am. Chem. Soc*. **1999**, *121*, 1707.

50. Fryzuk, M. D., Duval, P. B.; Patrick, B. O.; Rettig, S. J. *Organometallics* **2001**, *20*, 1608.

51. Liang, L.-C.; *Coord. Chem. Rev*. **2006**, *250*, 1152.

52. (a) Mindiola, D. J. *Acc. Chem. Res.* **2006**, *39*, 813. (b) Mindiola, D. J.; Bailey, B. C.; Basuli, F. *Eur. J. Inorg. Chem.* **2006**, 3135.

53. (a) Kilgore, U. J.; Tomaszewski, J.; Fan, H.; Huffman, J. C.; Mindiola, D. J. *Organometallics* **2007**, *26*, 6132. (b) Kilgore, U. J.; Sengelaub, C. A.; Fan, H.; Tomaszewski, J.; Pink, M.; Karty, J. A.; Baik, M.; Mindiola, D. J. *Organometallics* **2009**, *28*, 843.

54. (a) Fout, A. R.; Scott, J. L.; Miller, D. L.; Bailey, B. C.; Huffman, J. C.; Pink, M.; Mindiola, D. J. *Organometallics* **2009**, *28*, 331. (b) Bailey, B. C.; Fan, H.; Huffman, J. C.; Baik, M.; Mindiola, D. J. *J. Am. Chem. Soc.* **2007**, *129*, 8781.

55. Fryzuk, M. D.; Carter, A.; Rettig, S. J. *Organometallics* **1992**, *11*, 469-472.

56. (a) Fryzuk, M. D. *Can. J. Chem.* **1992**, *70*, 2839. (b) Fryzuk, M. D.; Berg, D. J.; Haddad, T. S. *Coord. Chem. Rev*. **1990**, *99*, 137. (c) Fryzuk, M. D.; Montgomery, C. D. *Coord. Chem. Rev.* **1989**, *95*, 1. (d) Cuenca, T.; Montejano, C.; Royo, P. *J. Organomet. Chem.* **1996**, *514*, 93-96.

57. (a) Fullmer, B. C.; Fan, H.; Pink, M.; Huffman, J. C.; Tsvetkov, N. P.; Caulton, K. G. *J. Am. Chem. Soc.* **2011**, *133*, 2571. (b) Ozerov, O. V.; Watson, L. A.; Pink, M.; Caulton, K. G. *J. Am. Chem. Soc*., **2007**, *129*, 6003. (c) Ishiyama, T.; Mizuta, T.; Miyoshi, K.; Nakazawa, H. *Organometallics* **2003**, *22*, 1096-1105.

58. Warren, T. H.; Schrock, R. R.; Davis, W. M. *Organometallics* **1998**, *17*, 308-321

59. Scott, M. J.; Lippard, S. J. *Inorganic Chimica Acta* **1997**, *263*, 287-299.

60. Gerber, L. C. H.; Watson, L. A.; Parkin, S.; Weng, W.; Foxman, B. M.; Ozerov, O. V. *Organometallics* **2007**, *26*, 4866-4868.

61. *POV-Ray – The Persistence of Vision Raytracer*, Dec. 2012, available at http://www.povray.org/

62. *Ortep-3 for Windows*, Farugia, L. *J. Appl. Crystallogr*. **1997**, *30*, 565.

63. See for example: (a) Kaupp, M. *Chem. Eur. J.* **1998**, *4*, 1678. (b) Kaupp, M. *Angew. Chem., Int. Ed.* **2001**, *40*, 3534. (c) Perrin, L.; Maron, L.; Eisenstein, O. *Faraday Discussions* **2003**, *124*, 25. (d) $[(^{t}Bu_3SiCC)_6Ta]^-$ is trigonal prismatic but $[(^{t}Bu_3SiCC)_6Zr]^{2-}$ is octahedral: Vaid, T. P.; Veige, A. S.; Lobkovsky, E. B.; Glassey, W. V.; Wolczanski, P. T.; Liable-Sands, L. M.; Rheingold, A. L.; Cundari, T. R. *J. Am. Chem. Soc*. **1998**, *120*, 10067. (e) $[Li(tmeda)]_2[ZrMe_6]$ was shown to have a trigonal prismatic environment about Zr in the solid state: Morse, P. M.; Girolami, G. S. *J. Am. Chem. Soc*. **1989**, *111*, 4114.

64. Fryzuk, M. D.; Corkin, J. R.; Patrick, B. O. *Can. J. Chem.* **2003,** *81*, 1376.

65. Fryzuk, M. D.; Carter. A.; Westerhaus, A. *Inorg. Chem.* **1985**, *24*, 642-648.

66. Crabtree, R. H. *The Organometallic Chemistry of the Transition Metals*, 3rd ed.; Wiley-Interscience: New York, **2001**, pp. 260-262.

67. (a) Churchill, M. R.; Youngs, W. J. *Inorg. Chem.* **1979**, *18*, 1930. (b) Diminnie, J. B.; Hall, H. D.; Xue, Z. *Chem. Commun*. **1996**, 2383.

68. Lockwood, M. A.; Fanwick, P. E.; Rothwell, I. P. *Organometallics* **1997** *16*, 3574.

69. Lockwood, M. A.; Fanwick, P. E.; Rothwell, I. P. *Chem. Commun.* **1996** 2013.

70. Weng, W. Ph.D. Thesis, Brandeis University, Waltham, MA, 2007.

71. (a) Procelewska, J.; Zahl, A.; Liehf, G.; Van Eldik, R.; Smythe, N. A.; Williams, B. S.; Goldberg, K. I. *Inorg. Chem.* **2005**, *44*, 7732. (b) Brown, M. P.; Puddephatt, R. J.; Upton, C. E. E. *J. Chem. Soc., Dalton Trans.* **1974**, 2457.

72. (a) Roy, S.; Puddephatt, R. J.; Scott, J. D.; *J. Chem. Soc., Dalton Trans.* **1989**, 2121. (b) Brown, M. P.; Puddephatt, R. J.; Upton, C. E. E. *J. Chem. Soc., Dalton Trans.* **1973**, *49*, C61.

73. (a) Anaikov, V. P.; Musaev, D. G.; Morokuma, K. *Eur. J. Inorg. Chem.* **2007**, 5390. (b) Hartwig, J. F. *Organotransition Metal Chemistry: From Bonding to Catalysis*; University Science Books: Sausalito, CA, 2009, pp 41-45.

74. R. Ghosh, T. J. Emge, K. Krogh-Jespersen and A. S. Goldman, *J. Am. Chem. Soc.*, 2008, 130, 11317-11327.

75. (a) Esteruelas, M. A.; Werner, H. *J. Organomet. Chem.* **1986**, *303*, 221. (b) Werner, H.; Wolf, J.; Ho¨hn, A. *J. Organomet. Chem.* **1985**, *287*, 395. (c) Intille, G. M. *Inorg. Chem.* **1972**, *11*, 695. (d) James, B. R.; Preece, M.; Robinson, S. D. *Inorg. Chim.Acta.* **1979**, *34*, L219. (e) Masters, C.; Shaw, B. L. *J. Chem. Soc. A.* **1971**, 3679.

76. Gatard, S.; Celenligil-Cetin, R.; Guo, C.; Foxman, B. M.; Ozerov, O. V. *J. Am. Chem. Soc.* **2006**, *128*, 2808.

77. Puri, M.; Gatard, S.; Smith, D. A.; Ozerov, O. V *Organometallics* **2011**, *30*, 2472.